Università di Pisa

Facoltà di Ingegneria
Corso di Laurea in Ingegneria Chimica

MODELLI DI SIMULAZIONE PER ANALISI E OTTIMIZZAZIONE DI SISTEMI ENERGETICI

Tesi di Laurea Specialistica in Ingegneria Chimica

Candidato:
Nicola Paoli

Relatori:
Ing. Gabriele Pannocchia
Prof. Ing. Roberto Lensi

Anno Accademico 2007/2008
Sessione di Laurea 30 Aprile 2009

UNIVERSITÀ DI PISA

Facoltà di Ingegneria

SIMULATION MODELS FOR ANALYSIS AND OPTIMIZATION OF GAS TURBINE CYCLES

MS Thesis in Chemical Engineering

Candidate:
Nicola Paoli

Supervisors:
Ing. Gabriele Pannocchia
Prof. Ing. Roberto Lensi

ACADEMIC YEAR 2007/2008

"It is not the strongest of the species that survives, nor the most intelligent, but the one most responsive to change."
— Charles Darwin

to my uncle Ing. Marco Mazzoni, R.I.P.

ABSTRACT

This Thesis deals with gas turbine cycle simulation models. In the first part it has been analysed the gas cycle theory and the models present in literature starting from the simplest ones to the most advanced ones.

In the second part different models have been developed using Aspen HYSYS, a widely used process modelling tool for conceptual design, optimisation, business planning, asset management, and performance monitoring. Furthermore, parametric analysis has been undertaken for each model to find out which variables have the most significant effect on overall efficiency. With these variables a model optimization has been conducted using the Hyprotech SQP optimiser, a rigorous sequential quadratic programming (SQP) optimisation solver.

We must become the change we want to see in the world

— Mohandas Gandhi

ACKNOWLEDGMENTS

I would like to give a special thanks to my supervisor, Dott. Ing. Gabriele Pannocchia, for his huge help, and thanks to his knowledge I could solve a lot of problems during this thesis.

I also acknowledge the help of Prof. Ing. Roberto Lensi who provided useful suggestions and comments during this work.

I want also to thank Ing. Andrea Micchi that patiently helped me and all the people at the CPC Lab, thanks guys.

I want to thank my parents for their constant support, Paolo and Sandra, my friends, starting from my computer advisers Marco Luisi and Francesco Monaci, and all the other people that believed in me: Luca Puccinelli, Roberta Rastelli, Franca Paoli, Stefania Mazzoni, Elisa Fabbri, Daniele Genick, Rebecca Borraccini, Matteo Ricci, Ettore Pea, Gabriele Bertozzi, Andrea Pulzone, Davide Bertellotti, Luca Rovai, Roberto Milazzo, Marco Barsanti, Andrea Andreotti, Christian Farnocchia, David Giunta, Marco Reggiannini, Andrea Mallegni, Luca Ghilarducci, Cristiano Pardini, Sonia Arrigoni, Giacomo Lamonaca, Simone Sardelli, Marco Rossi, Dario Brumini, Nico Simoncelli, Nicola Vandi, Valeria Liberti, Laura Sorrentino, and all the others.

CONTENTS

LIST OF FIGURES

LIST OF TABLES

1 INTRODUCTION

During the last few decades earth pollution and global warming have become relevant issues, particularly associated with energy generation industries. Thus, the scientists tried to create and optimize low emissions power plants in order to contain these major problems.

Natural gas, because of its clean burning nature, suits to become a very popular fuel for electricity generation. New technologies have allowed natural gas to play an increasingly important role in the clean generation of electricity. It is used as supply to gas turbine power plants, where it is burnt with air at medium-high pressure ($15 - 20$ bar) and the produced gases expand in a turbine, thus generating electrical energy. The exhaust hot gases from the gas turbine are generally used to heat a pressurized water stream ($50 - 100$ bar) and produce high pressure steam that drives a steam turbine, thus generating extra energy.

The growth of the gas turbine in recent years can be significantly associated with three factors:

- metallurgical advances that have made possible the employment of high temperatures in the combustor and turbine components,
- the cumulative background of aerodynamic and thermodynamic knowledge,
- the utilization of computer technology in the design and simulation of turbine airfoils and combustor and turbine blade cooling configurations.

Combining the above has led directly to improvements in compressor design (increases in pressure ratio), combustor design (regenerators, low NOx emissions), turbine design (single crystal blades, cooling), and overall package performance. Another contributing factor to the success of the gas turbine is the ability to simplify the control of this highly responsive machine through the use of computer control technology. Computers not only start, stop, and govern the gas turbine minute-to-minute operation (and its driven equipment) but can also report on the unit's health (diagnostics), and predict future failures (prognostics).

This thesis aims to evaluate the possible employment of rigorous process simulators in power system studies.

Different kinds of gas turbine power plant models starting from the simple gas cycle and steam cycle separately have been created and analysed. Subsequently these models have been combined together to create different kinds of combined cycle power plants from the simplest one to the advanced one.

These models have been realized using Aspen HYSYS, a widely used process modelling tool for conceptual design, optimization, business planning, asset management, and performance monitoring for oil & gas production, gas processing, petroleum refining, and air separation industries. After the models have been developed a rigorous sequential quadratic programming (SQP) optimization solver (*Hyprotech SQP optimizer*) has been used to achieve efficiency maximization in a range of frequently used pressures and temperatures.

Optimization is a key capability of process simulators and, therefore, they can play an important role in energy saving, and associated economical and environmental impact advantages.

The rest of this thesis is articulated as follows.

CHAPTER TWO starts with an overview of natural gas describing general properties, formation and principal uses. Furthermore it presents an introduction on gas turbine power plants outlining basic and simple configurations.

CHAPTER THREE analyses advanced gas turbine power plants such as different kinds of combined and cogenerative cycles.

CHAPTER FOUR deals with simulation models found in the literature about different kinds of advanced combined cycles.

CHAPTER FIVE describes the Aspen HYSYS models developed for the simple gas cycle, the steam cycle, and the simple combined cycle. Furthermore, it presents several parametric analysis and optimization studies in order to establish the most appropriate operating conditions for each cycle.

CHAPTER SIX describes advanced configuration models realized using Aspen HYSYS with an increasing level of details. It also presents parametric analyses and optimization studies.

CHAPTER SEVEN draws the main conclusions of this work and presents possible future implementations.

2 GAS TURBINE POWER PLANTS

Contents

2.1 INTRODUCTION

Natural gas, because of its clean burning nature, has become a very popular fuel for the generation of electricity. In the 1970's and 80's, the choices for most electric utility generators were coal or nuclear powered plants, but, due to economic, environmental, and technological changes, natural gas has become the fuel of choice for new power plants.

There are many reasons for this increased reliance: while coal is the cheapest fossil fuel for generating electricity, it is also the dirtiest, releasing the highest levels of pollutants into the air. Regulations surrounding the emissions of power plants have forced these electric generators to come up with new methods of generating power, while lessening environmental damage. New technology has allowed natural gas to play an increasingly important role in the clean generation of electricity.

2.2 NATURAL GAS OVERVIEW

Natural Gas is a vital component of the world's supply of energy. It is one of the cleanest, safest, and most useful of all energy sources. Natural gas is colourless, shapeless, and odourless in its pure form. Also it is combustible, and when burned it gives off a great deal of energy. Unlike other fossil fuels, however, natural gas is clean burning and emits lower levels of potentially harmful byproducts into the air.

Found in reservoirs underneath the earth, it is commonly associated with oil deposits. Production companies search for evidence of these reservoirs by using sophisticated technology that helps to find the locations, and drill wells in the earth where it is likely to be found. Once brought from underground, it is refined to remove impurities like water, other gases, sand, and other compounds. Some hydrocarbons are removed and sold separately, including propane and butane. Other impurities are also removed, like hydrogen sulfide (the refining of which can produce sulfur, which is then also sold separately). After refining, the clean natural gas is transmitted through a network of pipelines and, from these, it is delivered to its point of use.

2.2.1 General Properties of Natural Gas

Natural gas is a combustible mixture of hydrocarbon gases, it is formed primarily of methane (CH_4) and it can also include ethane (C_2H_6), propane (C_3H_8), butane (C_4H_{10}) and pentane (C_5H_{12}). The composition of natural gas can vary widely, table 2.1 outline the typical makeup of natural gas before it is refined.

It is considered 'dry' when it is almost pure methane, having had most of the other commonly associated hydrocarbons removed, when other hydrocarbons are present, the natural gas is 'wet'.

Table 2.1: Typical Composition of Natural Gas

Component	Formula	Composition %
Methane	CH_4	$70-90$
Ethane	C_2H_6	
Propane	C3H8	$0-20$
Butane	C_4H_{10}	
Carbon Dioxide	CO_2	$0-8$
Oxygen	O_2	$0-0.2$
Nitrogen	N_2	$0-5$
Hydrogen sulphide	H_2S	$0-5$
Rare gases	A, He, Ne, Xe	trace

In its pure form, it is tasteless, odourless and colourless and, when mixed with the requisite volume of air and ignited, it burns with a clean, blue flame. It is considered one of the cleanest burning fuels, producing primarily heat, carbon dioxide and water vapour. Natural gas is lighter than air, and tends to disperse into the atmosphere. In a confined state within a house, gas concentrations can reach explosive mixtures and when ignited, it causes great hazard to life and property.

In the natural gas combustion process, the principal reaction is the combustion of methane, in which several steps are involved. Methane is believed to form a formaldehyde (HCHO or H_2CO). The formaldehyde gives a formyl radical (HCO), which then forms carbon monoxide (CO). The process is called *oxidative pyrolysis*:

$$CH_4 + O_2 \rightarrow CO + H_2 + H_2O$$

Following oxidative pyrolysis, the H_2 oxidizes, forming H_2O, replenishing the active species and releasing heat. This occurs very quickly, usually in significantly less than a millisecond.

$$2H_2 + O_2 \rightarrow 2H_2O$$

Finally, the CO oxidizes, forming CO_2, and releasing more heat. This process is generally slower than the other chemical steps, and typically requires a few to several milliseconds to occur.

$$2CO + O_2 \rightarrow 2CO_2$$

The result of the above is the following total equation:

$$CH_4(g) + 2O_2(g) \rightarrow CO_2(g) + 2H_2O(l) + 890kJ/mol \quad (2.1)$$

Natural gas can be measured in a number of different ways. It can be measured by the volume it takes up at normal temperatures and pressures, commonly expressed in *normal cubic meters* (corresponding to 0°C at 101.325kPa). While measuring by volume is useful, natural gas can also be measured as a source of energy. Like other forms of energy, it is commonly measured and expressed in *British thermal units* (Btu)[1]. One Btu is the amount of natural gas that will produce enough energy to heat one pound[2] of water by one degree at normal pressure. When natural gas is delivered to a residence, it is measured by the gas utility in *therms* for billing purposes. A therm is equivalent to 100,000 Btu's of natural gas.

1 by convention 1MMBtu = 1.054615GJ. Conversely, 1GJ is equivalent to $26.8m^3$ of natural gas at defined temperature and pressure. So, 1 MMBtu is $28.263682m^3$ of natural gas at defined temperature and pressure

2 1 pound = 453.59237 grams (SI)

2.2.2 The Formation of Natural Gas

Natural gas is a fossil fuel like oil and coal. These fuels are, essentially, the remains of plants, animals and microorganisms that lived millions and millions of years ago. There are many different theories about the origins of methane and fossil fuels:

- **thermogenic methane**: similar to the formation of oil, it is formed from organic particles of organic matter, such as the remains of plant or animal, that are covered in mud and other sediment. Over long time, more and more sediment, mud and other debris are piled on top of the organic matter, which compresses it. This compression, combined with high temperatures found deep underneath the earth, break down the carbon bonds in the organic matter. At higher temperatures more natural gas is created, that is why it is usually associated with oil in deposits that are 1.5 to 3 kilometers below the earth's crust.

- **biogenic methane**: Methanogens, tiny methane producing microorganisms, chemically break down organic matter to produce methane. These microorganisms are commonly found in areas near the surface of the earth that are void of oxygen. Formation of methane in this manner usually takes place close to the surface of the earth, and the methane produced is usually lost into the atmosphere. In certain circumstances, however, it can be trapped underground and recoverable as natural gas.

- **abiogenic processes**: extremely deep under the earth's crust, there exist hydrogen-rich gases and carbon molecules. As these gases gradually rise towards the surface of the earth, they may interact with minerals that also exist underground, in the absence of oxygen. This interaction may result in a reaction, forming elements and compounds that are found in the atmosphere (including nitrogen, oxygen, carbon dioxide, argon, and water). If these gases are under very high pressure as they move towards the surface of the earth, they are likely to form methane deposits, similar to thermogenic methane.

Most of methane will simply rise to the surface and dissipate into the atmosphere, however, a great deal of this methane will rise up into geological formations (*Petroleum Traps*) made up of layers of porous, sedimentary rock, with a denser, impermeable layer of rock on top, that 'trap' the gas under the ground.

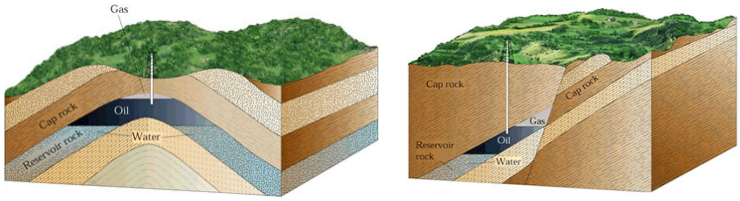

(a) *Anticlinal trap.* **(b)** *Fault trap.*

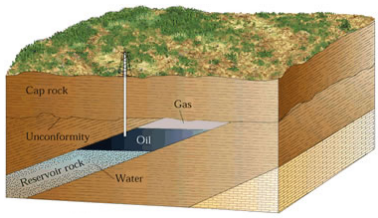

(c) *Stratigraphic trap.*

Figure 2.1: Examples of petroleum traps.

Geologists have classified petroleum traps (Figure 2.1) into two basic types:

1. **Structural traps**: formed because of a deformation in the rock layer that contains the hydrocarbons. Two common examples of structural traps are:
   - *Anticline* is a dome shape upward fold in the layers of rock, petroleum migrates into the highest part of the fold, and its escape is prevented by an overlying bed of impermeable rock;
   - *Fault trap*, when the impermeable formations on either side of the fault have been moved into a position that prevents further migration of petroleum;
2. **Stratigraphic traps**: formed when a reservoir bed is sealed by other beds or by a change in porosity or permeability within the reservoir bed itself. There are many different kinds of stratigraphic traps. In one type, a tilted or inclined layer of petroleum-bearing rock is cutoff or truncated by an essentially horizontal, impermeable rock layer.

Natural gas can be recovered by drilling a hole through the impermeable rock. Gas in these reservoirs is typically under pressure, allowing it to escape from the reservoir on its own.

2.2.3 Uses of Natural Gas

For hundreds of years, natural gas has been known as a very useful substance. The Chinese discovered a very long time ago that the energy in natural gas could be harnessed, and used to heat water. In the early days of the natural gas industry, the gas was mainly used to light streetlamps, and the occasional house. However, with much improved distribution channels and technological advancements, natural gas is being used in ways never thought possible.

There are so many different applications for this fossil fuel that it is hard to provide an exhaustive list of everything it is used for, and no doubt, new uses are being discovered all the time. Natural gas has many applications, commercially, residential, in industry, and even in the transportation sector. While the uses described here are not exhaustive, they may help to show just how many things natural gas can do.

Natural gas is used across all sectors, in varying amounts. The graph 2.2 gives an idea of the proportion of its use per sector. The industrial sector accounts for the greatest proportion of natural gas use, with the residential sector consuming the second greatest quantity of natural gas.

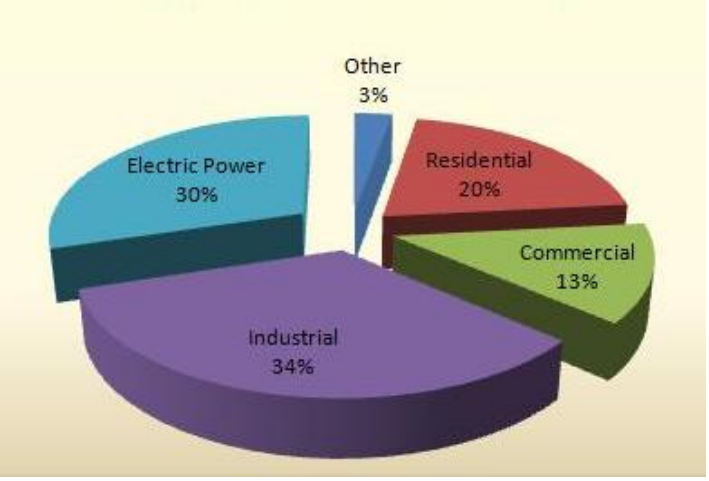

Figure 2.2: Natural gas use by sector.

2.2.4 Residential Uses

Natural gas has historically been much cheaper than electricity as a source of energy for the residential consumer. It has also a number of varied other appliances include space heaters, clothes dryers, fireplaces, barbecues, garage heaters, and outdoor lights.

Despite this massive increase in the proportion of homes using natural gas its actual volume consumed has not increased to the same degree due to increased efficiency of natural gas appliances. Modern top of the line gas furnaces can achieve efficiencies of over 90%, even low-end natural gas furnaces achieve high efficiencies, around 78%.

In addition to heating homes, natural gas can also be used to help cool houses, through natural gas powered air conditioning, more expensive than a comparable electric unit, but considerably more efficient and they require less maintenance.

Natural gas can also provide energy for these appliances at the home, by what is known as *distributed generation*.[3]

2.2.5 Commercial Uses

Commercial uses of natural gas are very similar to residential uses, The main one in this sector include space heating, water heating, and cooling.

There are three types of natural gas driven in commercial cooling processes:

- **Engine driven chillers**, which use a natural gas engine, instead of an electric motor, to drive a compressor. With these systems, waste heat from the gas engine can be used for heating applications, increasing energy efficiency;
- **Absorption chillers**, which provide cool air by evaporating a refrigerant like water or ammonia. These absorption chillers are best suited to cooling large commercial buildings, like office towers and shopping malls;
- **Gas-based desiccant systems**, which cool by reducing humidity in the air. Cooling this dry air requires much less energy than it would to cool humid air.

In addition, many buildings, because of their high electricity needs, have on-site their types of 'distributed generation' units.

3 to generate electricity right on the doorstep via natural gas fuel cells and microturbines

2.2.6 Natural Gas and Transport Sector

Natural gas has long been considered an alternative fuel for the transportation sector, in fact, the first internal combustion engine vehicle to run on natural gas was created by Etienne Lenoir[4] in 1860. In recent years, technology has improved to allow for a proliferation of natural gas vehicles, particularly for fuel intensive vehicle fleets, such as taxicabs and public buses.

Most natural gas vehicles operate using *Compressed Natural Gas* (CNG): this compressed gas is stored in similar fashion to a car's gasoline tank, attached to the rear, top, or undercarriage of the vehicle in a tube shaped storage tank. This natural gas fuels a combustion engine similar to engines fuelled by other sources. However, in a *Natural Gas Vehicle* (NGV), several components require modification to allow the engine to run efficiently on natural gas.

In addition to using CNG, some natural gas vehicles are fuelled by *Liquefied Natural Gas* (LNG). Some NGVs that exist today are bi-fuel vehicles, they can use gasoline or natural gas.

There are many reasons why NGVs are increasing in abundance and popularity:

- Natural gas is **very safe**: being lighter than air, in the event of an accident it simply dissipates into the air, instead of forming a dangerous flammable pool on the ground; this also prevents the pollution of ground water in the event of a spill. Natural gas fuel storage tanks on current NGVs are stronger and sturdier than gasoline tanks;
- Natural gas is an **economic** alternative to gasoline or other fuels. Traditionally, natural gas vehicles have been around 30% cheaper than gasoline vehicles to refuel, and in many cases the maintenance costs for NGVs is lower than traditional gasoline vehicles;
- NGVs, when designed to run on natural gas alone, are among the **cleanest** vehicles in the world; using an NGV means to decrease environmentally harmful emissions, producing, on average, 70% less carbon monoxide, 87% less non-methane organic gas, and 87% less NOx than traditional gasoline powered vehicles.

4 **Jean Joseph Étienne Lenoir** (January 12, 1822 - August 4, 1900) was a French-Belgian engineer. His interest in electroplating led him to make electrical inventions including an improved electric telegraph.

2.2.7 Uses in Industry

Industrial applications for natural gas are many, including the same uses found in residential and commercial settings. It is also used for waste treatment and incineration, metals preheating (particularly for iron and steel), drying and dehumidification, glass melting, food processing, and fuelling industrial boilers. Natural gas may also be used as a feedstock commonly found as a building block for methanol, which in turn has many industrial applications: natural gas is converted to what is known as *synthesis gas*, a mixture of hydrogen and carbon oxides formed through a process known as *steam reforming*[5]. This synthesis gas, once formed, may be used to produce methanol, which in turn is used to produce such substances as formaldehyde, acetic acid, and MTBE (methyl tertiary butyl ether) that is used as an additive for cleaner burning gasoline. Methanol may also be used as a fuel source in fuel cells.

Natural gas absorption systems are also being used extensively in industry to heat and cool water in an efficient, economical, and environmentally sound way.

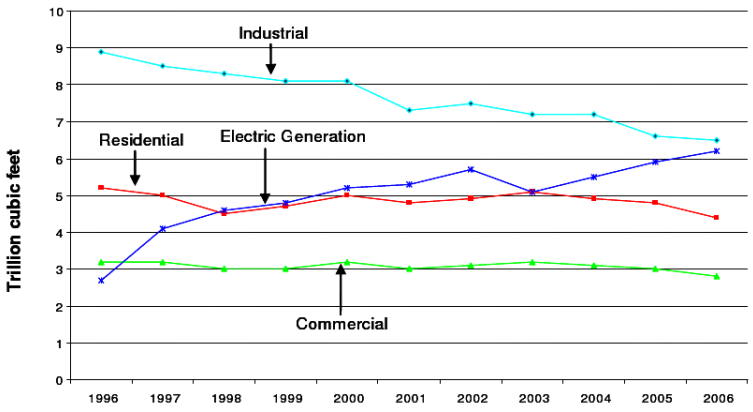

Figure 2.3: U.S. Delivery Volumes, 1996-2006.

5 natural gas is exposed to a catalyst that causes oxidization of the natural gas when brought into contact with steam

INFRARED HEATING UNITS (IR) An innovative and economic method of using natural gas to generate heat in an industrial setting. They are very useful in the metals industry, as they increase the efficiency of powder-coating manufacturing processes. Infrared heaters use natural gas to more efficiently and quickly heat materials used in this process. Natural gas is combined with a panel of ceramic fibers containing a platinum catalyst, causing a reaction with oxygen to dramatically increase temperature, without even producing a flame.

DIRECT CONTACT WATER HEATERS An application that works by having the energy from the combustion of natural gas transferred directly from the flame into the water. These systems are incredibly efficient at heating water. Normal industrial water heaters operate in the 60 - 70% energy efficiency range, however, direct contact water heaters can achieve efficiencies up to 99.7%. Obviously, this leads to huge cost savings in industries where hot water is essential.

INDUSTRIAL COMBINED HEAT AND POWER (CHP) AND COMBINED COOLING, HEAT, AND POWER (CCHP) PLANTS Natural gas may be used to generate electricity needed in a particular industrial setting; the excess heat and steam produced from this process can be harnessed to fulfill other industrial applications, including space heating, water heating, and powering industrial boilers.

INDUSTRIAL CO-FIRING A process in which natural gas is used as a supplemental fuel in the combustion of other fuels, such as coal, wood, and biomass energy. Adding natural gas to the combustion mix can have a two-fold effect: natural gas emits fewer harmful substances into the air than a fuel such as wood, since the energy needed to power the natural gas boiler remains constant, adding natural gas to the combustion mix can reduce harmful emissions; in addition, the operational performance of the boiler, including its energy efficiency, can be improved by supplementing with natural gas. This type of co-firing can also be used in the generation of electricity, whether on-site or in a centralized power plant.

2.3 GAS TURBINE POWER PLANTS

A conventional power plant receiving fuel energy (F), producing work (*W*) and rejecting heat (QA) to a sink at low temperature is shown in figure 2.4 as a block diagram. The objective is to achieve the least fuel input for a given work output as this will be economically beneficial in the operation of the power plant, thereby minimizing the fuel costs. However, the capital cost of achieving high efficiency has to be assessed and balanced against the resulting saving in fuel costs.

It is important to distinguish between a closed cyclic gas power plant (or heat engine) and an open circuit power plant. In the former, fluid passes continuously round a closed circuit, through a thermodynamic cycle in which heat (Q_B) received from a source at a high temperature, heat (Q_A) is rejected to a sink at low temperature and work output (*W*) is delivered, usually to drive an electric generator.

Figure 2.5a shows a gas turbine power plant operating on a closed circuit. The dotted chain control surface (Y) surrounds a cyclic gas turbine power plant (or cyclic heat engine) through which air or gas circulates, and the combustion chamber is located within the second open control surface (Z). Heat Q_B is transferred from Z to Y, and heat Q_A is rejected from Y. The two control volumes form a complete power plant.

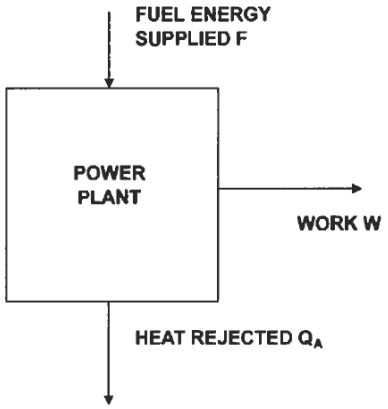

Figure 2.4: Basic power plant.

Usually, a gas turbine plant operates on 'open circuit', with internal combustion (Figure 2.5b). Air and fuel pass across the single control surface into the compressor and combustion chamber, respectively, and the combustion products leave the control surface after expansion through the turbine.

The open circuit plant cannot be said to operate on a thermodynamic cycle. However, its performance is often assessed by treating it as equivalent to a closed cyclic power plant, but care must be taken in such an approach.

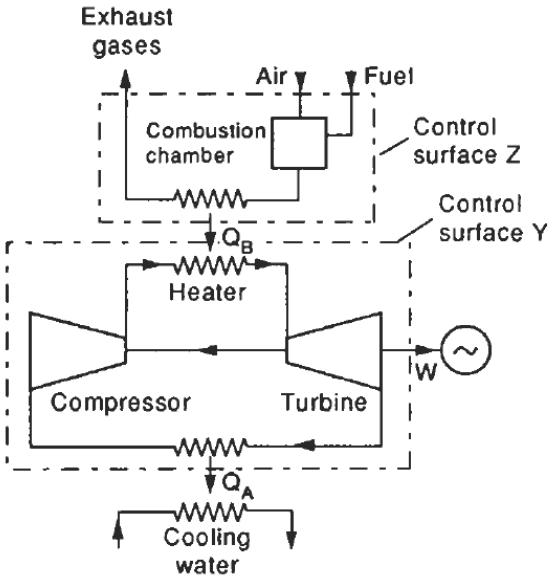

(a) *Closed circuit gas turbine plant.*

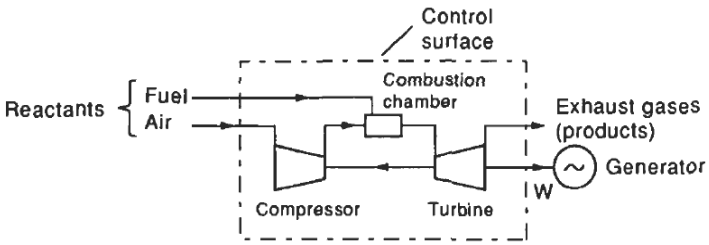

(b) *Open circuit gas turbine plant.*

Figure 2.5: Typical gas turbine plants.

The *Joule-Brayton (JB) constant pressure closed cycle* is the basis of the cyclic gas turbine power plant, with steady flow of air (or gas) through a compressor, heater, turbine, cooler within a closed circuit (Figure 2.6). The turbine drives the compressor and a generator delivering the electrical power, heat is supplied at a constant pressure and is also rejected at constant pressure.

An important field of study for power plants is that of the *combined plant*. A broad definition of a combined power plant (Figure 2.7) is one in which a 'higher' (upper or topping) thermodynamic cycle produces power, but part or all of its heat rejection is used in supplying heat to a 'lower' or bottoming cycle. The 'upper' plant is frequently an open circuit gas turbine while the 'lower' plant is a closed circuit steam turbine. Together they form a *combined cycle gas turbine* (CCGT) plant. The objective is to obtain greater work output for a given supply of heat or fuel energy by converting some of the heat rejected by the upper plant into extra work in the lower plant.

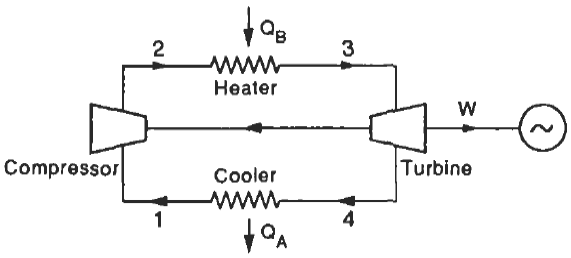

(a) *Cyclic gas turbine power plant.*

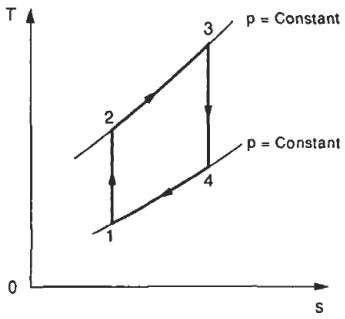

(b) *Temperature-Entropy Diagram.*

Figure 2.6: Joule-Brayton cycle.

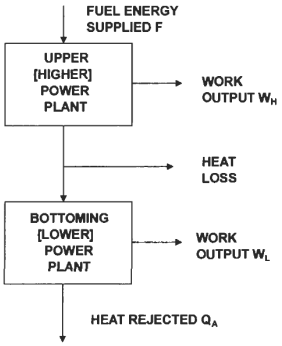

(a) *Block diagram.*

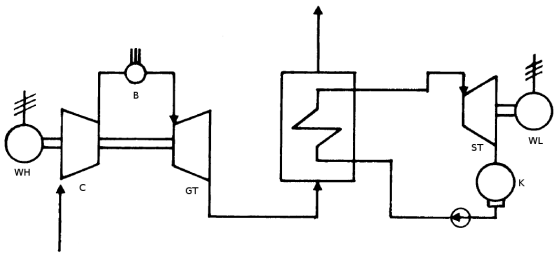

(b) *Scheme of a combined cycle power plant.*

Figure 2.7: Combined power plant.

The term *'cogeneration'* is referred to the *combined heat and power* (CHP) plant such as the one in Figure 2.8. Now the fuel energy is converted partly into electrical work (W) and partly into useful heat (Q_U) at a low temperature, but higher than ambient. The non-useful heat rejected is Q_{NU}.

Usually the heat is produced by the steam cycle of a combined cycle, that is why sometimes the term cogeneration is used mistakenly to describe combined cycles.

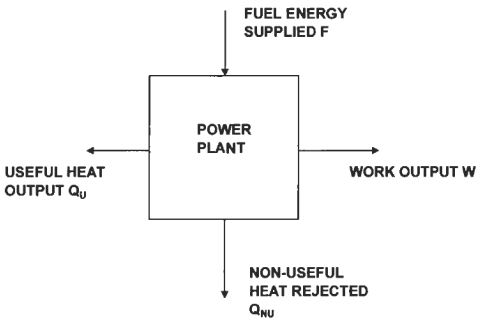

Figure 2.8: Cogeneration plant.

2.4 POWER PLANTS PERFORMANCE

2.4.1 Closed circuit gas turbine plant

For a cyclic gas turbine plant in which fluid is circulated continuously within the plant (e.g. the plant enclosed within the control surface Y in Figure 2.5a), one criterion of performance is simply the *thermal* or *cycle efficiency*,

$$\eta = \frac{W}{Q_B} \tag{2.2}$$

where W is the net work output and Q_B is the heat supplied.

The heat supply to the cyclic gas turbine power plant of figure 2.5a comes from the control surface Z. Within this second control surface, a steady-flow heating device is supplied with reactants (fuel and air) and it discharges the products of combustion. We may define a second efficiency for the 'heating device' (or boiler) efficiency,

$$\eta_B = \frac{Q_B}{F} = \frac{Q_B}{M_f[CV]_0} \tag{2.3}$$

Q_B is the heat transfer from Z to the closed cycle within control surface Y, which occurs during the time interval that M_f, the mass of fuel, is supplied and $[CV]_0$ is its calorific value per unit mass of fuel for the ambient temperature (T_0) at which the reactants enter. $F = M_f[CV]_0$ is equal to the heat (Q_0) that would be transferred from Z if the products were to leave the control surface at the entry temperature of the reactants, taken as the temperature of the environment, T_0.

The *overall efficiency* of the entire gas turbine plant, including the cyclic gas turbine power plant (within Y) and the heating device (within Z), is given by

$$\eta_O = \frac{W}{F} = \frac{W}{Q_B}\frac{Q_B}{F} = \eta\eta_B \tag{2.4}$$

2.4.2 Open circuit gas turbine plant

For an open circuit (non-cyclic) gas turbine plant (Figure 2.5b) a different criterion of performance is sometimes used, the *rational efficiency* (η_R). This is defined as the ratio of the actual work output to the maximum (reversible) work output that can be achieved between the reactants, each at pressure (P_0) and temperature (T_0) of the environment, and products each at the same P_0, T_0:

$$\eta_R = \frac{W}{W_{REV}} = \frac{W}{[-\Delta G_0]} \tag{2.5}$$

where $[-\Delta G_0] = G_{R0} - G_{P0}$ id the change in Gibbs function (from reactants to products).

$[-\Delta G_0]$ is not readily determinable, but for many reactions $[-\Delta H_0]$ is numerically almost the same as $[-\Delta G_0]$. Thus the rational efficiency of the plant is frequently approximated to

$$\eta_R \approx \frac{W}{[-\Delta H_0]} = \frac{W}{M_f[CV]_0} = \frac{W}{F} \tag{2.6}$$

where $[-\Delta H_0] = H_{R0} - H_{P0}$.

Many preliminary analyzes of gas turbines are based on the assumption of a closed 'air standard' cyclic plant, and for such analyzes the use of η as a thermal efficiency is entirely correct, but most practical gas turbines are of the open type and the rational efficiency should strictly be used, or at least its approximate form, the arbitrary overall efficiency η_O.

2.4.3 Energy utilization factor

For a gas turbine operating as a combined heat and power plant, the *energy utilization factor* (EUF) is better criterion of performance than the thermal efficiency. It is defined as the ratio of work output (W) plus useful heat output (Q_U) to the fuel energy supplied (F),

$$EUF = \frac{W + Q_U}{F} \tag{2.7}$$

2.5 IDEAL POWER PLANT PERFORMANCE

The second law of thermodynamics may be used to show that a cyclic heat power plant (or cyclic heat engine) achieves maximum efficiency by operating on a reversible cycle called the *Carnot*[6] *cycle* for a given (maximum) temperature of supply (T_{max}) and given (minimum) temperature of heat rejection (T_{min}). Such a Carnot power plant receives all its heat (Q_B) at the maximum temperature. The other processes are reversible, adiabatic and therefore isentropic (Figure 2.9). Its thermal efficiency is,

$$\begin{aligned} \eta_{CAR} &= \frac{W}{Q_B} = \frac{Q_B - Q_A}{Q_B} = \frac{T_{max}\Delta s - T_{min}\Delta s}{T_{max}\Delta s} \\ &= \frac{T_{max} - T_{min}}{T_{max}} = 1 - \frac{T_{min}}{T_{max}} \end{aligned} \tag{2.8}$$

The Carnot engine is a useful hypothetical device in the study of the thermodynamics of gas turbine cycles, for it provides a measure of the best performance that can be achieved under the given boundary conditions of temperature.

In his search for high efficiency, the designer of a gas turbine power plant will attempt to emulate these features of this cycle.

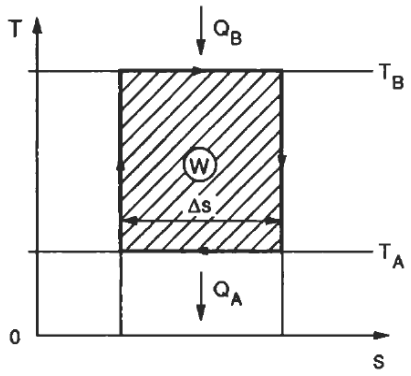

Figure 2.9: T,s diagram for a Carnot cycle.

6 **Nicolas Léonard Sadi Carnot** (1 June 1796 - 24 August 1832) was a French physicist and military engineer who gave the first successful theoretical account of heat engines [4].

2.6 BASIC GAS TURBINE CYCLES

Analyzing power plant thermodynamics the research of high thermal efficiency led us to emphasis on raising the maximum temperature T_{max} and lowering the minimum temperature T_{min} in emulation of the performance of the Carnot cycle. In a gas turbine plant, this search for high maximum temperatures is limited by material considerations and cooling of the turbine is required. This is usually achieved in 'open' cooling systems, using some compressor air to cool the turbine blades and then mixing it with the mainstream flow.

2.6.1 The reversible Joule-Brayton Cycle $[CHT]_R$

We use the original *Joule-Bryton*[7] *cycle* as a standard, an internally reversible closed gas turbine cycle (figure 2.10) with a maximum temperature $T_3 = T_B$ and a pressure ratio r. The minimum temperature is taken as T_A, the ambient temperature, so that $T_1 = T_A$. For unit air flow rate round the cycle, the heat supplied is $q_B = c_P(T_3 - T_2)$, the turbine work output is $w_T = C_P(T_3 - T_4)$ and the compressor work input is $w_C = c_P(T_2 - T_1)$.

Hence the thermal efficiency is

$$\begin{aligned}\eta = \frac{w}{q_B} &= \frac{C_P(T_3 - T_4) - C_P(T_2 - T_1)}{C_P(T_3 - T_2)} \\ &= 1 - \frac{(T_4 - T_1)}{(T_3 - T_2)} = 1 - \frac{\frac{T_3}{xT_1} - 1}{\frac{T_3}{T_1} - x} = 1 - \frac{1}{x}\end{aligned} \tag{2.9}$$

where $x = r^{(\gamma-1)/\gamma} = T_2/T_1 = T_3/T_4$ is the isentropic temperature ratio ($\gamma = c_P/c_V$).

Initially this appears to be an odd result as the thermal efficiency is independent of the maximum and minimum temperatures; however, each elementary part of the cycle, as shown in figure 2.10, has the same ratio of temperature of supply to temperature of rejection $T_S/T_R = x$. Thus each of these elementary cycles has the same Carnot type efficiency, equal to $1 - (T_R/T_S) = 1 - (1/x)$. Hence it is not surprising that the whole reversible cycle, made up of these elementary cycles of identical efficiency, has the same efficiency.

7 **George Brayton** (October 3, 1830 - December 17, 1892) was an American mechanical engineer who is noted for introducing the continuous combustion process that is the basis for the gas turbine.

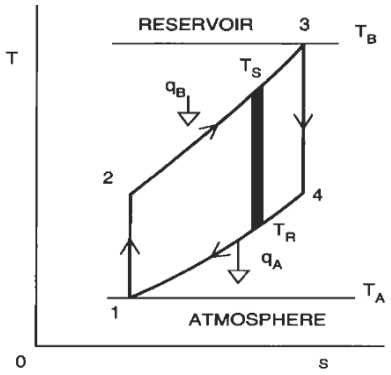

Figure 2.10: T,s diagram for reversible closed cycle.

However, the net specific work,

$$w = (w_T - w_C) = C_P T_1 \left[\frac{\theta}{x} - 1\right](x - 1) \tag{2.10}$$

does increase with $\theta = T_3/T_1$ at a given x. For a given θ, it is a maximum at $x = \theta^{1/2}$.

Although the $[CHT]_R$ cycle is internally reversible, external irreversibility is involved in the heat supply from the external reservoir at temperature T_B and the heat rejection to a reservoir at temperature T_A. So a consideration of the internal thermal efficiency alone does not provide a full discussion of the thermodynamic performance of the plant. If the reservoirs for heat supply and rejection are of infinite capacity, then it may be shown that the irreversibilities in the heat supply (q_B) and the heat rejection (q_A), respectively, both positive, are

$$\begin{aligned} i_B &= T_A \int_{T_2}^{T_B} (dq_B/T) - q_B T_A/T_B \\ &= [c_P T_A \ln(T_B/T_2) - (q_B T_A/T_B)] \end{aligned}$$

and

$$i_A = q_A - T_A \int_{T_A}^{T_4} (dq_B/T) = q_A - c_P T_A \ln(T_4/T_A)$$

But $T_B = T_3 = xT_4$ and $T_2 = xT_1 = xT_4$, so $(T_B/T_2) = (T_4/T_A)$,

$$\sum i = i_B + i_A = q_B[(q_A/q_B) - (T_A/T_B)] \tag{2.11}$$

With the two reservoirs at T_A and T_B, the maximum possible work is then

$$\begin{aligned} w_{max} &= w + \sum i = q_B - q_A + q_A - q_B(T_A/T_B) \\ &= q_B[1 - (T_A/T_B)] = \eta_{CAR} q_B \end{aligned} \tag{2.12}$$

where η_{CAR} is the Carnot efficiency.

2.6.2 The irreversible simple cycle $[CHT]_I$

A closed cycle $[CHT]_I$ with state points 1,2,3,4, is shown in figure 2.11. The specific compressor work input is given by

$$w_C = c_P\,(T_2 - T_1) = \frac{c_P\,(T_{2s} - T_1)}{\eta_C} = \frac{c_P T_1\,(x-1)}{\eta_C}$$

The specific turbine work output is

$$w_T = c_P(T_3 - T_4) = \eta_T c_P(T_3 - T_{4s}) = \eta_T c_P[1 - (1/x)]$$

so that the net specific work is

$$\begin{aligned} w = w_T - w_C &= c_P T_1\{\eta_T\theta[1-(1/x)] - [(x-1)/\eta_C]\} \\ &= c_P T_1 \frac{\alpha[1-(1/x)] - (x-1)}{\eta_C} \end{aligned} \tag{2.13}$$

where $\alpha = \eta_C\eta_T\theta$. The specific heat supplied is

$$q = c_P(T_3 - T_2) = c_P T_1[(\theta - 1) - (x-1)/\eta_C],$$

so that the thermal efficiency is given by

$$\eta = \frac{w}{q} = \frac{(\alpha - x)[1-(1/x)]}{\beta - x}, \tag{2.14}$$

where $\beta = 1 + \eta_C(\theta - 1)$.

The efficiency is a function of the temperature ratio θ as well as the pressure ratio r (and x), whereas it is a function of pressure ratio only for the reversible cycle $[CHT]_R$.

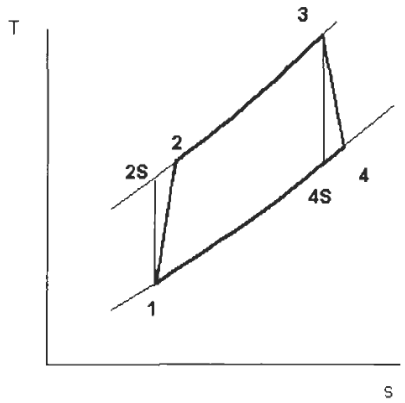

Figure 2.11: T,s diagram for irreversible closed cycle.

2.6.3 The [CBT] open circuit plant

In an open circuit gas turbine plants with combustion, real gas effects are present (in particular the changes in specific heats, and their ratio with temperature), together with combustion and duct pressure losses.

In [CBT] power plants, with fuel addition for combustion, f per unit air flow, the working fluid changes from air in the compressor, to gas products in the turbine, as indicated in figure 2.12. Real gas effects are present in this open gas turbine plant. Specific heats and their ratio are functions of f and T, and allowance is also made for pressure losses.

The flow of air through the compressor may be regarded as the compression of gas with properties $(c_{pa})_{12}$ and $(\gamma_a)_{12}$ (the double subscript indicates that a mean is taken over the relevant temperature range). The work required to compress the unit mass of air in the compressor is then represented as

$$w_C = (c_{pa})_{12} T_1 \frac{(x-1)}{\eta_C} \tag{2.15}$$

where $x = r^{(1/z)}$ and $z = (\gamma_a)_{12}/[(\gamma_a)_{12} - 1]$.

It is possible to represent in explicit form the pressure loss through the combustion chamber using a pressure loss factor $(\Delta p/p)_{23} = (p_2 - p_3)/p_2$, so that $(p_3/p_2) = 1 - (\Delta p/p)_{23}$. Similarly, the pressure loss factor through the turbine exhaust system is $(\Delta p/p)_{41} = (p_4 - p_1)/p_4$, so $(p_1/p_4) = 1 - (\Delta p/p)_{41}$.

The work generated by the turbine per unit mass of air after receiving combustion gas of mass $(1 + f)$ and subjected to a

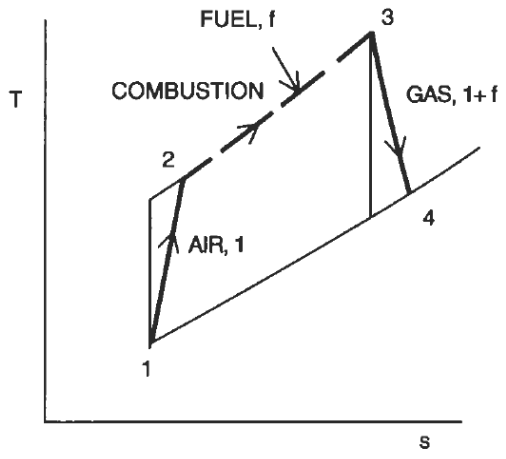

Figure 2.12: T, s diagram for irreversible open cycle.

pressure ratio of $r = [1 - (\Delta p/p)_{23}]/[1 - (\Delta p/p)_{41}]$, may then be written approximately as

$$w_T \approx (1 + f)\eta_T (c_{pa})_{12} T_3 [1 - (1 + \delta)/x^n]/n \tag{2.16}$$

$n = (c_{pa})_{12}/(c_{pg})_{34}$ and $\delta = \{[(\gamma_g)_{34} - 1] \sum(\Delta p/p)\}/(\gamma_g)_{34}$.

The appearance of n as the index of x in equation 2.16 need to be justified. Combustion in gas turbine usually involves substantial excess air and the molecular weight of the mixed products is little changed from that of the air supplied, since nitrogen is the main component gas for both air and products. Thus the mean gas constant (universal gas constant divided by mean molecular weight) is virtually unchanged by the combustion. It then follow that

$$\frac{1}{n} = \left[\frac{(\gamma_a)_{12} - 1}{(\gamma_a)_{12}}\right]\left[\frac{(\gamma_g)_{34} - 1}{(\gamma_g)_{34}}\right] \tag{2.17}$$

The *arbitrary overall efficiency* of the plant (η_0) is now defined as

$$\eta_0 = \frac{w}{[-\Delta H_0]} \tag{2.18}$$

where $[-\Delta H_0]$ is the change of enthalpy at temperature T_0 in isothermal combustion of a mass of fuel f with unit air flow. In the combustion process, assumed to be adiabatic,

$$[h_{a2} + f h_{f0}] = H_{g3} = (1 + f) h_{g3} \tag{2.19}$$

where h_{f0} is the specific enthalpy of the fuel supplied at T_0.

But from the calorific value process, with heat $[-\Delta H_0] = f[CV]_0$ abstracted to restore the combustion products to the temperature T_0,

$$[h_{a0} + f h_{f0}] = H_{g0} + [-\Delta H_0] = (1 + f) h_{g0} + [-\Delta H_0] \tag{2.20}$$

from equation 2.19 and 2.20:

$$\begin{aligned} f[CV]_0 &= (H_{g3} - H_{g0}) - (h_{a2} - h_{a0}) \\ &= (1 + f)(h_{g3} - h_{g0}) - (h_{a2} - h_{a0}) \\ &= (1 + f)(c_{pg})_{13}(T_3 - T_1) - (c_{pa})_{12}(T_2 - T_1) \end{aligned} \tag{2.21}$$

where the ambient temperature is now taken as identical to the compressor entry temperature (i.e. $T_0 = T_1$).

3 ADVANCED POWER PLANTS

Contents

3.1 INTRODUCTION

The single cycles may not achieve a high enough overall efficiency. The plant designer therefore explores the possibility of using a combined plant, which is essentially one plant thermodynamically on top of the other, the lower plant receiving some or all of the heat rejected from the upper plant.

If a higher mean temperature of heat supply and/or a lower temperature of heat rejection can be achieved in this way then a higher overall plant efficiency can also be achieved, as long as substantial irreversibilities are not introduced.

This chapter describes advanced gas turbine power plants such as different kinds of combined cycles and cogenerative cycles with more level of details.

3.2 THE COMBINED CYCLE GAS TURBINE (CCGT)

Considering an ideal combined power plant made up of two cyclic plants (H, L) in series (figure 3.1), heat that is rejected from the higher (topping) plant, of thermal efficiency η_H, is used to supply the lower (bottoming) plant, of thermal efficiency η_L, with no intermediate heat loss and supplementary heating. The work output from the lower cycle is

$$W_L = \eta_L Q_L \tag{3.1}$$

but

$$Q_L = Q_B(1-\eta_H) \tag{3.2}$$

where Q_B is the heat supplied to the upper plant, which delivers work

$$W_H = \eta_H Q_B \tag{3.3}$$

Thus, the total work output is

$$\begin{aligned} W &= W_H + W_L = \eta_H Q_B + \eta_L(\eta_H) Q_B \\ &= Q_B(\eta_H + \eta_L - \eta_H \eta_L) \end{aligned} \tag{3.4}$$

The thermal efficiency of the combined plant is therefore

$$\eta_{CP} = \frac{W}{Q_B} = \eta_H + \eta_L - \eta_H \eta_L \tag{3.5}$$

The thermal efficiency of the combined plant is greater than that of upper cycle alone by an amount of $\eta_L(1-\eta_H)$.

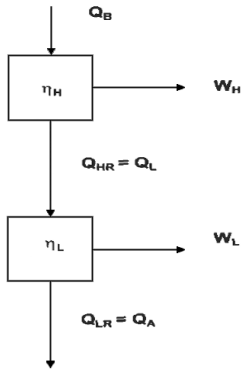

Figure 3.1: Ideal combined cycle plant.

The most developed and commonly used combined power plant involves a combination of open circuit gas turbine and a closed cycle steam turbine (*Rankine*[1] *cycle*), the so-called *CCGT*. Many different combinations of gas turbine and steam turbine plant have been proposed, but essentially there are two main types of CCGT.

In the first type, heating of the steam turbine cycle is by the gas turbine exhaust with or without additional firing (there is normally sufficient excess air in the turbine exhaust for additional fuel to be burnt, without an additional air supply). In the second, the main combustion chamber is pressurized and joint 'heating' of gas turbine and steam turbine plants is involved.

Most major developments have been of the first system, with and without additional firing of the exhaust. The firing is usually 'supplementary'-burning additional fuel in the *heat recovery steam generator* (HRSG) up to a maximum temperature of about 750 °C. However, full firing of exhaust boilers is used in the repowering of existing steam plants.

3.2.1 The exhaust heated (unfired) CCGT

Exhaust gases from the gas turbine are used to raise steam in the lower cycle without an additional fuel burning (figure 3.2). The temperatures of the gas and water/steam flows are as indicated. A limitation on this application lies in the HRSG. The choice of the evaporation pressure (p_C) is related to the temperature difference ($T_6 - T_C$) at the 'pinch point' as shown in the figure, and a compromise has to be reached between that pressure and the stack temperature of the gases leaving the exchanger, T_S (and the consequent 'heat loss').

The work output from the gas-turbine plant of figure 3.2 is

$$W_H = (\eta_O)_H F \tag{3.6}$$

where $(\eta_O)_H$ is the overall efficiency and F is the energy supplied in the fuel, $F = M_f[CV]_0$, where $[CV]_0$ is the enthalpy of combustion of the fuel of mass flow M_f.

The work output from the steam cycle is

$$W_L = \eta_L Q_L \tag{3.7}$$

in which η_L is the thermal efficiency of the lower (steam) cycle and Q_L is the heat transferred from the gas turbine exhaust.

1 **William John Macquorn Rankine** (5 July 1820 - 24 December 1872) was a Scottish engineer and physicist. He developed a complete theory of the steam engine and of all heat engines.

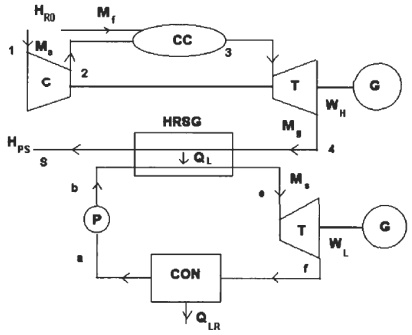

(a) *CCGT unfired scheme.*

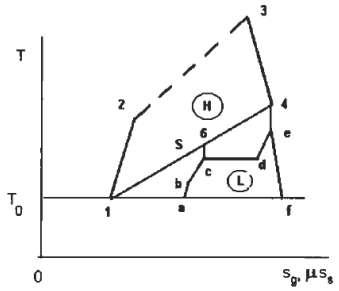

(b) *T,s diagram.*

Figure 3.2: CCGT with no supplementary firing.

Thus, the overall efficiency of the whole plant is

$$(\eta_O)_{CP} = \frac{W_H + W_L}{F} = (\eta_O)_H + \frac{\eta_L Q_L}{F} \tag{3.8}$$

If combustion is adiabatic, then the steady flow energy equation for the open-circuit gas turbine (with exhaust of enthalpy H_{PS} leaving the HRSG and entering the exhaust stack with a temperature T_S greater than that of the atmosphere, T_0) is

$$H_{R0} = H_{PS} + W_H + Q_L \tag{3.9}$$

so that

$$\begin{aligned} Q_L &= H_{R0} - H_{PS} - W_H \\ &= [H_{R0} - H_{P0}] - [H_{PS} - H_{P0}] - W_H \\ &= F - [H_{PS} - H_{P0}] - W_H \end{aligned} \tag{3.10}$$

where H_{P0} is the enthalpy of products leaving the calorimeter in a 'calorific value' experiment, after combustion of fuel M_f at temperature T_0.

The overall efficiency of the combined plant may then be written as

$$\begin{aligned}(\eta_O)_{CP} &= (\eta_O)_H + \eta_L[1 - W_H/F - [H_{PS} - H_{P0}]/F] \\ &= (\eta_O)_H + \eta_L - (\eta_O)_H\eta_L - \eta_L[H_{PS} - H_{P0}]/F \\ &= (\eta_O)_H + \eta_B\eta_L - \eta_B(\eta_O)_H\eta_L \\ &= (\eta_O)_H + (\eta_O)_L - (\eta_O)_H(\eta_O)_L\end{aligned} \tag{3.11}$$

where

$$\eta_B = 1 - \frac{[H_{PS} - H_{P0}]}{F[1 - (\eta_O)_H]} \tag{3.12}$$

the term $\eta_L[H_{PS} - H_{P0}]/F$ corresponds to the 'heat loss'. The extent of this reduction in overall efficiency depends on how much exhaust gases can be cooled and could theoretically be zero if they emerged from the HRSG at the (ambient) temperature of the reactants. In practice this is not possible, as corrosion may take place on the tubes of the HRSG if the dew point temperature of the exhaust gases is above the feed water temperature. We shall find that there may be little or no advantage in using feed heating in the steam cycle of the CCGT plant.

3.2.2 The exhaust heated (fired) CCGT

The exhaust gases from the gas turbine contain substantial amounts of excess air, since the main combustion process has to be diluted to reduce the combustion temperature to well below that which could be obtained in stechiometric combustion, because of the metallurgical limits on the gas turbine operating temperature. This excess air enables supplementary firing of the exhaust to take place and higher steam temperatures may then be obtained in the HRSG. The T, s diagram for a combined plant with supplementary firing is illustrated in figure 3.3 (again the steam entropy has been scaled). Introduction of regenerative feed heating of the water is of doubtful value. Supplementary heating generally lowers the overall efficiency of the combined plant. Essentially this is because a fraction of the total heat supplied is utilized to produce work in the lower cycle, of lower efficiency than that of the higher cycle.

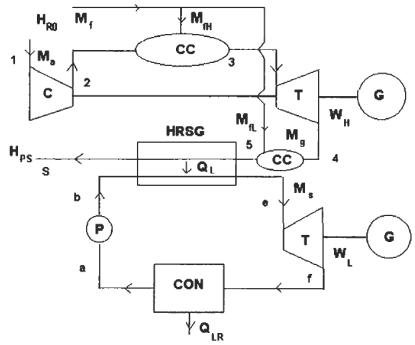

(a) *CCGT fired scheme.*

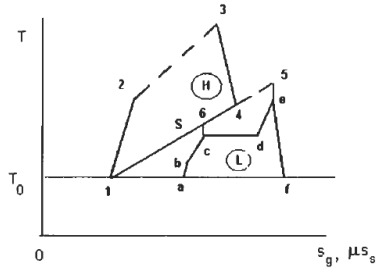

(b) *T,s diagram.*

Figure 3.3: CCGT with supplementary firing.

3.2.3 A parametric calculation

We describe a parametric 'point' calculation of the efficiency of a simple CCGT plant, firstly with no feed heating. It is supposed that the main parameters of the gas turbine upper plant (pressure ratio, maximum temperature, and component efficiencies) have been specified and its performance $(\eta_O)_H$ determined (figure 3.2 shows the T, s diagram for the two plants and the various state points).

For the steam plant, the condenser pressure, the turbine and pump efficiencies are also specified. There is also a single phase of water/steam heating, with no reheating. The feed pump work term for the relatively low pressure steam cycle is ignored, so that $h_b \approx h_a$.For the HRSG two temperature differences are prescribed:

1. the upper temperature difference, $\Delta T_{4e} = T_4 - T_e$;
2. the 'pinch point' temperature difference, $\Delta_{T_{6c}} = T_6 - T_c$.

With the gas temperature at turbine exit known (T_4), the top temperature in the steam cycle (T_e) is then obtained from (1). It

is assumed that this is less than the prescribed maximum steam temperature.

If an evaporation pressure (p_c) is pre-selected as a parametric independent variable, then the temperatures and enthalpies at c and e are found, from (2) the temperature T_6 is also determined. If there is no heat loss, the heat balance in the HRSG between gas states 4 and 6 is

$$M_g(h_4 - h_6) = M_s(h_e - h_c) \tag{3.13}$$

where M_g and M_s are respectively the gas and steam flow rates.

Thus, by knowing all the enthalpies the mass flow ratio $\mu = M_s/M_g$ can be obtained. As the entry water temperature T_b has been specified (as the condenser temperature approximately), a further application of the heat balance equation for the whole HRSG,

$$(h_4 - h_s) = \mu(h_e - h_b) \tag{3.14}$$

yields the enthalpy and temperature at the stack (h_S, T_S).

Even for this simplest CCGT plant, iterations on such a calculation are required, with various values of p_c, in order to meet the requirements set on T_e, the steam turbine entry temperature, and T_s (the calculated value of T_s has to be such that the dew point temperature of the gas (T_{dp}) is below the economizer water entry temperature (T_b) and that may not be achievable). But with the ratio μ satisfactorily determined, the work output from the lower cycle W_L can be estimated and the combined plant efficiency obtained from

$$\eta_O = \frac{W_H + W_L}{M_f[CV]_0} \tag{3.15}$$

as the fuel energy input to the higher cycle and its work output is already known.

This is essentially the approach adopted by Rufli [33] in a comprehensive set of calculations: he assumed that the economizer entry water temperature T_b is raised above the condenser temperature by feed heating, which was specified for all his calculations. The T , s diagram is shown in figure 3.4. The feed pump work terms are neglected so that $h_a \approx h_{b'}$ and $h_{a'} \approx h_b$.

Knowing the turbine efficiency, an approximate condition line for the expansion through the steam turbine can be drawn (to state f' at pressure $p_{b'}$) and an estimate made of the steam enthalpy $h_{f'}$. If a fraction of the steam flow m_s is bled at this point then the heat balance for a direct heater raising the water from near the condenser temperature T_a to T_b is approximately

$$M_s(h_{f'} - h_b) = M_s(1 - m_s)(h_b - h_a) \tag{3.16}$$

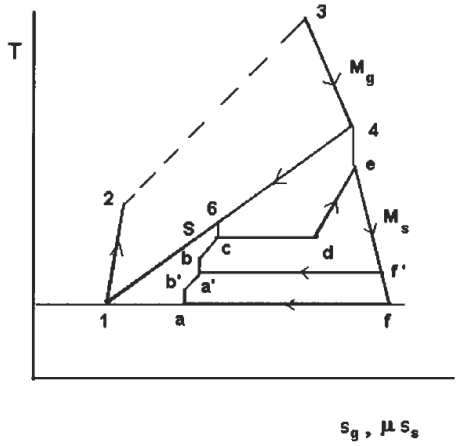

Figure 3.4: CCGT plant with feed water heating.

and m_s can be determined. The work output from the steam cycle can then be obtained (allowing for the bleeding of the steam from the turbine) as

$$W_{L'} = M_s\,[(h_e - h_{f'} + (1 - m_s)(h_{f'} - h_f)] \tag{3.17}$$

where feed pump work terms have been neglected (the feed pumping will be split for the regenerative cycle with feed heating).

With the fuel energy input known from the calculation of the gas turbine plant performance, $F = M_f[CV]_0$, the combined plant efficiency is determined as

$$(\eta_O)_{CP} = \frac{W_H + W_{L'}}{F} \tag{3.18}$$

The reason for using feed heating to set the entry feed water temperature at a level T_b above the condenser temperature T_a is that T_b must exceed the dew point temperature T_{dp} of the exhaust gases. If T_b is below T_{dp} then condensation may occur on the outside of the economizer tubes (the temperature of the metal on the outside of the tubes is virtually the same as the internal water temperature because of the high heat transfer on the water side). With T_b T_{dp} possible corrosion will be avoided.

Rufli also investigated whether raising the steam at two pressure levels showed any advantage. He found that there is an increase of about $2-3\%$ on overall efficiency resulting from two stages of heating rather than a single stage.

3.2.4 Regenerative feed heating

For a comprehensive discussion on feed heating in a CCGT plant, we may refer to Kehlhofer's practical book on CCGTs [15]. A summary of this discussion is given below.

Kehlhofer takes the gas turbine as a 'given' plant and then concentrates on the optimization of the steam plant. He discusses the question of the limitation on the stack and water entry temperatures in some detail, their interaction with the choice of p_C, in a single pressure steam cycle, and the choice of two values of p_C in a dual pressure steam cycle. Considering the economizer of the HRSG he also argues that the dew point of the gases at exhaust from the HRSG must be less than the feed-water entry temperature. For sulphur free fuels the water dew point controls, whereas for fuels with sulphur a 'sulphuric acid' dew point (at a higher temperature) controls. Through these limitations on the exhaust gas temperature, the choice of fuel with or without sulphur content (distillate oil or natural gas, respectively) has a critical influence ab initio on the choice of the thermodynamic system.

For the simple single pressure system with feed heating, he first points out that the amount of steam production (M_S) is controlled by the pinch point condition if the steam pressure (p_C) is selected. However, with fuel oil containing sulphur, the feed-water temperature at entry to the HRSG is set quite high (T_b is about 130 °C), so the heat that can be extracted from the exhaust gases beyond the pinch point $[M_S(h_c - h_b)]$ is limited. The condensate can be brought up to T_b by a single stage of bled steam heating, in a direct contact heater, the steam tapping pressure being set approximately by the temperature T_b.

Kehlhofer then suggests that more heat can be extracted from the exhaust gases, even if there is a high limiting value of Tb (imposed by use of fuel oil with a high sulphur content). It is thermodynamically better to do this without regenerative feed heating, which leads to less work output from the steam turbine. For a *single pressure system with a pre-heating loop*, the extra heat is extracted from the exhaust gases by steam raised in a low pressure evaporator in the loop (as shown in figure 3.5). The evaporation temperature will be set by the 'sulphuric acid' dew point (and feed water entry temperature $T = 130°C$). The irreversibility involved in raising the feed water to temperature T_b is split between that arising from the heat transfer from gas to the evaporation (pre-heater) loop and that in the deareator/feed heater. The total irreversibility is just the same as that which would have

occurred if the water had been heated from condenser temperature entirely in the HRSG.

Kehlhofer explains that the pre-heating loop must be designed so that the heat extracted is sufficient to raise the temperature of the feed water flow from condenser temperature T_a to $T_{a'}$ (figure 3.4). The available heat increases with live steam pressure (p_c),for selected $T_b (\approx T_a)$ and given gas turbine conditions, but the heat required to preheat the feed water is set by $(T_{a'} - T_a)$. The live steam pressure is thus determined from the heat balance in the pre-heater if the heating of the feed water by bled steam is to be avoided. However the optimum (low) live steam pressure may not be achievable because of the requirement set by this heat balance.

Kehlhofer regards the *two pressure system* as a natural extension of the single pressure cycle with a low pressure evaporator acting as a pre-heater. Under some conditions more steam could be produced in the LP evaporator than is required to pre-heat the feed water and this can be used by admitting it to the turbine at a low pressure. For a fuel with high sulphur content (requiring high feed water temperature (T_b) at entry to the HRSG), a dual pressure system with no low pressure water economizer may have two regenerative surface feed heaters and a pre-heating loop. For a sulphur free fuel (with a lower T_b), a dual pressure system with a low pressure economizer may have a single-stage deareator/direct contact feed heater using bled steam.

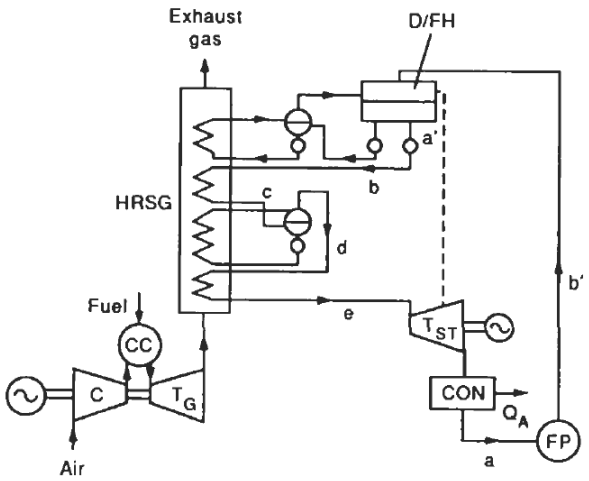

Figure 3.5: Single pressure steam cycle system.

3.3 ADVANCED CCGT PLANTS

In some plants, analysing the HRSG, we can find the use of sections with more than one water stream exchanging simultaneously with the exhaust gas. Nevertheless this particular section arrangement is limited to the case in which the two water streams are in the same phase (e.g. two liquid streams or two superheated vapour streams). In addition to these trends, in order to increase the efficiency of the combined plant, two strategies can be considered[11]:

1. optimization of the HRSG and of the steam cycle;
2. gas to gas recuperation in the gas cycle.

Another interesting opportunity is related to the use of postcombustion coupled with gas to gas recuperation, and optimization of the HRSG.

3.3.1 HRSG optimization

In order to provide better heat recovery in the HRSG, more than one pressure level is used. With a single-pressure HRSG typically more or less 30% of the total plant output power is generated in the steam turbine. A dual-pressure arrangement can increase the power output of the steam cycle by up to 10%, and an additional 3% can result by choosing a triple-pressure cycle [22].

Modern combined cycle power plants with a triple-pressure HRSG with steam reheat can easily reach efficiencies above 55%. A gas turbine with steam cooling of the turbine blades and nozzles, coupled with an advanced HRSG, is expected to operate at an efficiency level of 60%.

The technology of the combined plants leads to the utilization of gas turbine outlet temperatures (i.e. of the inlet gas to the HRSG) superior to 580°C (853 K) and in some cases of the order of 647°C (920 K). The requirements for the increase of the exhaust gas inlet temperature to the HRSG are due to the fact that it does not make use of the section with parallel liquid streams. So the key for increasing the output of the steam cycle, seems to be the greater extension possible of the inlet temperature of the exhaust gas to the HRSG.

The thermodynamic optimization of the HRSG yields the minimization of exergy losses, taking into account only irreversibility due to the temperature difference between the hot and the

cold stream [17]. From the exergy balance, the exergy losses in the HRSG are given by

$$I_{HRSG} = Ex_{g,in} + Ex_{w,in} - Ex_{vap,out} \tag{3.19}$$

The analysis is based on the concept of temperature effectiveness of the HRSG sections, in [5] Franco and Casarosa shows how the use of the gas side effectiveness leads to solve the optimization problem referring to a reduced number of independent variables. The analysis reveals that it seems convenient to use as much as possible a section with more than one water stream. The systematic use of sections with two or more water streams and the approach of the upper steam temperature to the critical value are the key elements for an increase of the efficiency of the whole combined plant. This approach to the critical condition is not found in the existing plants, but it is usually recommended that the saturated vapour stay below 160 bar and 350°C[10].

For a given HRSG configuration, the efficiency of the steam bottoming cycle shows an asymptotic trend, as shown in figure 3.6 for the 3PRSH. It appears reasonable to assume an upper limit value for the inlet temperature of the exhaust gas to the HRSG. This means that, the increase in the HRSG inlet temperature over a value of 823 K determines a less meaningful increase in the efficiency of the steam cycle. This is confirmed by the analysis of the exergy losses in the HRSG and of the total exergy losses, obtained by adding to this term the irreversibility due to expansion and the residual exergy of the vapour at the end of the expansion.

Figures 3.7a and 3.7b show the scheme of the HRSG sections and the corresponding thermodynamic steam cycle of the 3PRSH

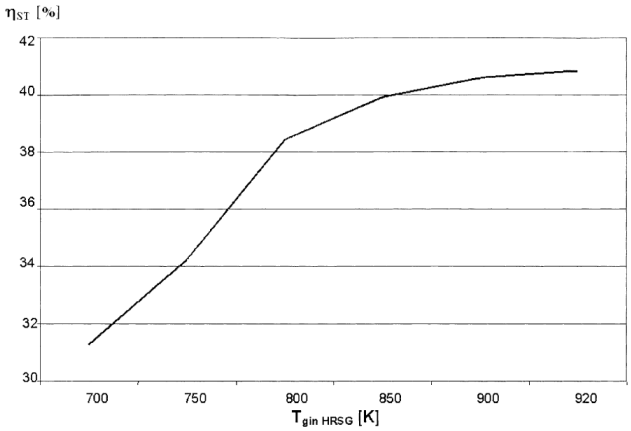

Figure 3.6: Steam cycle efficiency vs gas temperature.

configuration. From the analysis of the general data it is deduced that, from a purely thermodynamic point of view, a complication of the HRSG and consequently of the steam cycle using 2PRSH or 3PRSH configuration is justified and an inlet temperature of the exhaust gas of 823 K can be considered sufficient in order to obtain exergy loss in the HRSG comparable with that due to the expansion in the steam turbine. Moreover it is noted that with an optimized two or three pressure level HRSG configuration, with an inlet temperature to the HRSG of 823 K, the exergy loss in the HRSG is lower than that due to the steam expansion in the turbine.

Coupling an optimized triple pressure level HRSG with superheaters (3PRSH) with an optimized Brayton cycle, it seems possible to obtain efficiencies of about 60%.

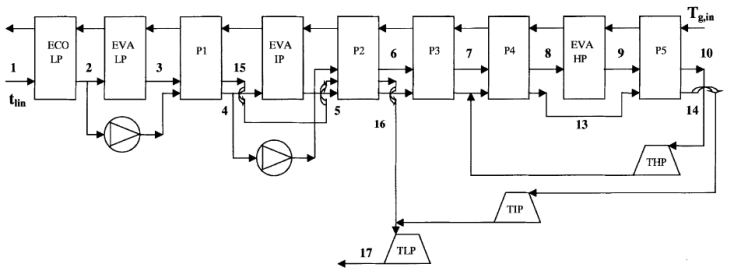

(a) *Scheme of a three pressure level HRSG with reheater (3PRSH).*

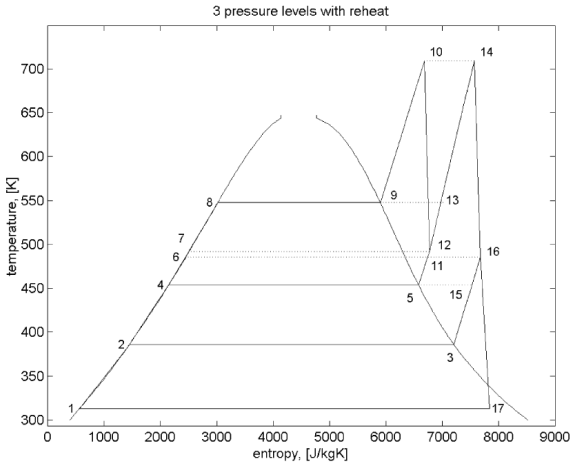

(b) *Thermodynamic scheme of a three pressure level HRSG with reheater (3PRSH).*

Figure 3.7: Three pressures HRSG with reheater.

3.3.2 Brayton cycle with gas to gas recuperation and optimized HRSG

The first strategy to obtain an increase of the combined cycle plant efficiency is represented by the possibility of exploring the optimization of the HRSG with regeneration. In this case the best results can be obtained working with a pressure ratio in the range between 8 and 15. This is due to the fact that, for higher pressure ratios, the regenerator does not influence the gas turbine efficiency because the temperature at the exit of the compressor is similar to that at the exit of the gas turbine. For these pressure ratios it is possible to obtain plant efficiencies higher than 60%. For each pressure ratio two relative maximum of the efficiency can be obtained. The first maximum corresponds to an inlet temperature of the exhaust gas to the HRSG of about 800 K (limited temperature drop in the regenerator and predominant heat recovery). The second maximum is obtained for an inlet temperature in the HRSG of about $650 - 670$ K (higher temperature drop in the regenerator and limited heat recovery). In both the cases it is possible to obtain an increase of the combined plant efficiency of about 1.5% in comparison with the case of a Brayton cycle with an optimized HRSG and without gas to gas regeneration.

3.3.3 Brayton cycle with postcombustion, gas to gas recuperation and optimized HRSG

A very interesting opportunity to furtherly increase the efficiency of the combined cycle plant is represented by exploring the concept of gas to gas recuperation and postcombustion, with the thermodynamic scheme shown in figure 3.8. Optimizing the gas cycle, choosing ad hoc the pressure ratio and the intermediate pressure, using a regenerator and optimizing the HRSG it seems possible an increase of about $7 - 8\%$ in comparison with the classical arrangement of the combined cycle. So resorting to a Brayton cycle with postcombustion, gas to gas recuperation (regeneration), and an optimized 2PRSH or 3PRSH, it is possible to approach an efficiency of 65% for the combined plant.

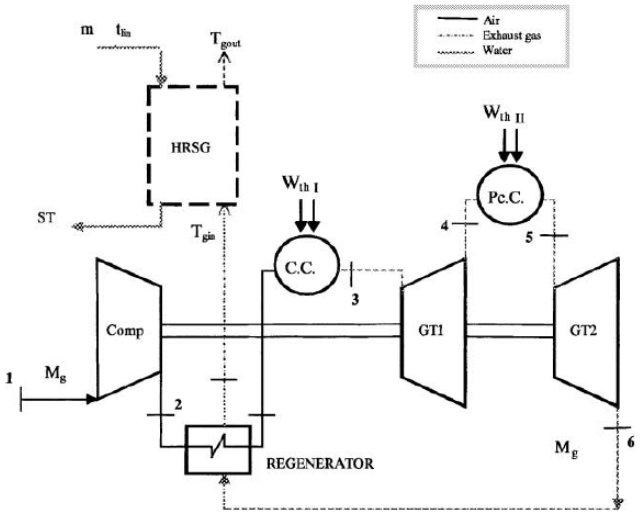

(a)

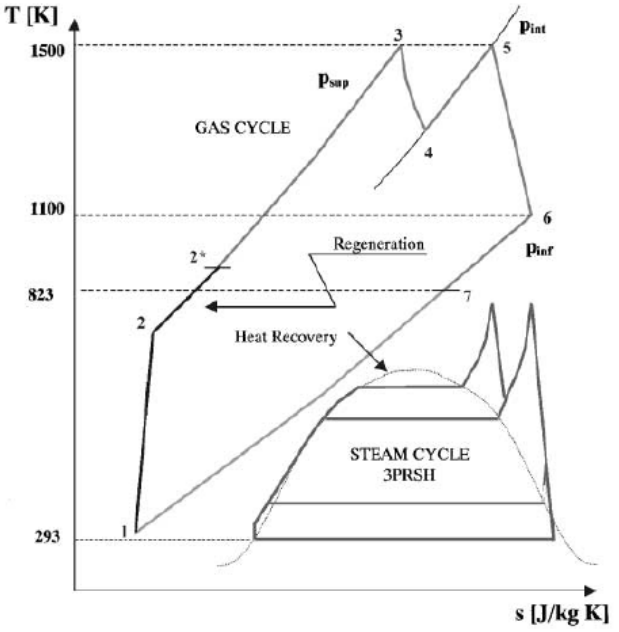

(b)

Figure 3.8: Advanced Brayton cycle.

3.3.4 Brayton cycle with partial gas to gas recuperation

For a given HRSG configuration, the efficiency of the steam bottoming cycle is the function of HRSG inlet gas temperature, it appears that there is an upper limit value for the inlet temperature of the exhaust gas to HRSG. This means that, the increase in HRSG inlet temperature over a value of 590°C will lead to a less increase in the efficiency of steam bottoming cycle. If the temperature is higher than 590°C, it is necessary to use part of its exhaust energy in gas turbine side. For instance GEPG9351 gas turbine, the exhaust gas temperature reaches 615°C at base load and even higher than 640°C under 75% load. An interesting method[36] used to increase the efficiency of the combined cycle plant is to heat the compressed air through partial gas to gas recuperation heat exchanger, with the thermodynamic scheme shown in figure 3.9. The compressed air from compressor is divided into two streams, one directly to combustion chamber and the other to the exchanger and then to combustion chamber, in which part of the compressed air takes in the heat released from the gas turbine exhaust gas. The gas temperature can be regulated by controlling the ratio of the two flows. Partial gas to gas recuperation does not decrease the steam bottoming cycle efficiency, but can save the fuel consumption in Brayton cycle and increase the topping cycle efficiency.

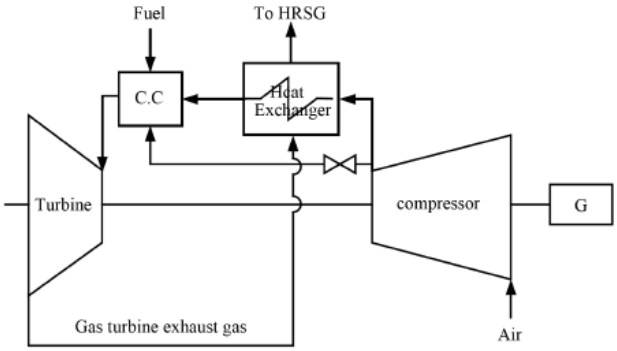

Figure 3.9: GTCC with partial gas to gas recuperation.

3.4 THE COGENERATION PLANTS

Cogeneration by definition, is the generation of electricity and useful heat from the same primary fuel source (figure 3.10). Cogeneration (Combined Heat and Power CHP) plants can typically capture 75% or more of the energy released by the primary fuel as against the 33% capture rate for conventional generation plants. With the deregulation and dismantling of state owned power monopolies and the increased global emphasis placed on efficient, sustainable and environmentally friendly energy development, cogeneration based power plants are increasingly sought after by power producers within appropriate constraints.

Although, cogeneration plants include different types of heat sources, the most common method used involves the exhaust gases from a gas turbine. Of course, a cogeneration plant would require higher thermal demand in comparison to the electrical demand. The thermal demand could be for heating water or producing steam for driving a steam turbine or for on plot / off plot process requirement.

A basic combined cycle cogeneration configuration consists of one or more gas turbines used in conjunction with a dedicated Heat Recovery Steam Generator (HRSG) connected in their exhaust path. The steam produced in the HRSG (at one or more pressure levels) is fed to a steam turbine driving an electric generator. The steam extraction from the steam turbine, after suitable conditioning is normally used to supply an external user.

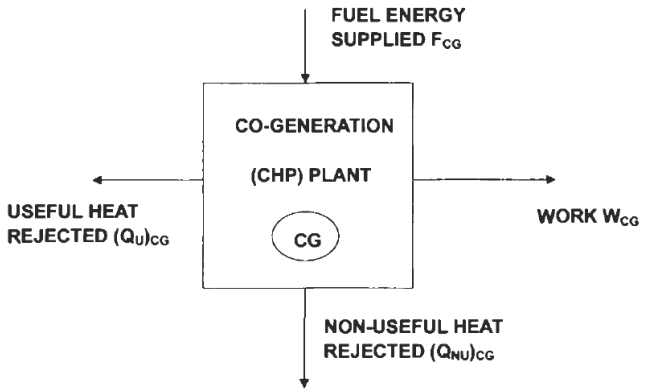

Figure 3.10: Cogeneration (CHP) plant.

Figure 3.11a illustrates a typical unfired combined cycle cogeneration system configuration. The system is shown with one gas turbine, one HRSG and one condensing type steam turbine configuration. Typically, in this configuration the steam turbine will be able to provide additional electrical power upto half the power output of the gas turbine.

The gas turbine and the steam turbine are shown in 'decoupled' (ie. not on the same shaft) condition. The process steam could be the extracted inter-stage output of the steam turbine or could also be taken from the main steam header after suitable steam conditioning for export or could be a mix of both. The NOx injection steam and/or the bypass damper are added, to respectively meet the emission requirements and stand alone gas turbine operations.

Figure 3.11b illustrates a typical supplementary fired combined cycle cogeneration system configuration. The supplementary firing could use the same fuel as the gas turbine or an off gas or a by-product from the external steam user as fuel. The supplementary firing can add a great deal of flexibility in the operation of the plant. Also, through supplementary firing, increase in steam production can be achieved with only a marginal increase in costs. In those cases, where the fuel for duct firing can be obtained from the external steam consumer (for eg, an oil refinery), pricing scheme based on net energy traded can be implemented.

There are many index that explain the primary energy saving using a CHP plant, the most used is the *fuel energy saving ratio* (FESR), defined as the ratio between the CHP plant primary energy saving instead of using two different plants, electric and thermal power plants, and the primary energy needed for the two processes separately:

$$\begin{aligned} FESR &= \frac{E_S - E_C}{E_S} = 1 - \frac{E_C}{E_S} \\ &= 1 - \frac{E_C}{E_{ES} + E_{TS}} = 1 - \frac{E_C}{\frac{E_E}{\eta_{ES}} + \frac{E_T}{\eta_{TS}}} \end{aligned} \tag{3.20}$$

where:

- $E_S = E_{ES} + E_{TS}$: primary energy from fossil fuel used to produce separately electric and thermal energy using two distinct plants;
- E_{ES}: primary energy from fossil fuel to produce only electric energy;
- E_{ES}: primary energy from fossil fuel to produce only heat using an industrial boiler;

- E_C: primary energy from fossil fuel referred to the fuel's lower heating value, consumed in the CHP plant to produce electric energy E_E and thermal energy E_T;
- E_E: net electric energy from a CHP plant;
- E_T: net thermal energy from a CHP plant;
- η_{ES}: net electric efficiency for an energy production plant ($= 0.38$ for standard plants, $= 0.5$ for advanced plants);
- η_{TS}: net thermal efficiency for a thermal generator plant ($= 0.9$, $= 0.8$ for teleheating plants).

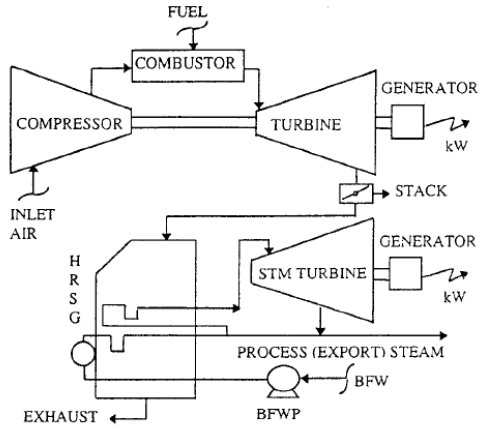

(a) *unfired combined cycle.*

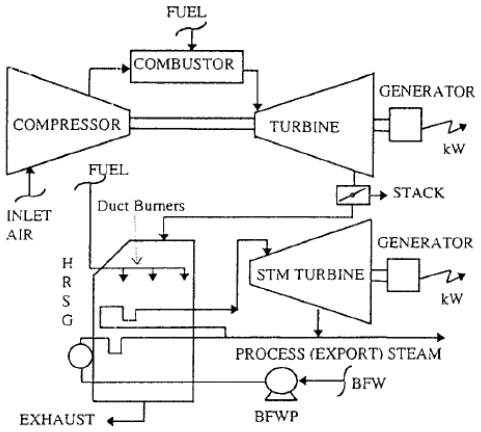

(b) *supplementary fired combined cycle.*

Figure 3.11: Typical cogeneration systems.

For completing evaluate the CHP plant benefits instead of using two different plants, we have to consider also another saving that CHP plants determine on transmission and distribution on the national electric system losses. It is generally used a coefficient p in the FESR expression, correlated to the electric efficiency ($p = 1 - 4.3/100$ for a low tension net or $p = 1 - 2.8/100$ for a medium tension net). Thus the FESR becomes

$$FESR = 1 - \frac{E_C}{\frac{E_E}{\eta_{ES} p} + \frac{E_T}{\eta_{TS}}} \tag{3.21}$$

Another criterion of performance sometimes used is an *'artificial' thermal efficiency* (Ecabert efficiency) for the electric production in a CHP plant, defined as the ratio between the produced energy and the primary energy used for the electric energy production, as the difference between the primary energy of the commercial fossil fuel used in the plant and the useful thermal energy production:

$$R_E = \frac{E_E}{E_C - \frac{E_T}{\eta_{TS}}} \tag{3.22}$$

4 SIMULATION MODELS

Contents

4.1 INTRODUCTION

In this section different kinds of gas turbine and combined cycles gas turbine models found in the literature have been proposed.

There are several different combined cycle configurations and control variations available from various manufacturers. These configurations may incorporate steam injection from the heat recovery system to control NOx emissions, Heat Recovery Steam Generator (HRSG) supplementary firing, multiple steam generation pressure levels, reheat or nonreheat steam cycles and integral HRSG deaerators.

In addition gas turbines may modulate gas flows to different degrees and control turbine firing or exhaust temperatures over given ranges of operation. Each of these options has a unique power response characteristic.

4.2 GAS TURBINE MODELS

The gas turbine modeled is assumed to only operate in a simple cycle with no heat recovery, however, this may not be always the case in CCPPs in order to exploit their high efficiency [3].

With CCPPs the airflow is controlled to maintain a high exhaust temperature, even when partly loaded. The airflow is adjusted via inlet guide vanes (IGV), which change geometry to adjust the airflow from the compressor.

4.2.1 Physical models

Physical models derive the model directly from dynamic physical thermodynamic properties and laws. They involve utilizing laws governing thermodynamic behaviour in the Brayton cycle [6], [7] along with some simplifying assumption to obtain the differential equations representing the dynamic gas turbine behaviour. These laws include conservation of mass, conservation of power and conservation of energy [8], [16]. Below is an example of the differential equations adopted from [1]. Equation 4.1 is the conservation balance of total mass while equation 4.2 refers to the conservation balance of internal energy in the gas turbine

$$\frac{dm}{dt} = \dot{m_{in}} - \dot{m_{out}} \tag{4.1}$$

$$\frac{dU^*}{dt} = \dot{m_{in}} i^*_{in} - \dot{m_{out}} i^*_{out} + Q + W \tag{4.2}$$

where m represents the mass, U represents the internal energy, i refers to the specific enthalpy, Q is the heat input and W is the work done. Over the years, many different types of gas turbine have been developed for different applications. For power generation, the gas turbines are essentially split into two distinct types, *heavy duty industrial gas turbine* (single shaft)[1] and the *aero-derivative type gas turbine* (twin/multiple shaft)[2] [7]. Other authors (especially those having a mechanical engineering background) [8] also utilize physical laws as well as thermodynamic laws in order to derive the equations representing gas turbine dynamics. They model different components of the gas turbine such as ducting, compressors, combustors and air blades.

1 The *single shaft gas turbine* has compressor, combustor and turbine connected on a single shaft, this makes the overall inertia of the gas turbine larger

2 the *aero derivative type gas turbine* has the gas generator and the power turbine mechanically separated. Different speed settings for the compressor and the power turbine allow to achieve higher efficiencies at part load.

4.2.2 Rowen's model

This model [31] entails a simplified mathematical model for heavy duty gas turbines. The following assumptions were made:

1. it is a heavy duty gas turbine operated in a simple cycle with no heat recovery;
2. fairly constant speed is maintained between 95% and 107% of the rated speed;
3. it operates at an ambient temperature of 15°C and at an ambient pressure of 101.325 kpa.

Since then, the model has been utilized to investigate the impacts of governor on system operation. It was derived from, and validated against the actual operation data and found to be adequate for a real life implementation. It is shown in figure 4.1 in a simplified block diagram format representing the single shaft gas turbine along with the control and fuel system. Control system of the gas turbine has three control loops, the speed control, temperature control and acceleration control. These three control functions are all inputs into a minimum value selector (represented by the low value select block). Output of the low value select represents the least fuel control actions among the three control actions. The speed control loop corresponds directly to the governor and can be operated either in the standard droop configuration or in isochronous mode. The temperature control loop represents the limitation of the gas turbine output due to temperature.

Exhaust temperature is measured using a series of thermocouples incorporating radiation shields as shown in the model.

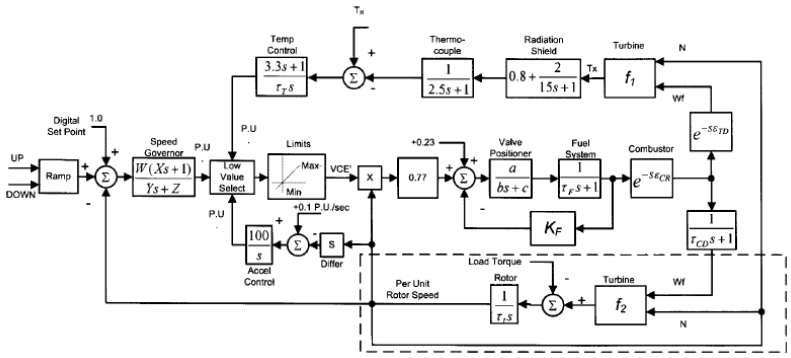

Figure 4.1: Rowen's model.

An acceleration control loop, in order to prevent the overspeeding of the generator in the event of a sudden loss of load, is also implemented in the model and represented by the third input into the low value select.

Dynamics of the turbine in the Rowen's model is essentially made of the function blocks f_1 and f_2, the delays associated with transport of the exhaust gas and the combustion process as well as the time lag block with a time constant of T_{CD}. Function block f_1 (a function of fuel flow and rotor speed) calculates the exhaust temperature of the turbine. Block f_2 calculates the turbine torque output of the gas turbine and again is a function of the fuel flow and rotor speed. The functions f_1 and f_2 are reproduced below

$$f_1 = TR - af_1(1 - wf_1) - bf_1(speed)$$

$$f_2 = af_2 + bf_2(wf_1) - cf_2(speed)$$

where af_1, af_2, bf_1, bf_2, cf_2 represent coefficients and constants in the equations while TR refers to the rated exhaust temperature, speed refers to the speed deviation of the rotor wf_1 refers to the fuel flow.

Rowen extended in [32] his original model, to include IGVs and their effect on the gas turbine dynamics, especially the exhaust temperature. Though the IGVs are included, the control loops for the speed and acceleration control remain essentially the same. The IGV controls can be seen in figure 4.2.

Function f_1, which calculates the exhaust temperature, is now augmented to include the impacts of the changing airflow as well as ambient temperature. A new function, f_3, is included in the model to calculate the exhaust flow calculation. Similarly to the first model, this new model has also been used to study the governor and the gas turbine operation. Since it enabled a more accurate modelling of a gas turbine operation installed as part of a CCPP, many researchers have utilized it for studies involving CCPPs [2], [38]. The augmented function, f_1'[3], incorporates the effect of the IGV, fuel flow, ambient temperature and rotor speed, where T_r refers to the rated exhaust temperature, T_a refers to the ambient temperature,W_f represents the fuel flow and N refers to the rotor speed. New function, f_3, calculates the flow of exhaust gases from the gas turbine:

$$f_3 = N\frac{519}{T_a + 460}(Ligv)^{0.257}$$

where T_a refers to the ambient temperature,$Ligv$ represents the output of the IGV and N refers to the rotor speed.

3 $f_1' = \frac{T_r - 815(N^2 - 4.21N + 4.42)0.82(1 - W_f) + 1300(1 - N) + 3.5(MaxIGV - IGV)}{1 + (1 + 0.0027(59 - T_a)}$

Further simplifications of the Rowen's model can be made in order to suit the different operating conditions of different gas turbines. According to [32], for a simple operation of the gas turbine without any heat recovery, the IGVs would only be in operation during the start up and the shut down of the gas turbine. However, the IGVs are also modulated at part load operation when the gas turbine is used as a part of a combined cycle plant. During normal operation of the gas turbine, the IGV would usually not be in operation, hence, the portion pertaining to the IGV (shown in figure 4.2, above the $\approx$ symbol) can be omitted. With the IGV section omitted, the model would be reduced to the original one shown in [31]. The acceleration control loop can also be omitted if frequency variations are not greater than 1% (as the machine is operating in a relatively 'stiff' system [31] where over speeding is unlikely to happen unless a load-loss situation arises) as well as the temperature control loop when the control of the gas turbine is dominated by the governor (diminishing the action of the temperature control signal). With only one signal remaining, the low value select can also be omitted. Finally, since the papers [31], [32] are based on specific models of GE gas turbines, namely the $5001 - 9001$ series, the various constants featuring in need to be derived separately for other types of turbines.

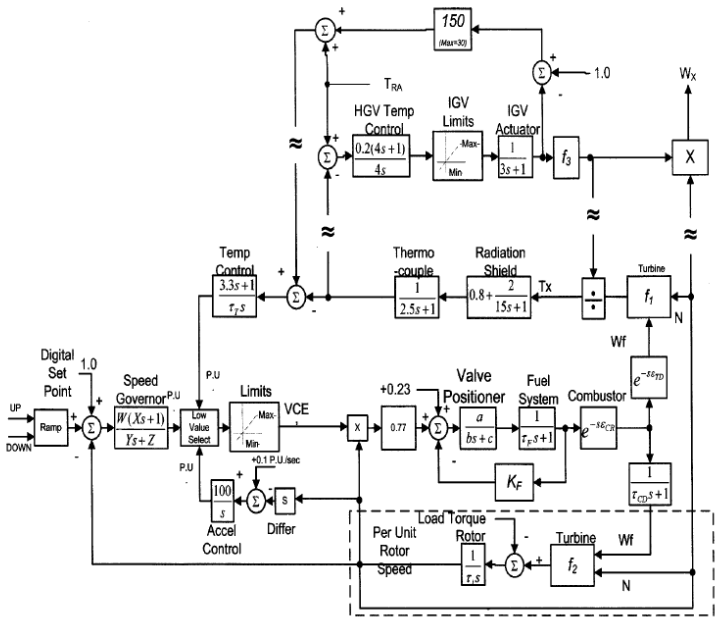

Figure 4.2: Rowen's model with IGVs.

4.2.3 IEEE model

The IEEE model is split into two parts, one pertaining to the controls of the gas turbine (the temperature control loop, the air flow control loop and the fuel flow control loop) and the other representing the thermodynamic properties of the turbine. The gas turbine model is applied to a constant speed simple cycle gas turbine with variable guide vanes in order to maintain a constant firing temperature for low greenhouse gases emission. Comparison of the IEEE model to that presented in Rowen's first paper [31] reveals that the main difference is the control action necessary to maintain a high firing temperature (turbine inlet temperature). A beneficial by product of the high firing temperature is low NOx gasses emission level. The IEEE model assumed a fixed compressor ratio, which is only valid for a relatively constant rotor speed. Figure 4.3 shows the corresponding control scheme of the gas turbine which is similar to that shown in the Rowen's model previously. However, as the modulating actions of the guide vanes are modeled [27] an additional air flow control loop is included. Additionally, the control block A, which essentially schedules the air flow, W, is a nonlinear function of equation 4.4 and equation 4.5. The calculation required by block A have to be solved via solvers such as the *Newton Raphson method* due to the nonlinear nature of equation 4.4 and equation 4.5.

Figure 4.4 below shows the block diagram representing the necessary calculations in order to derive the mechanical power output of the gas turbine. The connections in the block diagram

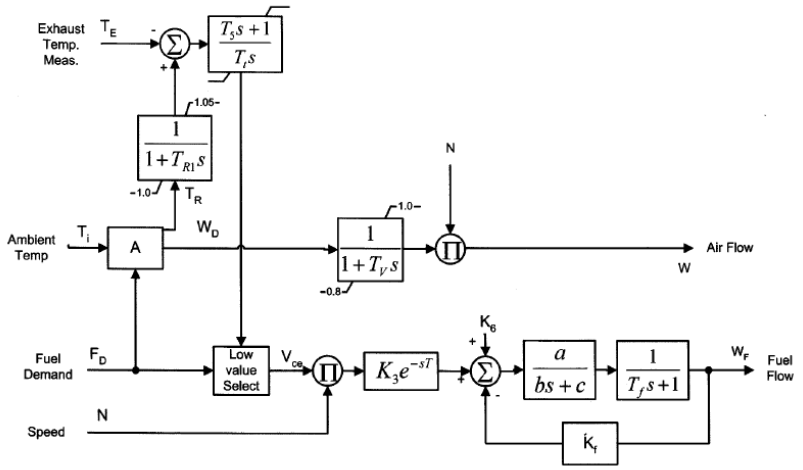

Figure 4.3: IEEE model controls.

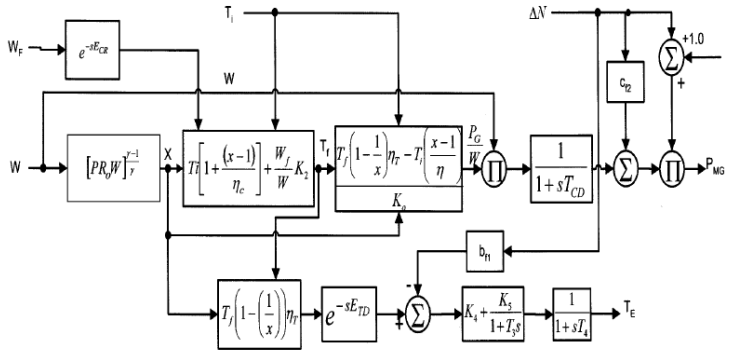

Figure 4.4: IEEE model thermodynamic equations.

are essentially based on the isentropic efficiencies equations [7] for the compressor and the power balance equation. The E_{cr} and E_{td} parameters (in figure 4.4) refer to the time constants related to the time delays. The following equations are stated below for the completeness of the discussion:

$$T_R = T_f[1 - (1 - \frac{1}{x})\eta_T] \tag{4.3}$$

$$x = [PR_0 W]^{\frac{\gamma-1}{\gamma}} \tag{4.4}$$

$$W = \frac{P_G K_0}{T_F(1 - \frac{1}{x})\eta_T - T_i \frac{(x-1)}{\eta_C}} \tag{4.5}$$

$$T_f = T_D + \frac{W_f K_2}{W} = T_i[1 + \frac{(x-1)}{\eta_C}] + \frac{W_f}{W} K_2 \tag{4.6}$$

where T_R is the reference exhaust temperature in per unit of the absolute firing temperature at rated conditions, T_f the turbine inlet temperature in pu of design absolute firing temperature, x the cycle isentropic pressure ratio parameter, η_T the turbine efficiency, PR_0 the design cycle pressure ratio (P_{in}/P_0), γ is the ratio of specific heats (c_p/c_v), W is the air flow in pu of design air flow (W_0), P_G is the power output in pu of rated, $K_0 = (kW_0 3413)/(W_0 T_{f0} c_p)$ where kW_0, W_0, T_{f0}, c_p are the base net output (kW), air flow (lbs/sec), turbine inlet temperature (°R), average specific heat (BTU/lb x °F), W_{f0} is the design fuel flow in per unit of design air flow, T_i is the compressor inlet temperature in pu of design absolute firing temperature, η_C is the compressor efficiency, T_D is the compressor discharge temperature in per unit of design absolute firing temperature, W_f is the fuel flow in per unit of design air flow (W_0), $K_2 = \Delta T_0/T_{f0}$ is the design combustor temperature rise in pu of absolute firing temperature.

Based on the isentropic efficiencies of the compressor and the turbines, equation 4.3 and equation 4.6 can be derived accordingly. The ideal adiabatic process is isentropic, however, in reality this is not exactly the case. This results in inefficiencies in the adiabatic processes, i.e., turbine and compressor isentropic efficiencies (η_T and η_C) respectively. A brief derivation based on the compressor efficiency is shown below while more details can be found in [6], [7]. Bearing in mind that the temperature change for the ideal compressor cycle is $T_{02} - T_{01}$ (Temperature of cycle $1-2$ in figure 2.6), the real temperature change would be $T'_{02} - T_{01}$. Compressor isentropic efficiency is defined as

$$\eta_C = \frac{C_p \Delta T'_0}{C_p \Delta T_0} = \frac{T'_{02} - T_{01}}{T_{02} - T_{01}} \tag{4.7}$$

where C_p refers to the mean heat capacity of the gas and T'_0 refers to the change in temperature in reality while T_0 refers to the temperature change in the ideal process. Pressure ratio of the cycle is linked to temperature [6], therefore equation 4.7 can be further developed into

$$T_{02} - T_{01} = \frac{1}{\eta_C}(T'_{02} - T_{01}) = \frac{T_{01}}{\eta_C}(\frac{T'_{02}}{T_{01}} - 1)$$

Neglecting the pressure loss in the combustor, P_{02} is equal to P_{03}. Therefore the ratio of P_{02}/P_{01} is equivalent to the cycle pressure ratio, x, turbine inlet pressure divided by ambient pressure. Hence T_{02}, which is T_D (compressor discharge temperature), can be calculated by equation 4.8. Considering that T_{01} as the ambient temperature equation 4.8 can be seen to be equivalent to the T_D section in equation 4.6.

$$T_{02} - T_{01} = \frac{T_{01}}{\eta_C}((\frac{P_{02}}{P_{02}})^{\frac{\gamma-1}{\gamma}} - 1)$$

$$T_{02} = T_{01} + \frac{T_{01}}{\eta_C}(x - 1) \tag{4.8}$$

Using turbine isentropic efficiency instead, equation 4.3 can be similarly worked out as shown above. A detailed derivation of both equations is shown in [7]. It should be noted that the temperatures in the IEEE model are worked out in absolute temperature, K. The IEEE model has also been further developed in [35] to take into account effects such as the use of a part of the overall air flow in order to cool the turbine blades. The enhanced model [35] was found to be able to simulate the dynamic behaviour of the gas turbine with the required accuracy.

4.2.4 Aero-Derivative model

The previous models focused on heavy duty or single shaft gas turbines. As there are many aero derivative gas turbines, a model for an aero-derivative gas turbine was also developed. These gas turbines are essentially derived from jet engines and often utilized to exploit their better efficiencies at part load operation compared to the heavy duty gas turbine. In this case the compressor is connected on a different shaft as compared to the power turbine, it is able to rotate at different speeds and achieve better compressor ratio and hence better overall performance. Figure 4.5 shows the overall block diagram for the twin shaft gas turbine adopted from [13]. The gas turbine is split into the engine, connected to the compressor, and the turbine, connected the the generator shaft. The block diagram is similar to the Rowen's model. However, instead of a single speed signal going into the low value selector, there are now two speed signals, one is the speed of the engine (which determines the speed of the compressor) and the other is the speed of the turbine (which corresponds to the speed of the turbine or the generator). Also the turbine characteristics indicated by functions $f_1 - f_4$ in the twin shaft model (figure 4.5), can be obtained from the operation characteristics of the turbine itself. These functions are derived based on the operating curves such as the electrical power versus fuel flow, or the exhaust temperature versus fuel flow. The ultimate model parameters are then obtained through a trial and error process in order to fine tune the parameters till the responses are matched to the actual gas turbine response.

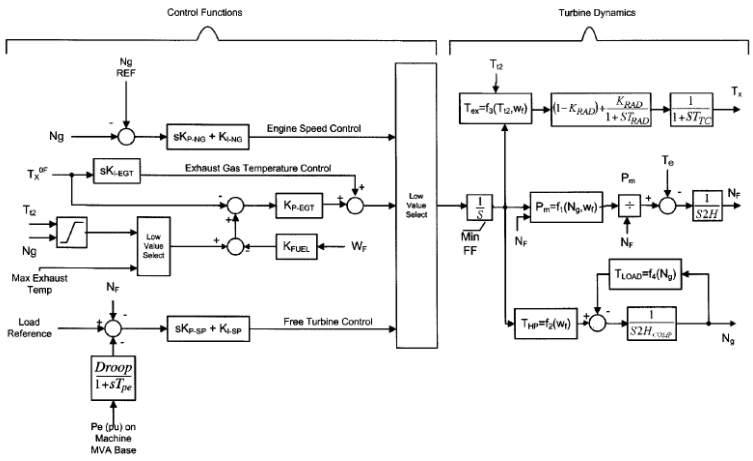

Figure 4.5: Twin shaft turbine.

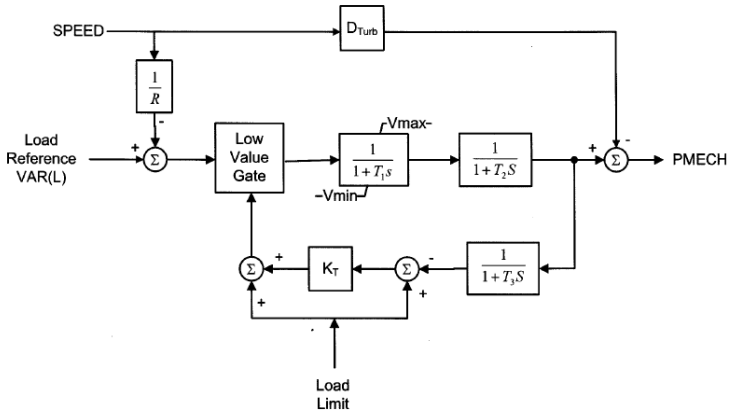

Figure 4.6: GAST Model.

4.2.5 GAST Model

Figure 4.6 shows the GAST model which was one of the most commonly used dynamic models for the governor [24]. This was partly due to the simplicity of the model and partly due to the fact that it was once WECC compliant. Even though it was one of the most widely used models it has now been found to be deficient in certain areas [24]. It is unable to model the gas turbine operation accurately when the temperature control loop becomes active, and to replicate system oscillations around the final settling frequency. The GAST Model is no longer WECC compliant and it has been superseded by other, more accurate models such as the GGOV1 model discussed below.

4.2.6 WECC/GGOV1 model

Over the years, numerous trips of large generating plants in the *Western Electricity Coordinating Council* (WECC) have been observed. This has been attributed to the inaccurate modelling of many of the thermal unit governors in the WECC. Since early 2001, WECC has proposed new criteria for *Frequency Responsive Reserves* (FRR) making the need to develop a more accurate governor model for dynamic simulations imperative [29]. A model shown in Figure 4.7 was developed using measured responses and data collected from two trip tests performed on the 18th May 2001. The tests had revealed that only 40% of the expected governors responded (based on the simulations). The principal reason for the large discrepancy between the expected and measured governor responses is that base loaded and load limited turbine

units were not modeled properly. These units were found to be predominantly thermal units including gas turbines. Using a block diagram format, thermal units were modeled with separate elements such as the governor element, supervising element and the load management element. It should be noted that the GGOV1 model is a general model for all thermal units and the developed model can be utilized for representing gas turbines with suitable parameters in the various control blocks. Governor element essentially pertains to the basic governor and is a typical PID configuration. The droop can be implemented via a feedback signal of valve position or electrical power. The supervising element represents a load limit imposed by the operation of the power plant and in case of a gas turbine. The supervising limit represents the exhaust temperature limit. L_{dref} in the model represent this load limit and is given in terms of turbine power instead of exhaust temperature directly. This limit is imposed in the gas turbine model with a curve that relates exhaust temperature to several other engine variables [29]. The load management element will regulate the turbine power to the setpoint P_{mwset}, simulating effectively the adjustments necessary due to the AGC commands. Turbine dynamics is essentially considered to be in direct proportion with fuel flow (the relevant time constants are longer compared to the turbine time constants) and hence can be simply represented by a single lead-lag block. Many of the GAST models previously used in the system were replaced by the developed GGOV1 model.

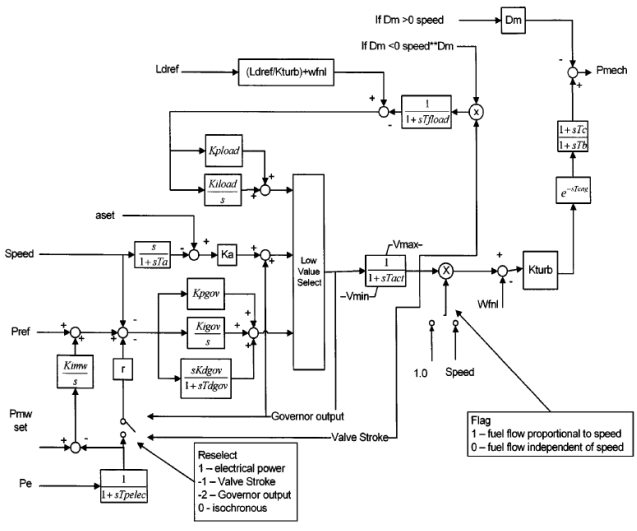

Figure 4.7: GGOV1 Model.

4.2.7 CIGRE model

Recognizing the increasing importance of the gas turbines, a CIGRE Task Force for gas and steam turbines in combine-cycle power plants, has developed a model of combined cycle power plant as shown in figure 4.8 [3]. Similar to the Rowen's model, there are three major control loops feeding into a low value select. These control loops represent the speed/load governor, the acceleration control loop and the temperature control loop. However there are certain differences in the control representation. There is an additional outer loop plant control represented by the MW set to maintain the unit's output at a prespecified MW level. The minimum fuel flow in this model is represented by the limit V_{min}. Turbine dynamics is modeled by the second-order block instead of calculating the torque function as in Rowen's model. The exhaust temperature is not explicitly calculated, instead, the temperature control is provided via a signal calculated via a function $F(x)$ as shown in the figure 4.8. This function is obtained from curves which relate exhaust temperature to turbine variables such as rotor speed. By choosing appropriate values for different control parameter constants, any desired mode of governor action can be simulated. A set of example parameters for the gas turbine model can be found in [3]. The CIGRE model is similar to the GGOV1 model, however, it specifically models a gas turbine instead of a generic thermal unit (hence the explicit modelling of the temperature limit).

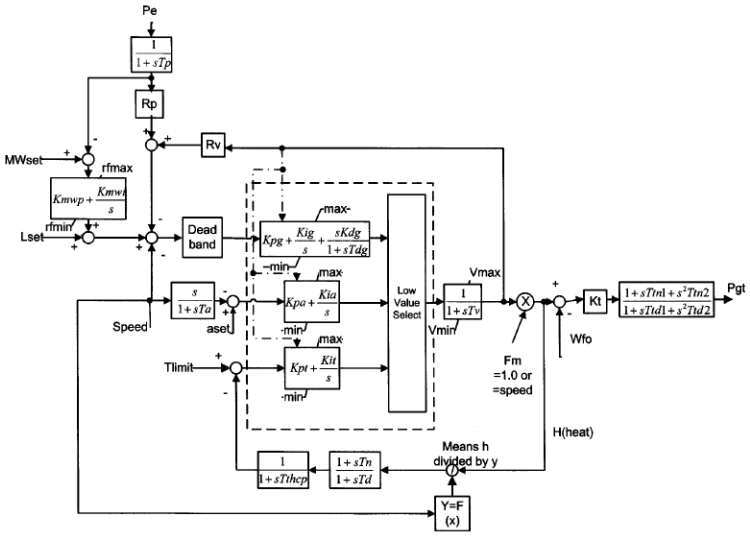

Figure 4.8: CIGRE Model.

4.2.8 Frequency dependent model

Many of the models mentioned before are not suitable for determining the frequency dependency of the gas turbine. To be able to analyse incidents with abnormal system frequency behaviour, the frequency dependence of the gas turbine model must be taken into account. This was the main aim of [18] and a model which is based on the physical principles is developed in order to clarify the effects that shaft speed and ambient temperature has on shaft speed. A brief explanation of the various effects that frequency and ambient condition have on power output is shown in [30].

Changes in frequency are equivalent to changes in shaft speed and would result in a change in airflow. This change then translates firstly into a change in the pressure ratio across the compressor and secondly into a change in fuel level (in order to maintain the given firing temperature).

These changes will directly affect the maximum power output [30]. A similar relation is reported between the ambient temperature and the maximum power output, however changes in ambient temperature have a much more severe impact compared to changes in rotor speed. The paper [30] also discusses the characteristics of the axial compressor and the physical principles of the gas turbine.

The overall block diagram of the frequency dependent model is shown in figure 4.9a. Again, the control scheme is similar to that found in the previous models, such as the Rowen's model.

Figure 4.9b shows the thermodynamic equations representing the dynamic behaviour of the gas turbine. Unlike the Rowen's model, where only the output power and the exhaust temperature were necessary, this model calculates the compressor pressure ratio and the exhaust gas flow in addition to exhaust temperature and mechanical power output. Equations representing the impact of IGVs have also been incorporated into the model. The various parameters of the model (e.g., A_0, A_1 and A_2, etc.) are obtained directly from the test data of actual machines. Based on this model, a CCPP model for investigating frequency excursions was developed and tested in [19], it is shown in detail in section 4.3.2. Malaysia black out was quoted in the paper as an example of the abnormal frequency event, as well as the formation of electrical power islands with a power imbalance. This study found that the dependency of the output of the gas turbine on frequency and ambient temperature is significant and that both, the temperature control and the governor play critical role during such abnormal frequency operations.

Interestingly enough, the frequency dependent model is based on similar equations to those used in the IEEE models. However, instead of a fixed compressor ratio with small deviations, the frequency dependent model assumed a generic form representing the dependence of the pressure ratio on frequency deviations as well as ambient temperature.

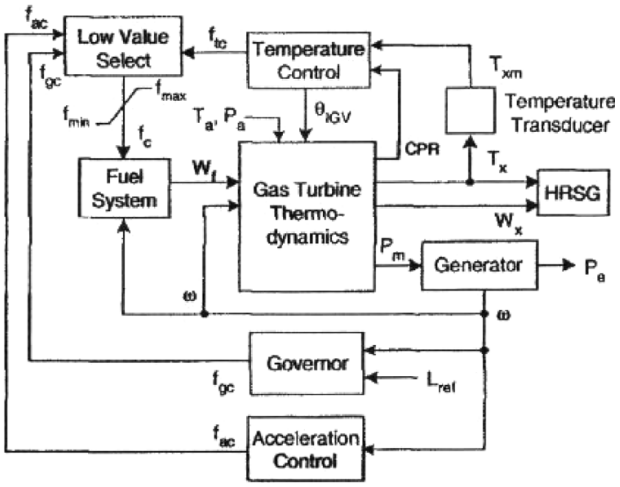

(a) *Frequency dependent gas turbine model.*

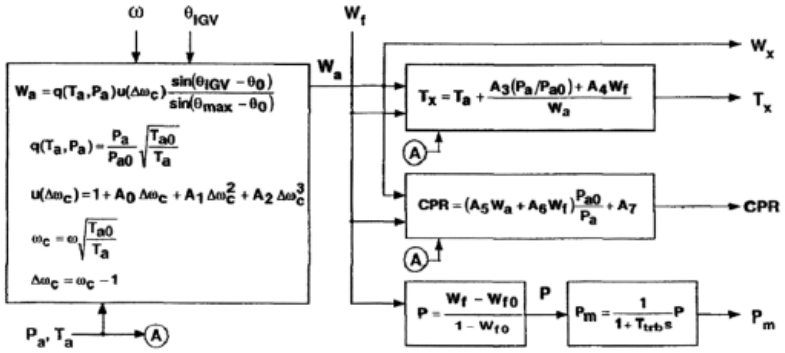

(b) *TD equations for frequency dependent GT.*

Figure 4.9: Frequency dependent gas turbine.

4.3 COMBINED CYCLE MODELS

4.3.1 Prime Mover - 1995

This model [27] is referred to a typical combined cycle plant configuration, shown in figure 4.10. This arrangement consists of an unfired three pressure level with a single shaft gas turbine, HRSG and single steam turbine operating at steam conditions of 1250 psi/950°F and 450 psi/475°F. The low pressure drum provides steam for feedwater deaeration. The steam turbine has no uncontrolled extraction and all feedwater deaeration is accomplished with low temperature gas turbine exhaust heat in an integral HRSG deaerator. 1250 psi high pressure throttle steam and the 450 psi admission steam expand to a condenser pressure of 2" Hg. The steam turbine operates under sliding pressure with initial pressure regulation at low load conditions.

In multiple gas turbine unit combined cycle configurations, the steam flows are generally combined as shown in figure 4.10 for admission to a single steam turbine. The gas turbine units modulate in parallel to provide good partial load performance which also results in uniform steam mixing conditions. The gas turbines are provided with variable compressor inlet guide vanes to maintain good steam conditions over partial load ranges. These guide vanes reduce gas turbine compressor air flow thus decreasing stack loss and maintaining high gas turbine exhaust temperature at reduced gas turbine loads.

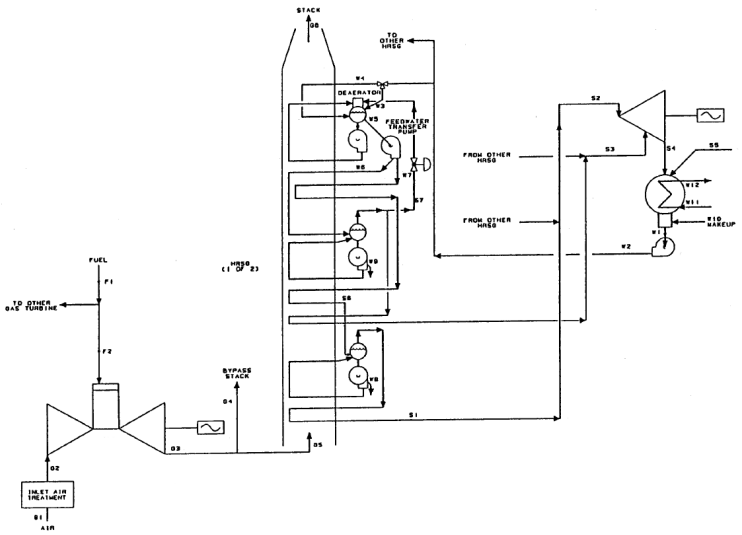

Figure 4.10: Two pressure HRSG.

The range of guide vane operation and control strategy may vary somewhat among turbine manufacturers, however, the basic objective is to maintain high steam temperature operation at lower loads.

Figure 4.11a shows the chain of submodels of the combined cycle described above, identifying the input and output variables of each submodel and the coupling between the blocks. From left to right these blocks are: the speedload control, the fuel and air flow controls, the gas turbine and the heat recovery boiler with steam turbine.

Figure 4.11b shows the speed governor. The inputs to the speed governor are the load demand V_L and the speed deviation ΔN. The output is a fuel demand signal, F_D.

The gas turbine model is the one shown in section 4.2.3. The control scheme for fuel and air flow rates is the one shown in figure 4.3. Inlet guide vanes are modulated to vary air flow over a limited range. This allows maintaining high turbine exhaust temperatures and thus, steam cycle efficiency at reduced loads.

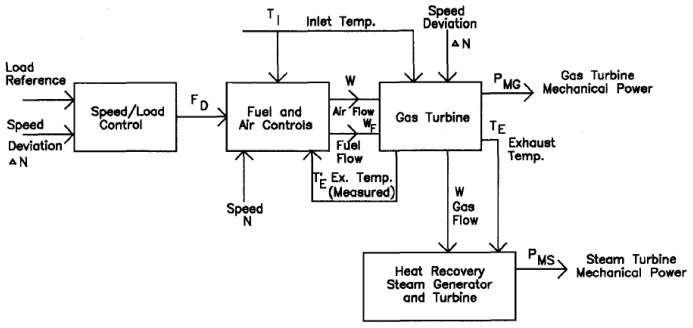

(a) *Combined cycle model.*

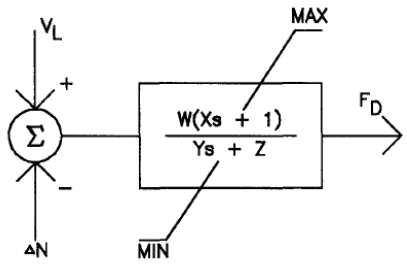

(b) *Speed load controls.*

Figure 4.11: Combined cycle model.

Over this load range, the fuel and guide vanes are controlled to maintain constant gas turbine inlet temperature.

This is functionally accomplished by scheduling air flow with load demand F_D and setting the turbine exhaust temperature reference, T_R (equation 4.3), to that value which is calculated to result in the desired load with the scheduled air flow at constant turbine inlet temperature.

The per unit air flow required to produce a specified power generation at the given gas turbine inlet temperature T_f is given by the turbine power balance (equation 4.5).

Combustor pressure drop, specific heat changes and detailed treatment of cooling flows has been deleted for purposes of illustration of the general unit behaviour. These performance effects have been incorporated into equivalent compressor and turbine efficiency values. Also for practical purposes the steady state gas flow through the turbine is considered the same as air flow through the compressor (W).

Equations 4.5 and 4.4 determine the air flow W and pressure ratio parameter, x, for a given power generation, P_G, at a specified per unit ambient temperature, T_i. The reference exhaust temperature, T_R is then given by equation 4.3, with $T_f = 1.0$. The air flow must of course be subject to the control range limits.

Block A in figure 4.3 contains the calculation of desired air flow W_D and desired exhaust temperature reference T_R, over the design range of air flow variation through vane control. These desired values of W_D and T_R are functions of F_D (desired turbine output from speedhoad controls) and ambient temperature T_i and are determined by the solution of equations 4.5 and 4.4 with appropriate limits on W_D and T_R.

The response of the vane control is modeled with a time constant T_V with non windup limits corresponding to the i vane control range. The actual ar flow W is shown as product of vane opening and shaft speed. The exhaust temperature reference T_R is fed through a time lag and appropriate limits to the exhaust temperature controls.

The measured exhaust temperature T'_E is compared with the limit value T_R and the error acts on the temperature controller. Normally T'_E is less than T_R causing the temperature controller to be at the MAX limit (about 1.1 pu). Should T'_E exceed T_R, the controller will come off limit and integrate down to the point where its output takes over as the demand signal for fuel, V_{ce}, through the "low select" block. The fuel valve positioner and fuel flow control yield the fuel flow signal W_F as another input to the gas turbine model.

Figure 4.4 shows the relationships used to develop gas turbine mechanical power P_{MG} and exhaust temperature T_E.

The gas turbine net output (turbine power less compressor power) is determined from equation 4.5 where T_f is the calculated turbine inlet temperature, and the air flow W is specified by the inlet guide vane schedule and compressor speed. The turbine inlet temperature T_f is determined from the combustor heat balance (equation 4.6).

The gas turbine exhaust temperature T_E is now given by equations 4.3 and 4.4 using the turbine inlet temperature, equation 4.6.

Mechanical power P_{MG} is shown to be a function of T_f and flow rate of combustion products (W). Since in many applications speed deviations can be significant, the speed effects are also included.

The blocks involving dynamics include the combustor time delay E_{CR}, the compressor discharge volume time constant T_{CD} and the turbine and exhaust system transport delay E_{TD}. The location of the time constants and time delays in the block diagram of figure 4.4 does not necessarily follow their relation to the process physics. For instance the compressor volume time constant T_{CD} is located downstream of the turbine power block P_G/W. This does not alter the effect of this time constant on the variable of interest which is P_{MG}.

It should be noted that the effect of this time constant on the output of the HRSG is negligible compared to the storage lags in the steam generator.

The radiation shield and thermocouple lags are used to develop the measured exhaust temperature T'_E from the actual exhaust temperature T_E.

The HRSG steam system reacts to the changes in gas turbine exhaust flow W, and exhaust temperature, T_E. The transient gas heat flux to the high and low pressure steam generation sections may be closely approximated by using the relations for constant gas side effectiveness.

The exhaust gas and steam absorption temperatures through the HRSG shown in figure 4.10, are indicated in figure 4.12.

$$\eta_{g1} = \frac{T_{ex} - T'}{T_{ex} - T_{m1}} \qquad \eta_{g2} = \frac{T' - T''}{T' - T_{m2}}$$

where T' and T'' are the gas pinch point temperatures shown in figure 4.12 and, T_{m1}, T_{m2} are the average metal temperatures in the HP and LP evaporation sections, respectively.

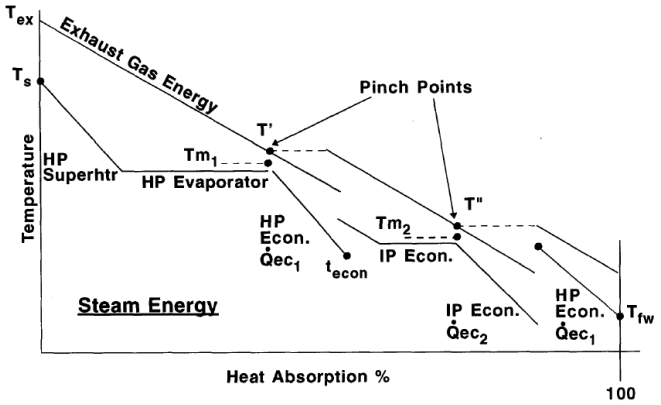

Figure 4.12: Exhaust gas vs steam absorption temp.

The gas heat absorption by the respective HRSG section is then given by:

$$Q_{g1} = W\eta_{g1}(T_{ex} - T_{m1}) + (Q_{ec1} + Q'_{ec1})$$
$$Q_{g2} = W\eta_{g1}(T' - T_{m2}) + (Q_{ec2} + Q_{ec1})$$

where $Q_{ec1,2}$ are the HP and IP economizer heat fluxes. The respective economizer heat absorption is approximated by using the generic constant effectiveness expression.

$$Q_{ec} = n_{ec}(T_g - T_i)m$$

where

Q_{ec}: the heat flux absorbed by the heating section,

T_g: hot side gas temperature,

T_i: cold side water temperature,

m: flow rate water.

The relations above are listed to illustrate the physics of the process involved in the block "Gas Path Relations" of figure 4.13. This level of modelling detail is not justified except where studies of plant controls are the principal objective. Figure 4.13 develops a lumped parameter simplified structure of the HRSG and steam turbine model following the approach described in [9].

Given the heat fluxes absorbed by the high pressure and intermediate pressure steam generators, Q_{G1} and Q_{G2}, steam pressure in each drum P_{DH} and P_{DI} is developed by integrating the difference between steam generation and steam flow out of each section. Steam generation follows, heat flux (Q_{g1}, Q_{g2}) with

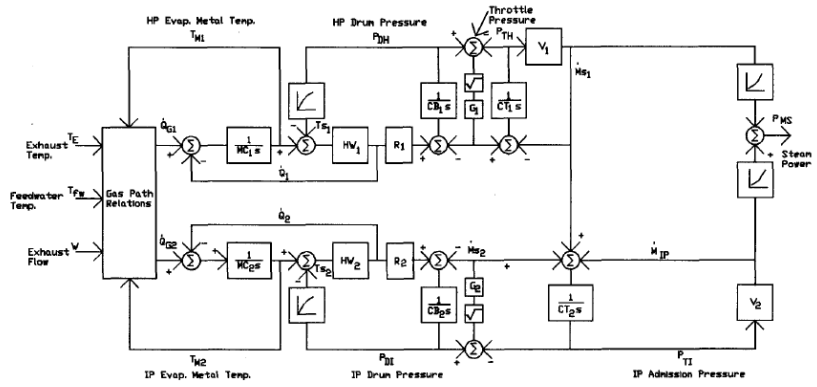

Figure 4.13: Steam system model.

a short lag due to metal heat capacitance (MC_1, MC_2) and heat transfer film coefficient (HW_1, HW_2). The heat fluxes from metal to the steaming mixture are proportional to the temperature differences between metal and steaming mixture ($T_{M1} - T_{S1}$) for the high pressure boiler and ($T_{M2} - T_{S2}$) for the intermediate pressure boiler. The saturation temperature T_{S1} and T_{S2} are functions of drum pressures (P_{DH}, P_{DI}) for the high pressure and intermediate pressure boilers respectively. Steam generations are proportional to the heat fluxes through the constant R_1 and R_2. The boiler and steam leads inner volume is split in two lumped volumes whose storage constants are shown as C_{B1} and C_{T1} for the high pressure boiler and C_{B2} and C_{T2} for the low pressure boiler. The changes in gas heat flux are established by the gas temperature profile which tends to peg about the pinch points as shown by the dotted gas characteristics shown in figure 4.12. This is the point of closest approach of the gas to the evaporator metal temperature. The IP sections therefore experience higher temperature difference as exhaust temperature decreases. The deaerator is assumed pegged at constant pressure.

The steam flow rates between the two volumes in each boiler is determined from the pressure drop relationship with flow rate being proportional to square root of pressure drop (proportionality constants G_1 and G_2).The flow rate to the high pressure turbine is proportional to the valve coefficient V_1 and throttle pressure. The turbine pressure at the point of the low pressure steam admission is shown to be proportional to turbine flow coefficient V_2 and total steam flow $m_{S1} = m_{S2}$ with a small time constant C_{T2} to account for steam volume effects. The steam turbine mechanical power is a function of the steam flow rates m_{S1} and m_{S2}.

4.3.2 Kunitomi, Kurita - 2003

This model [19] is not intended for simulation if startup or shoutdown of CCPP, it is generally applicable for initial CCPP loading above 50%.

The gas turbine consist of an axial compressor, a combustion chamber and a turbine (figure 4.14). The air is compressed and then mixed with fuel in the combustion chamber. The hot gas resulting from the combustion process is expanded through the turbine to drive a generator and the compressor. Pertinent input variables of the gas turbine are fuel mass flow (W_f) and air mass flow (W_a) which depend on IGV angle (θ_{IGV}), shaft speed (ω), ambient temperature (T_a), and atmospheric pressure (P_a). Pertinent output variables are net mechanical power output (P_{mGT}), exhaust gas mass flow (W_x), exhaust gas temperature (T_x), and compressor pressure ratio (CPR). The gas turbine model is the one described in section 4.2.8 based on [18]. The airflow speed factor characterizes the frequency dependency of the GT output. The physically based structure of the model reveals the possibility of determining the parameters of the air flow speed factor form the loading test made at different ambient temperatures. The GT model is base on the following assumptions:

- W_f solely determines P_{mGT},
- $W_x = W_a$ since W_f is negligibly small compared to W_a,
- the shaft power required to drive the compressor is constant,
- the only significant dynamic effects are the time lags between changes in fuel command and changes in W_f and between changes in W_f and changes in P_{mGT}.

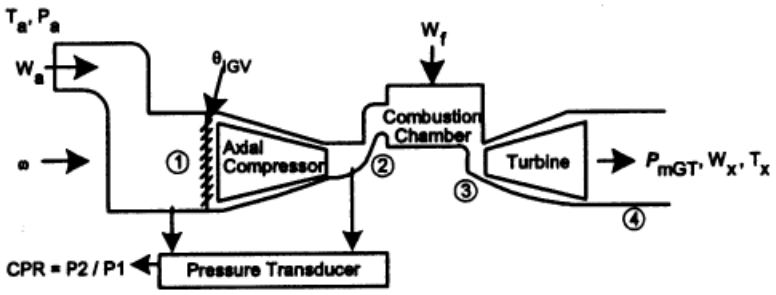

Figure 4.14: Gas turbine configuration.

HRSG and steam turbine performances of the detailed design model of an example plant led to the following observations and simplifying assumptions:

- The feed water energy gains in the economizers and in the evaporators are additive and there is no need to model the economizers separately. The feed water adjustment is fast, and there is no need to model the feed water system or drum level controls,
- The temperature and flow variations in the condenser have insignificant effects and there is no need to model the attemperators (ATT) or the bypass flows. The water flows to the attemperators in the HP and reheat lines have insignificant effects and they can be assumed constant without substantial loss of accuracy,
- The enthalpy of the steam at the each turbine inlet is constant since the steam temperature is held constant.

Figure 4.15 show pertinent components of the HP, IP, and LP sections, respectively. The pertinent variables are steam pressures and flows, valve positions of MCV, IPAV, ICV, LPAV, and bypass valves. Figure 4.16 show models of the HP, IP, and LP sections, respectively. The controls are site specific, and the structure and parameters of the control models need to be adjusted for each site. Figure 4.17 define the model structure of a CCPP example. The input variables to the plant model are the ambient air temperature (T_a) and pressure (P_a), electrical power output of the generator (P_e), and load reference (L_{ref}). The pertinent controls are:

- *GT controls*: as identified previously [18], including temperature control, IGV control, governor, and acceleration control. The acceleration control limits the acceleration rate of the turbine by limiting the fuel flow. Its primary function is to limit turbine acceleration during plant start-up. It may become active during a partial load rejection. The acceleration control signal (X_{AC}) is transferred to the ST valve controls.
- *ST controls*: including inlet pressure controls, inlet pressure limiters, and bypass valve controls for MCV, IPAV, and LPAV, which regulate, limit, and relieve the steam pressure at the valve inlet points. Also included is the ST speed control, which operates upon an excessive overspeed of the turbine.

- *PLU control*: which affects both GT and ST. The PLU control issues two signals, the PLU signal and Load Rejection Occurrence (LRO) signal, if the difference between the mechanical power to the generator and the electrical power exceeds a specified value (e.g. 0.4 p.u.) and if the electrical power decreases faster than a specified rate (e.g. 0.35 p.u./s). With a PLU signal, the ICV and LPAV close completely. With a LRO signal, the MCV and IPAV close is set for a no-load, full-speed value completely, and of 100.3%. Once the unbalance is removed, the PLU signal is automatically reset but not the LRO signal.

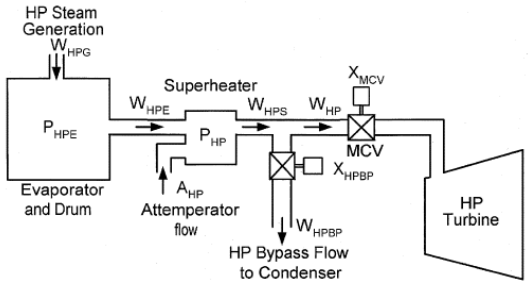

(a) *HP section configuration.*

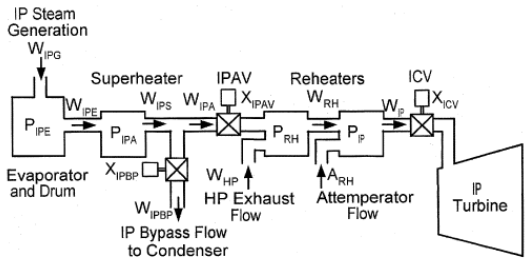

(b) *IP section configuration.*

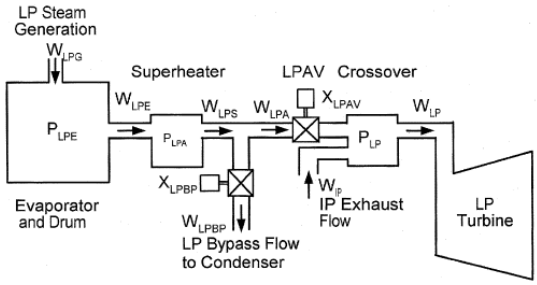

(c) *LP section configuration.*

Figure 4.15: HRSG configuration.

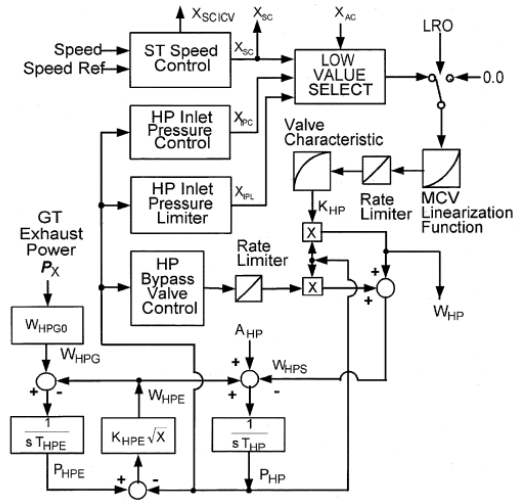

(a) *HP section model.*

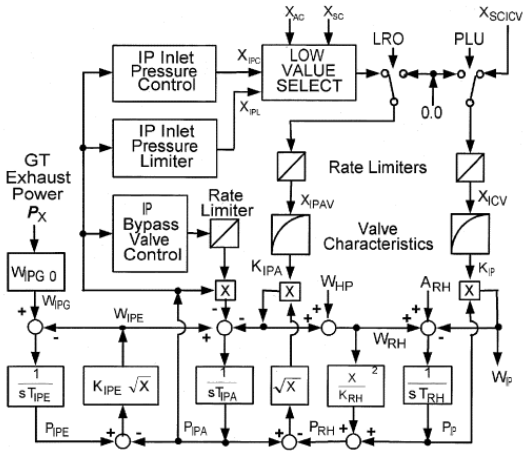

(b) *IP section model.*

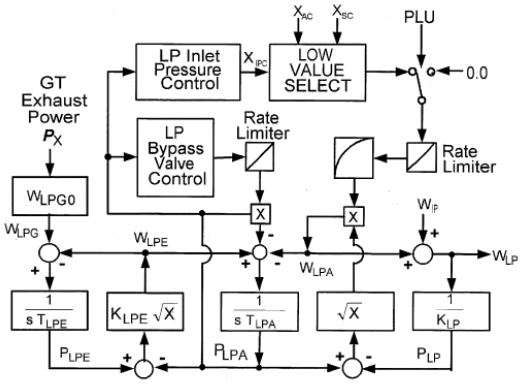

(c) *LP section model.*

Figure 4.16: HRSG model.

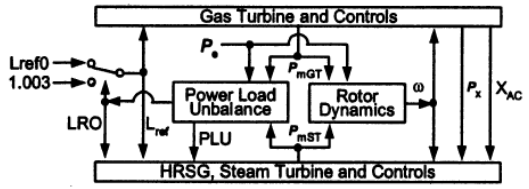

(a) *Plant model structure.*

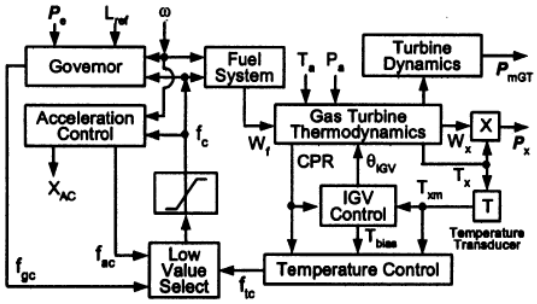

(b) *Model structure for GT and controls.*

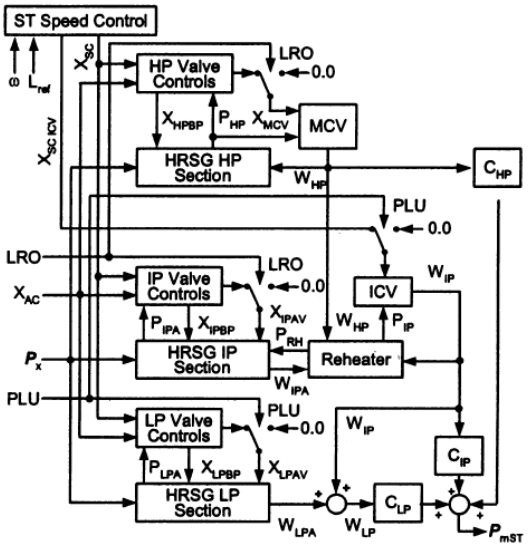

(c) *Model structure of HRSG, ST and controls.*

Figure 4.17: Model structure.

4.3.3 Lalor, Ritchie - 2005

Further implementations in CCPP control systems has been made in [20].

Assumptions made in this study include the following:

- fuel flow is negligible with respect to airflow, so that the volume of exhaust gases may be assumed equal to the volume of air flowing through the compressor, and the pressure ratios are the same across both the compressor and the gas turbine (i.e., no air is extracted for cooling);
- The timescale of interest is up to 20 s following a system disturbance, so that the response of the steam turbine can be considered negligible;
- Acceleration control generally only comes into play during unit start up and shut down;
- As steady-state conditions are initially assumed, the acceleration control loop can be neglected.

The gas turbine model used in this study has been adapted from that developed by Rowen [31], [32], by making reference to more recent CCGT models [3], [2], [27]. An outline of the structure is shown in figure 4.18, the relevant equations are:

$$\begin{aligned} F1 : T_x = [T_r - 453((aN + b)^2 + 4.12)((aN + b) + \\ + 4.42)0.82(1 - W_f)] + 722(1 - (aN + \\ + b)) + 1.94(Maxigv - igv) \end{aligned}$$

$$F2 : Torque = 1.3(W_f - 0.23) + 0.5(1 - N)$$

$$F3 : W_x = N(L_{igv})^{0.257}$$

where T_x is the exhaust gas temperature, T_r is the rated turbine exhaust temperature, a is the scaling factor for frequency sensitivity of GT exhaust temperature calculation, b is a constant, N is the speed pu, W_f is the fuel flow pu and L_{igv} is the inlet guide vane position pu.

The required inputs to the model are the steady-state set point of the unit and the ambient temperature and pressure.

The effect of ambient temperature on the rating of the gas turbine is incorporated as a correction factor, developed from historical data, which is applied to the unit set-point input. This differs from previous models, where ambient temperature was either neglected or incorporated inside the model structure, for example, within the exhaust temperature calculations [31], [32].

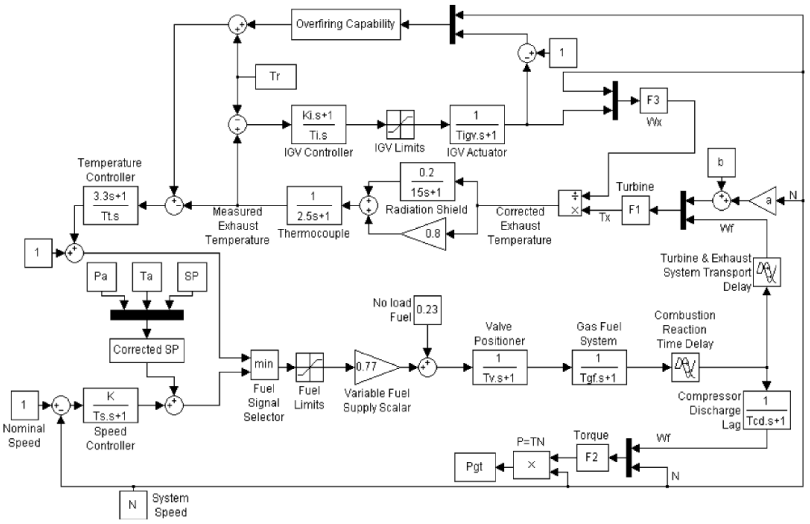

Figure 4.18: Gas turbine model.

The effect of ambient pressure on the gas turbine output, which is not addressed in some models, was also incorporated in a similar way.

All parameters are given in per unit, with the exception of temperature and pressure, which are measured in °C and mbar, respectively.

There are two key control loops on a gas turbine: speed control and temperature control. Under normal operating conditions, speed control regulates the fuel supply and takes the form of a simple droop governor. The outputs from both the speed and temperature controllers are fed into a minimum block, such that the lesser of the two signals determines the fuel flow into the gas turbine, within allowable limits.

There is a no-load fuel requirement in a gas turbine, generally about 23% of maximum, so the controllers regulate the fuel flow between this minimum point and the maximum.

In previous models [31]-[2], fuel flowing from the fuel pump into the gas turbine was obtained as a function of the system speed. For this study, the fuel supply is assumed independent of frequency and depends only on the control signal.

In the model illustrated in figure 4.18, the system speed input to the turbine calculation of exhaust temperature F1 incorporates a scaling mechanism to regulate the frequency sensitivity of the unit. This was developed to take into account the variations in frequency sensitivity conditional on technology and age of

CCGT units, which were evident on examination of responses of the different units.

The system speed N is multiplied by a scalar, a, and then, a constant, b, is added, such that $a + b = 1$.

Since the actual exhaust temperature depends on the airflow into the combustor, the exhaust temperature from the turbine calculation, F1, is modulated using the calculated airflow through the compressor.

The temperature of the exhaust gases is then 'measured', with the appropriate time delays incorporated.

The airflow is regulated using an IGV controller. The calculated exhaust temperature is compared with the rated exhaust temperature such that if there is a difference, the IGVs control airflow in order to bring the temperature back to the rated value. However, as airflow also depends on the speed of the compressor, the expected airflow, due to IGV position, is modulated using the actual speed, yielding the calculated flow.

The model is also equipped with an over-firing capability, which allows the temperature limits to be increased for a short period of time during a frequency transient.

5 SIMPLE CYCLES SIMULATION

Contents

5.1 INTRODUCTION

Aspen HYSYS is a widely used process modelling tool for conceptual design, optimization, business planning, asset management, and performance monitoring for oil & gas production, gas processing, petroleum refining, and air separation industries. It is a core element of AspenTech's AspenONE® Process Engineering applications.

In this chapter simple HYSYS models have been developed. The first model represents a simple gas cycle, the second one a simple steam cycle and the third one a simple combined cycle.

For each model, a parametric analysis has been conducted to evaluate the significant variables and a process optimization has been realized using those variables.

Numerical optimization goals have been achieved using the *Hyprotech SQP optimizer*, a rigorous sequential quadratic programming (SQP) optimization solver.

5.2 NATURAL GAS

All simulations are based on the Bolivian natural gas, whose composition is shown in tabular 5.1.

Table 5.1: Composition of Bolivian Natural Gas

Component	Formula	Composition %
Methane	CH_4	91.79
Ethane	C_2H_6	5.58
Propane	C3H8	0.97
i-Butane	C_4H_{10}	0.03
n-Butane	C_4H_{10}	0.02
i-Pentane	C_5H_{12}	0.05
n-Pentane	C_5H_{12}	0.05
Carbon Dioxide	CO_2	0.08
Nitrogen	N_2	1.42
Hydrogen sulphide	H_2S	0.01

In HYSYS, all necessary information pertaining to pure component flash and physical property calculations are contained within the Fluid Package. This approach allows to define all the required information inside a single entity. We decided to use the thermodynamic model *Peng-Robinson*.

During the definition of the fluid package, we also define the reactions that take place in the combustion chamber, where natural gas is mixed with the air coming from the compressor. The reactions in the combustion chamber are:

$$
\begin{aligned}
CH_4 + 2O_2 &\rightarrow CO_2 + 2H_2O \\
C_2H_6 + 3.5O_2 &\rightarrow 2CO_2 + 3H_2O \\
C_3H_8 + 5O_2 &\rightarrow 3CO_2 + 4H_2O \\
i - C_4H_10 + 6.5O_2 &\rightarrow 4CO_2 + 5H_2O \\
n - C_4H_10 + 6.5O_2 &\rightarrow 4CO_2 + 5H_2O \\
i - C_5H_12 + 8O_2 &\rightarrow 5CO_2 + 6H_2O \\
n - C_5H_12 + 8O_2 &\rightarrow 5CO_2 + 6H_2O \\
H_2S + 1.5O_2 &\rightarrow SO_2 + H_2O \\
SO_2 + 0.5O_2 &\rightarrow SO_3 \\
N_2 + O_2 &\rightarrow 2NO \\
NO + 0.5O_2 &\rightarrow NO_2
\end{aligned}
$$

5.3 THE SIMPLE GAS TURBINE CYCLE

The simple gas turbine cycle (CHT) has been modelled using Aspen HYSYS as shown in figure 5.1. The air, at atmospheric conditions, enters the plant and goes to a compressor, in which the pressure increases from the atmospheric one up to 20 bar. The compressed air is mixed with the natural gas flow, set at the same pressure and atmospheric temperature. The obtained stream enters a combustion chamber modelled as a Gibbs reactor where the reactions defined before occur. This kind of reactor calculates the exiting compositions such that the phase and chemical equilibria of the outlet streams are attained. The condition that the Gibbs free energy of the reacting system is at a minimum at equilibrium is used to calculate the product mixture composition. After the combustion the gases are sent to a gas turbine and expanded to atmospheric pressure.

Compressors and expanders models can have shafts that are physically connected to the unit operation. Linking compressors and expanders in HYSYS means the speed of each linked unit operation is the same and the sum of the duties of each linked compressor or expander and the total power loss equals zero.

It has been specified the natural gas pressure and mass flow and the air mass flow. The pressure of compressed air is calculated by HYSYS using the automatic mixer pressure assignment, selecting *Equalize all* in the mixer parameters design.

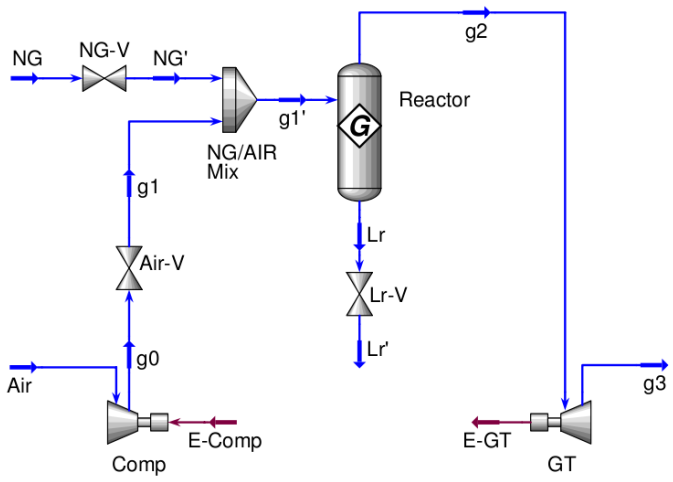

Figure 5.1: Gas turbine HYSYS model.

5.3.1 Parametric Analysis

The gas turbine model needs some constraints in order to represent the real behaviour of a gas turbine plant. The temperature of the exhausted gas cannot exceed the 1250°C because of mechanical problem in the gas turbine and the compression must be below 20 bar. Aspen HYSYS has an interesting tool, *Adjust*, in which the user sets the target variable value and specifies an adjusted variable used to reach the target value. The temperature of exhaust gas (1250°C) has been set as target variable and the air mass flow as adjusted variable (*ADJ-2* in figure 5.2). Everytime the user changes the manipulated variable, the adjust regulates the air mass flow to reach the temperature set point.

The model efficiency has been expressed as

$$\eta_{GC} = \frac{E_{gt} - E_{Comp}}{\dot{m}_{NG}[LHV]_{NG}} = \frac{E_{net}}{\dot{m}_{NG}[LHV]_{NG}} \tag{5.1}$$

where E_{Comp} is the compressor work, E_{gt} is the gas turbine power, $\dot{m}_{NG}$ is the natural gas mass flow and $[LHV]_{NG}$ is the natural gas lower heating value.

In order to make a good parametric analysis, the net power output has been set to 50 *MW* using another adjust (*ADJ-1* in figure 5.2) with the natural gas mass flow as adjusted variable. This can be done connecting the adjust directly to a spreadsheet in which the net power is specified using the equation $E_{net} = E_{gt} - E_{comp}$, or setting the gas turbine power as the target variable and selecting *another object* as source in the adjust target value section, and the compressor power as *matching value object*, with an offset of 50 *MW*.

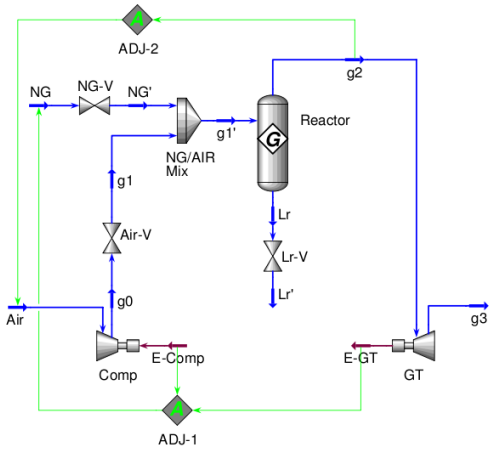

Figure 5.2: Gas turbine HYSYS model-adjusts.

The *Aspen HYSYS Databook* provides the user with a convenient way to examine the flowsheet in more detail. He can use the Databook to monitor key variables under a variety of process scenarios, and view the results in a tabular or graphical format.

For the parametric analysis, the simulation can be run for a range of natural gas pressure (e.g., 1400 kPa through 2200 kPa in 10 kPa increments) by changing the pressure specified for natural gas feed in the worksheet. The changes can be automate using the *Case Studies* feature in the Databook.

For a 50 MW net power production, the results are shown in figure 5.3. The efficiency increases with the pressure with a sort of logarithmic trend, the natural gas flow decrease with the pressure and the air mass flow has a minimum at 1570 kPa.

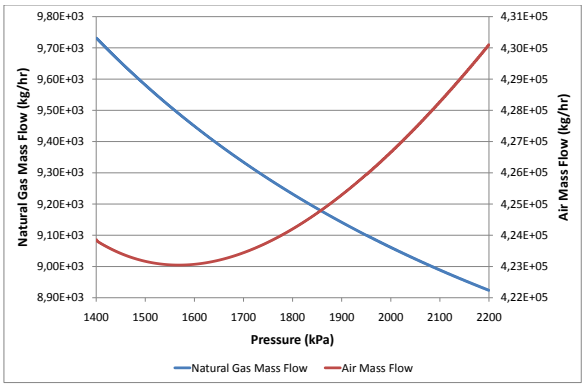

(a) *Mass flow variation with pressure.*

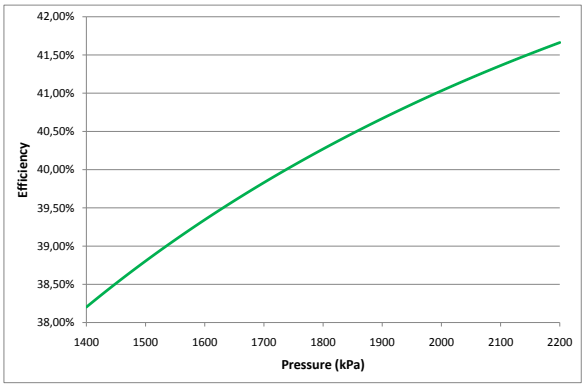

(b) *Efficiency rise with pressure.*

Figure 5.3: Parametric analysis of GTPP.

5.3.2 Optimization

Aspen HYSYS contains a multi-variable *steady state Optimizer*. Once the flowsheet has been built and a converged solution has been obtained, the optimizer is used to find the operating conditions which minimize (or maximize) an *Objective Function*. The object-oriented design of HYSYS makes the optimizer extremely powerful, since it has access to a wide range of process variables for the optimization study.

The following terminology is used in describing the Optimizer:

- *Primary Variables*: These are the variables imported from the flowsheet whose values are manipulated in order to minimize (or maximize) the objective function. You set the upper and lower bounds for all of the primary variables, which are used to set the search range, as well as for normalization.
- *Objective Function*: The function which is to be minimized or maximized. There is a great deal of flexibility in describing the Objective Function. Primary variables can be imported and functions defined within the Optimizer Spreadsheet, which possesses the full capabilities of the main flowsheet spreadsheet.
- *Constraint Functions*: Inequality and Equality Constraint functions can be defined in the Optimizer Spreadsheet. An example of a constraint is the product of two variables satisfying an inequality (for example, $-A * B < K$).

The optimization solver used is the *Hyprotech SQP*, a rigorous Sequential Quadratic Programming (SQP) optimization solver. This solver features step size restriction, decision variable and objective function scaling, and a problem-independent and scale-independent relative convergence test. The algorithm also ensures that the model is evaluated only at points feasible with respect to the variable bounds. The Hyprotech SQP requires the use of Derivative Utilities, a component of the HYSYS.RTO RealTime Optimization package available as a plug-in to the basic HYSYS software package. The Derivative utility is one of two utilities used by HYSYS.RTO to provide the primary interface between the flowsheet model and the solver. Their primary purpose is to collect appropriate optimization objects, which are then exposed to solvers to meet a defined solution criteria.

The variables used in the gas turbine model are the natural gas mass flow and pressure, and the air mass flow. The plant efficiency (equation 5.1) has been set as objective function and

Table 5.2: Gas turbine model data

Parameter	Symbol	Standard	Optimized	Unit
Natural Gas	Mass Flow ($\dot{m}_{NG}$)	9527	9039	kg/h
	Pressure (P_{NG})	15.4	20	bar
Air	Mass Flow ($\dot{m}_{Air}$)	$4.23 \cdot 10^5$	$4.21 \cdot 10^5$	kg/h
	Pressure (P_{air})	1	1	bar
Compressor	Adiabatic Effic. (η_{AE})	88	88	%
	Polytropic Effic. (η_{PE})	91.4	91.6	%
	Duty (E_{Comp})	$4.68 \cdot 10^4$	$5.31 \cdot 10^4$	kW
Reactor	Efficiency (η_R)	99.9	99.9	%
	Fuel line pressure ($P_{g1'}$)	15.2	19.8	bar
	g2 Temperature (T_{g2})	1250	1259	°C
Turbine	Adiabatic Effic. (η_{AE})	90	90	%
	Polytropic Effic. (η_{PE})	86.4	85.9	%
	Duty (E_{gt})	$9.68 \cdot 10^4$	$1.03 \cdot 10^5$	kW
	g3 Temperature (T_{g3})	601.9	560.9	°C
Efficiency	Effic. (η_{GC})	39.02	41.08	%

the hot gas temperature (1000°C< T_{g2} <1260°C) and the net power output (49950 kW < E_{net} < 50050 kW) are set as process constraints. The optimized data are shown in table 5.2.

After the optimization, the natural gas mass flow decreases unlike its pressure that increases to the limit imposed in the derivative utility. The efficiency increases up to 41.08%, very similar to the real gas turbine efficiency: for instance the GE LM6000 model (figure 5.4) has an efficiency of 41.0% with a pressure ratio of 27.9 or the GE PGT25+ with an efficiency of 39.6% and a pressure ratio of 21.6.

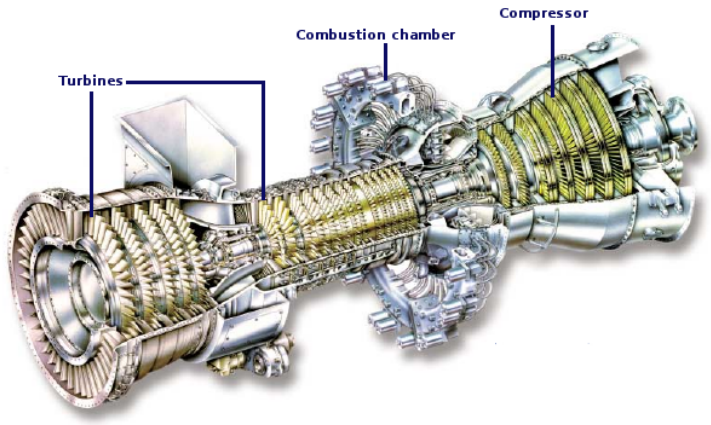

Figure 5.4: GE LM6000 gas turbine.

5.4 THE SIMPLE STEAM CYCLE

The steam cycle model is a closed cycle based on the *Rankine cycle* with superheat (figure 5.5). There are four processes in the Rankine cycle, each changing the state of the working fluid. These states are identified by number in figure 5.5:

- *Process 1-2*: the water is pumped from low to high pressure, as the fluid is a liquid at this stage the pump requires little input energy;
- *Process 2-3'*: the high pressure liquid enters a boiler where it is heated at constant pressure by an external heat source to become a superheated vapour;
- *Process 3'-4*: the vapour expands through a turbine, generating power, this decreases the temperature and pressure of the vapour, and some condensations may occur;
- *Process 4-1*: the wet vapour enters a condenser where it is condensed at a constant pressure and temperature to become a saturated liquid. The pressure and temperature of the condenser is fixed by the temperature of the cooling coils as the fluid is undergoing a phase-change.

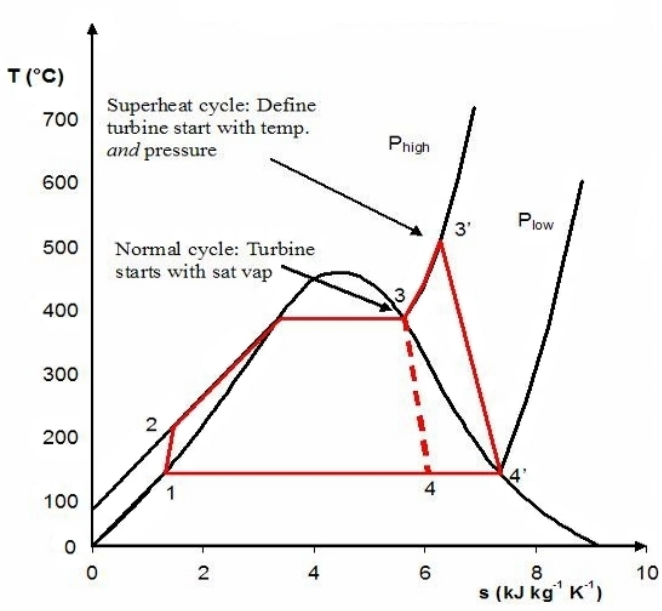

Figure 5.5: Rankine cycle's T-s diagram.

In an ideal Rankine cycle the pump and turbine would be isentropic, processes 1-2 and 3-4 would be represented by vertical lines on the Ts diagram and more closely resemble that of the Carnot cycle.

In a real Rankine cycle, the pump compression and the turbine expansion are not isentropic. In other words, these processes are non-reversible and entropy is increased during the two processes. This somewhat increases the power required by the pump and decreases the power generated by the turbine.

The steam cycle HYSYS model is represented in figure 5.6. It has been specified the mass flow, the high pressure (s2 stream), the temperature of superheated vapour (s3 stream), the pressure after the steam turbine (s4 stream) and the temperature after the cooler (s1 stream).

There is a limitantion concerning the superheated vapour temperature due to steam turbine's material problems, it must be set below $550 - 565$ °C (the creep limit of stainless steel). This low critical temperature (compared with a gas turbine cycle) explains why the Rankine cycle is often used as a bottom cycle in the combined cycle gas turbine power stations.

Furthermore, the increase of the high pressure causes the decrease of vapour fraction after the steam turbine. As the water condenses, water droplets hit the turbine blades at high speed causing pitting and erosion, gradually decreasing the life of turbine blades and efficiency of the turbine. The high pressure must be set below 100 bar.

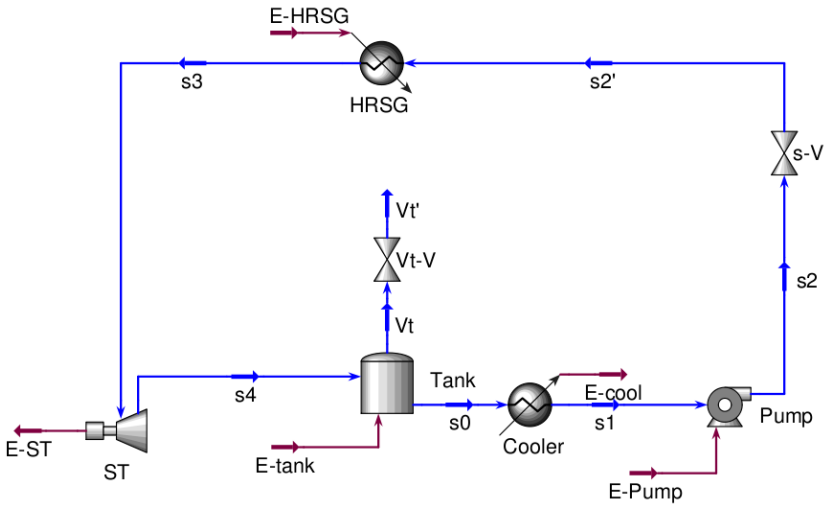

Figure 5.6: Steam cycle model.

5.4.1 Parametric Analysis

In order to make a significant parametric analysis, a net power output of 50 *MW* has been set using an adjust (*ADJ-1* in figure 5.7) which has the s2 stream mass flow as the adjusted variable.

The thermodynamic efficiency of the steam cycle has been defined as the ratio of net power output to heat input, the work required by the pump is often around 1% of the turbine work output:

$$\eta_{SC} = \frac{E_{ST} - \frac{E_{pump}}{0.60}}{E_{HRSG}} = \frac{E_{net}}{E_{HRSG}} \tag{5.2}$$

where E_{st} is the steam turbine power and $(E_{pump}/0.6)$ is the real pump work necessary to compress the liquid stream (0.6 is the conversion factor from electric to mechanical work).

The high and low pressure has been used as independent variables to analyse the model behaviour.

Figure 5.8 shows the efficiency variation and the water mass flow needed to satisfy the 50 *MW* set point variations with pressures.

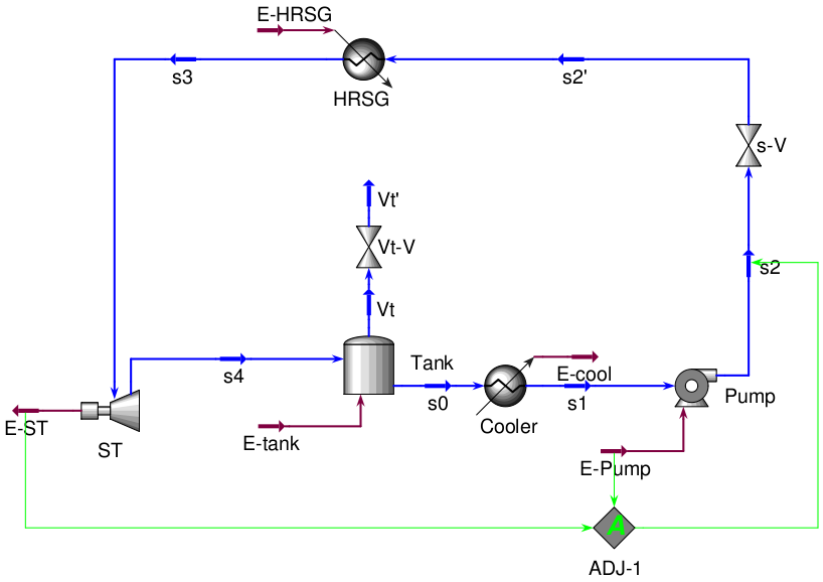

Figure 5.7: Steam cycle model-adjust.

It appears that the efficiency increases, and the water mass flow decreases, when the high pressure is at his higher value and the low pressure is at is lower value.

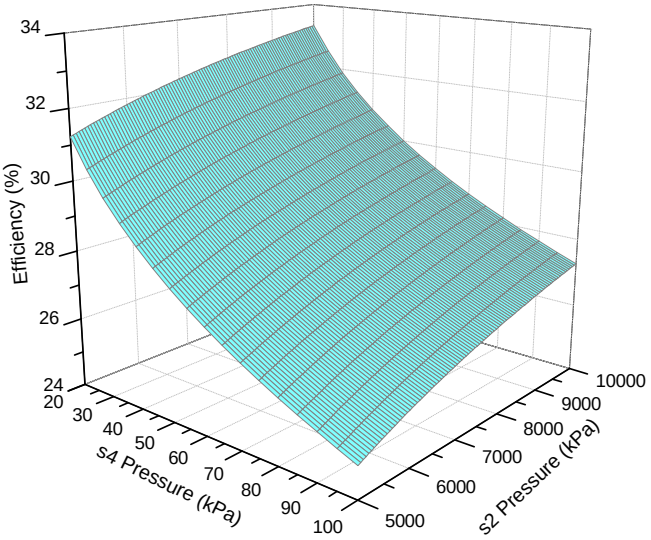

(a) *Efficiency variation with pressures.*

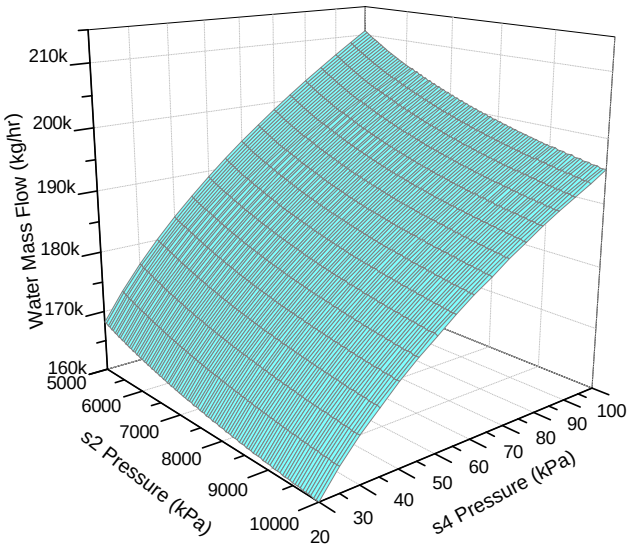

(b) *Mass flow variation with pressures.*

Figure 5.8: Steam cycle parametric analysis.

5.4.2 Optimization

The optimization variables used in this model are:

- the pressure in stream s2 (high pressure);
- the water mass flow;
- the superheated vapour temperature;
- the pressure in stream s4 (low pressure).

The optimization objective function is the plant efficiency expressed by equation 5.2, and the constraint variable is the s3 temperature (535°C< T_{s3} <565°C).

After the optimization it has been reached an efficiency of 35.04%. The optimizer indicates as high pressure the pressure limit of 100 bar. Analysing the vapour phase fraction in the low pressure stream it appears around 89.71%, this is a quite low level and the steam turbine may be affected by a low life expectancy. Further optimizations have been made setting the high pressure limit to 70 bar and 90 bar reaching an efficiency of 33.18% and 34.01% with a vapour phase fraction over 90%.

Table 5.3: Steam cycle model data

Parameter	Symbol	Standard	Optimized	Unit
s2 Stream	Mass Flow ($\dot{m}_w$)	$1.58 \cdot 10^5$	$1.57 \cdot 10^5$	kg/h
	Pressure (P_{s2})	70	100	bar
	Temperature (T_{s2})	33.80	34.07	°C
HRSG	Duty (E_{HRSG})	$5.35 \cdot 10^8$	$5.35 \cdot 10^8$	kJ/h
	Delta P (ΔP_{HRSG})	0.60	0.60	bar
s3 Stream	Temperature (T_{s3})	550.0	565.0	°C
	Pressure (P_{s3})	69.2	99.2	bar
Turbine	Adiabatic Effic. (η_{AE})	90	90	%
	Polytropic Effic. (η_{PE})	87.7	87.6	%
	Duty (E_{st})	$5.01 \cdot 10^5$	$5.21 \cdot 10^5$	kW
Condenser	Duty (E_{cond})	$3.59 \cdot 10^8$	$3.49 \cdot 10^8$	kJ/h
	Delta P (ΔP_c)	0.1	0.1	bar
Pump	Delta P (ΔP_p)	69.95	99.95	bar
	Duty (E_p)	407.82	582.70	kW
	Adiabatic Effic. (η_p)	75	75	%
Efficiency	Effic. (η_{SC})	33.62	35.02	%

5.5 SIMPLE COMBINED CYCLE

The easiest way to represent a combined cycle with Aspen HYSYS is using only one heat exchanger as heat recovery steam generator (HRSG), and one steam turbine, as shown in figure 5.10. The gas cycle is the same as in section 5.3 with a compression pressure of 18 bar in the standard model. In the steam cycle, liquid water is pumped up to 70 bar, vaporized through the HRSG by the exhausted hot gas from the gas turbine and expanded in a steam turbine. The low pressure steam becomes liquid in the condenser and stored in a tank to close the cycle. In this case it has been specified a minimum approach of 50°C in the HRSG to allow a vapour superheating inside the heat exchanger (figure 5.9).

The air compressor adiabatic efficiency has been set to 88% and the efficiency of all the turbines to 90% leaving HYSYS to evaluate the polytropic efficiencies.

Combined cycle constraints are the combination of the gas cycle and steam cycle constraints. The exhausted gas temperature before the gas turbine must be below 1250°C and the steam temperature after the HRSG must be below 565°C. This is realized using two adjusts, the first one referred to the gas temperature and operating on the air mass flow (*ADJ-2*, figure 5.11) and the second one manipulating the water mass flow to set the correct vapour temperature (*ADJ-3*, figure 5.11).

Standard combined cycle plants have an efficiency from 50% to 55% (the new advanced GE combined cycles can reach the 60%).

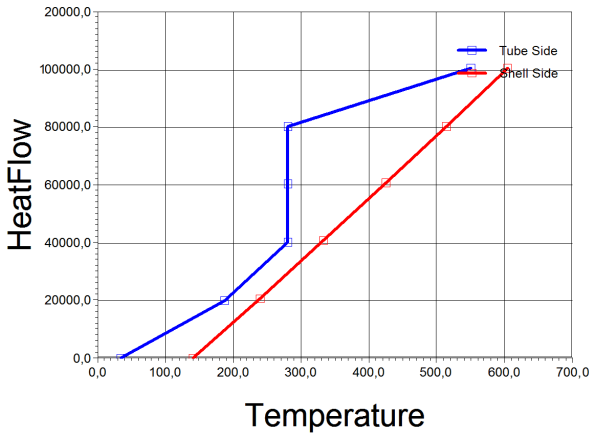

Figure 5.9: HRSG Temperature vs Heat flow.

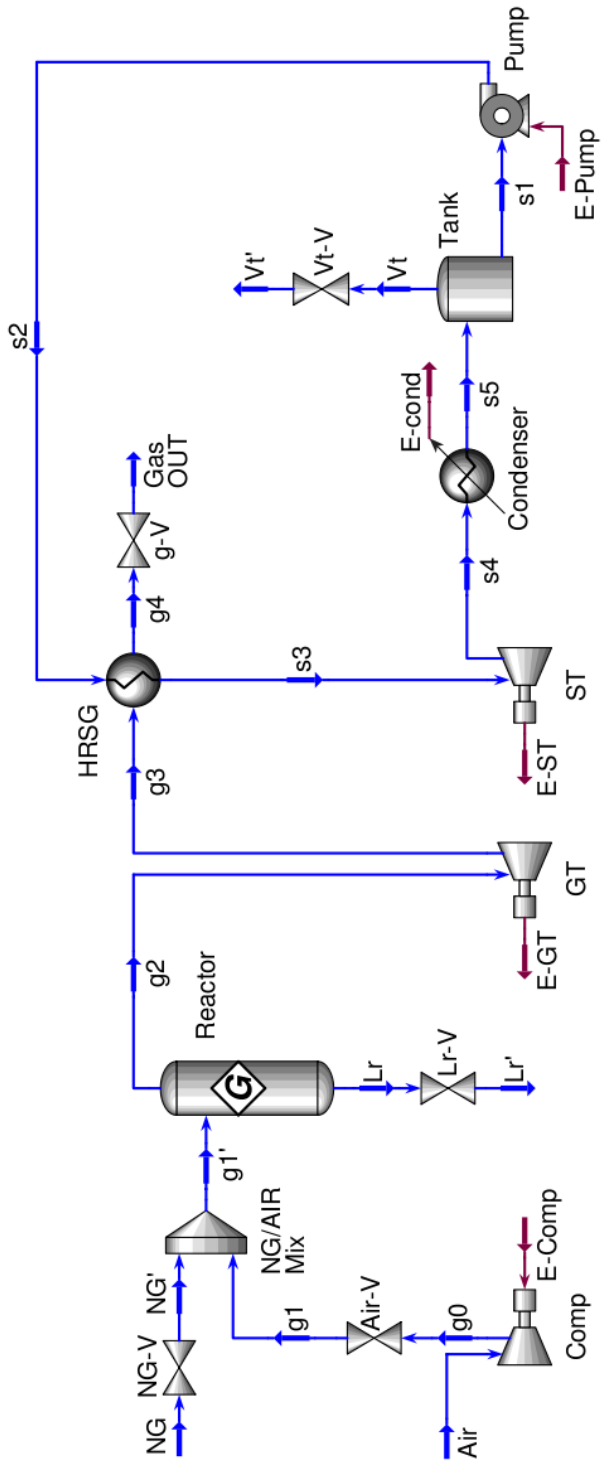

Figure 5.10: Simple combined cycle model.

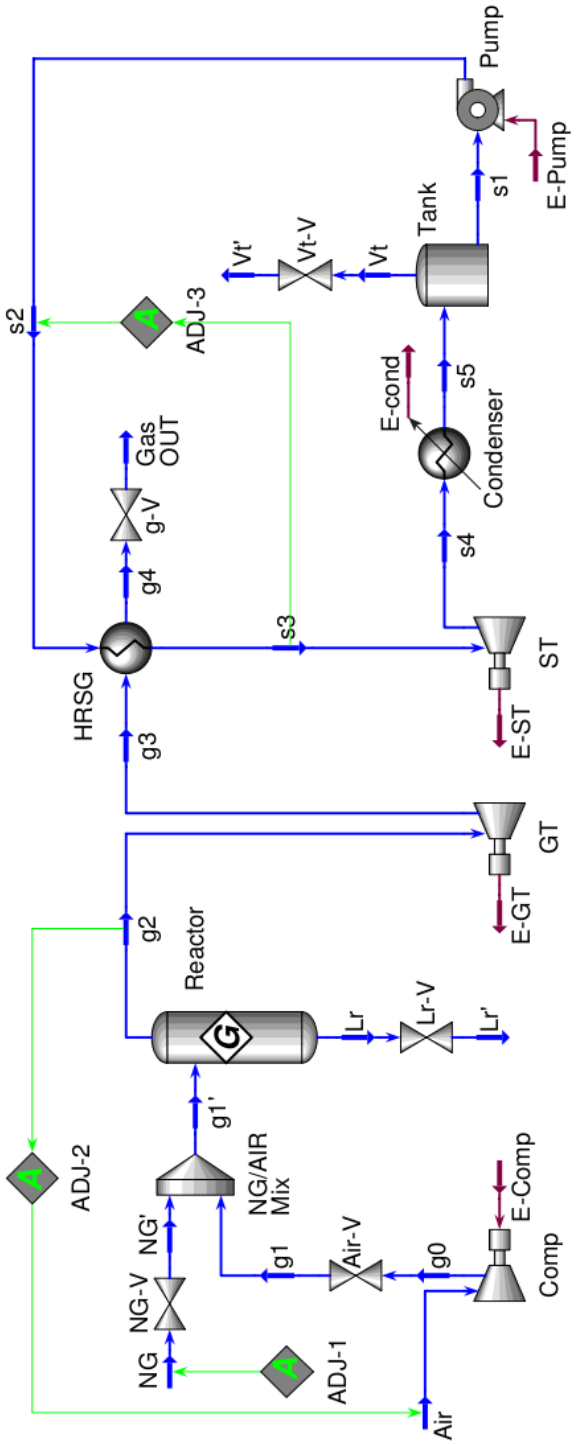

Figure 5.11: Simple combined cycle model-adjusts.

5.5.1 Parametric Analysis

In order to make a satisfying analysis, a plant net power of 100 *MW* has been set using an adjust (*ADJ-1* in figure 5.11) operating on the natural gas mass flow, linked to a spreadsheet in which is defined the net power output (E_{netCC}).

The *combined cycle efficiency* is expressed by

$$\begin{aligned} \eta_{CC} &= \frac{(E_{gt} - E_{Comp}) + (E_{st} - E_{pump}/0.6)}{\dot{m}_{NG}[LHV]_{NG}} \\ &= \frac{E_{netCC}}{\dot{m}_{NG}[LHV]_{NG}} \end{aligned} \tag{5.3}$$

where E_{st} is the steam turbine power and $(E_{pump}/0.6)$ is the real pump work necessary to compress the liquid stream (0.6 is the conversion factor from electric to mechanical work).

In the analysis is also evaluated the *work ratio* (RW):

$$RW = \left(\frac{E_{st} - E_{pump}/0.6}{E_{gt} - E_{Comp}}\right) = \frac{E_{netSC}}{E_{netGC}}$$

this parameter represents the different contribution between gas cycle and steam cycle.

The variables used in this analysis are the natural gas pressure from 14 bar to 21 bar and the water high pressure (s2 stream) from 60 bar to 100 bar. The efficiency variation analysis is represented in figure 5.12.

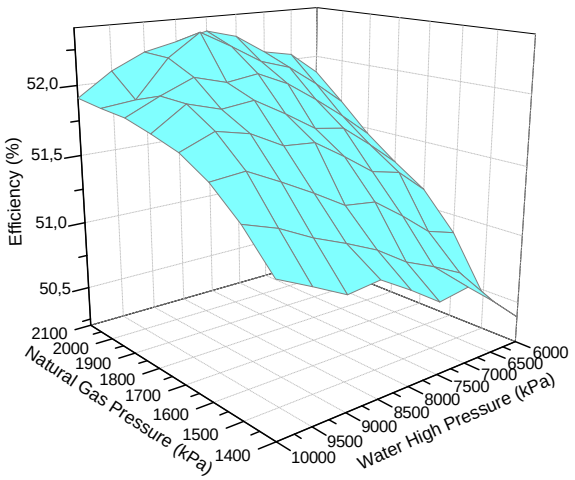

Figure 5.12: Efficiency vs Pressures.

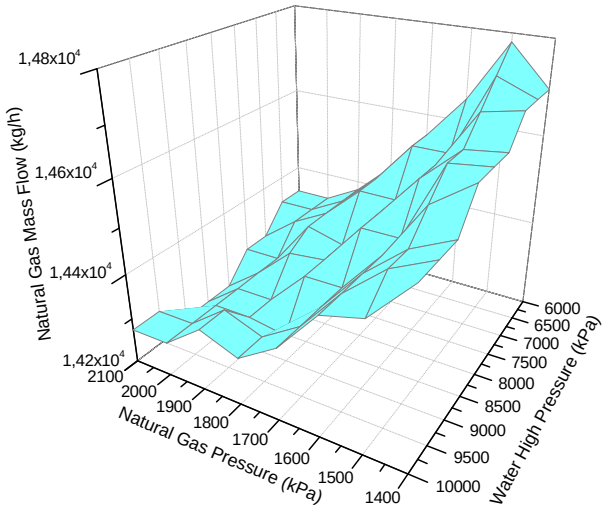

Figure 5.13: Natural Gas mass flow vs Pressures.

In this case the parametric analysis is not so simple because there is not only one possible equilibrium stage for a single combination of pressures. By the way we can see that the natural gas mass flow increases when the two pressures are lower in order to maintain the specified net power (figure 5.13). The water mass flow (figure 5.14) increases when the the natural gas pressure is low to maintain the net power output, but it increases also with the water pressure in order to maintain the steam temperature below 565°C.

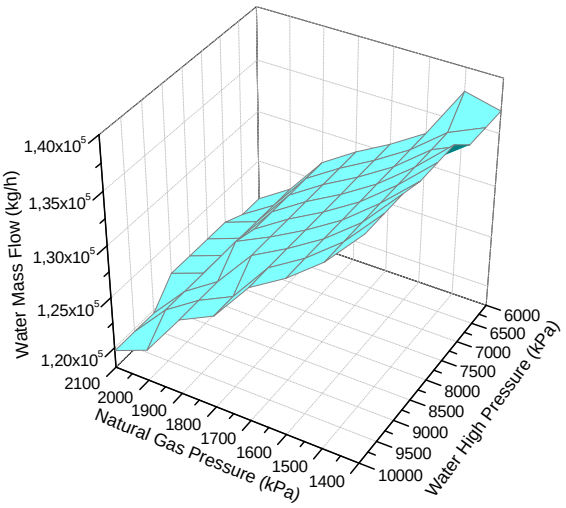

Figure 5.14: Water mass flow vs Pressures.

5.5.2 Optimization

The SQP optimization variables are the natural gas mass flow and pressure, the air mass flow, the water mass flow and high and low water's pressures (stream s2 and stream s4 in figure 5.10). After the optimization the efficiency is increased from 50.89% to 52.02%. We also witnessed a mass flows decrease correlated to an increase in pressures.

Table 5.4: Simple combined cycle model data

Parameter	Symbol	Standard	Optimized	Unit
Natural Gas	Mass Flow ($\dot{m}_{NG}$)	$1.461 \cdot 10^4$	$1.423 \cdot 10^4$	kg/h
	Pressure (P_{NG})	18.00	19.90	bar
Air	Mass Flow ($\dot{m}_{Air}$)	$6.707 \cdot 10^5$	$6.692 \cdot 10^5$	kg/h
	Pressure (P_{air})	1	1	bar
Compressor	Adiabatic Eff. (η_{Ac})	88	88	%
	Polytropic Eff. (η_{Pc})	91.5	91.6	%
	Duty (E_{Comp})	$8.05 \cdot 10^4$	$8.43 \cdot 10^4$	kW
Reactor	Efficiency (η_R)	99.9	99.9	%
	g1′ Pressure ($P_{g1'}$)	17.80	19.70	bar
	g2 Temperature (T_{g2})	1251	1250	°C
Gas Turbine	Adiabatic Eff. (η_{Agt})	90	90	%
	Polytropic Eff. (η_{Pgt})	86.8	86.5	%
	Duty (E_{gt})	$1.43 \cdot 10^5$	$1.50 \cdot 10^5$	kW
	g3 Temperature (T_{g3})	645.9	613.9	°C
HRSG	UA (UA_{HRSG})	$4.32 \cdot 10^6$	$4.27 \cdot 10^6$	kJ/h°C
	Delta P shell (ΔP_{sh})	0.30	0.30	bar
	Delta P tube (ΔP_{tb})	0.60	0.60	bar
	s2 Temperature (T_{s2})	33.8	33.8	°C
	s3 Temperature (T_{s3})	554.5	563.9	°C
	GasOut Temp. (T_{gO})	129.3	139.9	°C
s2 Stream	Mass Flow ($\dot{m}_w$)	$1.180 \cdot 10^5$	$1.069 \cdot 10^5$	kg/h
	Pressure (P_{s2})	70.00	70.07	bar
Steam Turbine	Adiabatic Eff. (η_{Ast})	90	90	%
	Polytropic Eff. (η_{Pst})	87,8	87.7	%
	Duty (E_{st})	$3.77 \cdot 10^4$	$3.45 \cdot 10^4$	kW
	s4 Pressure P_{s4}	0.15	0.15	bar
Condenser	Delta P (ΔP_{cond})	0.10	0.10	bar
	Duty E_{cond}	$2.67 \cdot 10^8$	$2.43 \cdot 10^8$	kJ/h
Pump	Adiabatic Eff. (η_{Ap})	75	75	%
	Delta P (ΔP_p)	69.95	70.02	bar
	Duty (E_p)	305.35	276.99	kW
Efficiency	Net Eff. (η_{CCGT})	50.89	52.02	%
	RW	55.29	52.01	%

6 ADVANCED CYCLES SIMULATION

Contents

6.1 INTRODUCTION

In this chaper HYSYS models for advanced cycles have been realized with more level of details. The first advanced model wants to develope a detailed heat recovery steam generator, splitting it in three heat exchanger, each one dedicated to a peculiar application (economizing, evaporation and superheating). The second model is a multifunctional model, which can work as either a combined cycle with three steam turbines or as a cogenerative plant with two external utilities represented by two heat exchangers with a specific power setting. The third model is based on a plant with a three pressure heat recovery steam generator and three steam turbines.

Furthermore, parametric analysis has been undertaken for each model to find out which variables have the most significant effect on overall efficiency (or on the fuel energy saving ratio for the cogenerative model). With these variables a model optimization has been conducted using the Hyprotech SQP optimiser.

6.2 CCGT WITH THREE HEAT EXCHANGER

During the heat recovery steam generator (HRSG) design, we have to consider three primary coil types:

1. *Economizer Section* (preheater or preheat coil): it is used to preheat the feedwater being introduced to the system. It is normally located in the colder gas downstream of the evaporator. Since the evaporation temperature is constant, the amount of heat that may be removed from the flue gas is limited due to the approach to the evaporator, whereas the economizer inlet temperature is low, allowing the flue gas temperature to be taken lower;

2. *Evaporator Section*: it may consist of one or more coils. In these coils, the effluent (water), passing through the tubes is heated to the saturation point and evaporated;

3. *Superheater Section*: it is used to dry the saturated vapour being separated in the steam drum. In some units it may only be heated to little above the saturation point where in other units it may be superheated to a significant temperature for additional energy storage.

An implementation of the simple model is to use three heat exchangers as heat recovery steam generator, each one dedicated to a specific operation (figure 6.1). In the economizer the liquid is heated up to the evaporation temperature, in the evaporator we have the phase transition at constant temperature and in the superheater the vapour reaches $\simeq$ 550°C. In this way we can have a better exchange between exhaust gas and water, this is deductible from the gas outlet temperature that decreases compared with the model with only one heat exchanger as heat recovery steam generator. The pressure drops in the exchangers are set to 10 kPa shell side and to 20 kPa tube side.

This model has two more degrees of freedom, so it has been specified the vapour fraction in *s2a* (= 0) and *s2b* (= 1) streams allowing the evaporator to work at constant temperature making only the phase transition.

We have also set an evaporator minimum approach of 10°C to avoid temperature crosses. Thus the gas from the evaporator has a temperature 10°C higher than the water coming from the economizer.

The compressor adiabatic efficiency is set, as usual, to 88% and the turbine adiabatic efficiency is set to 90%. The reactor conversion is 99%.

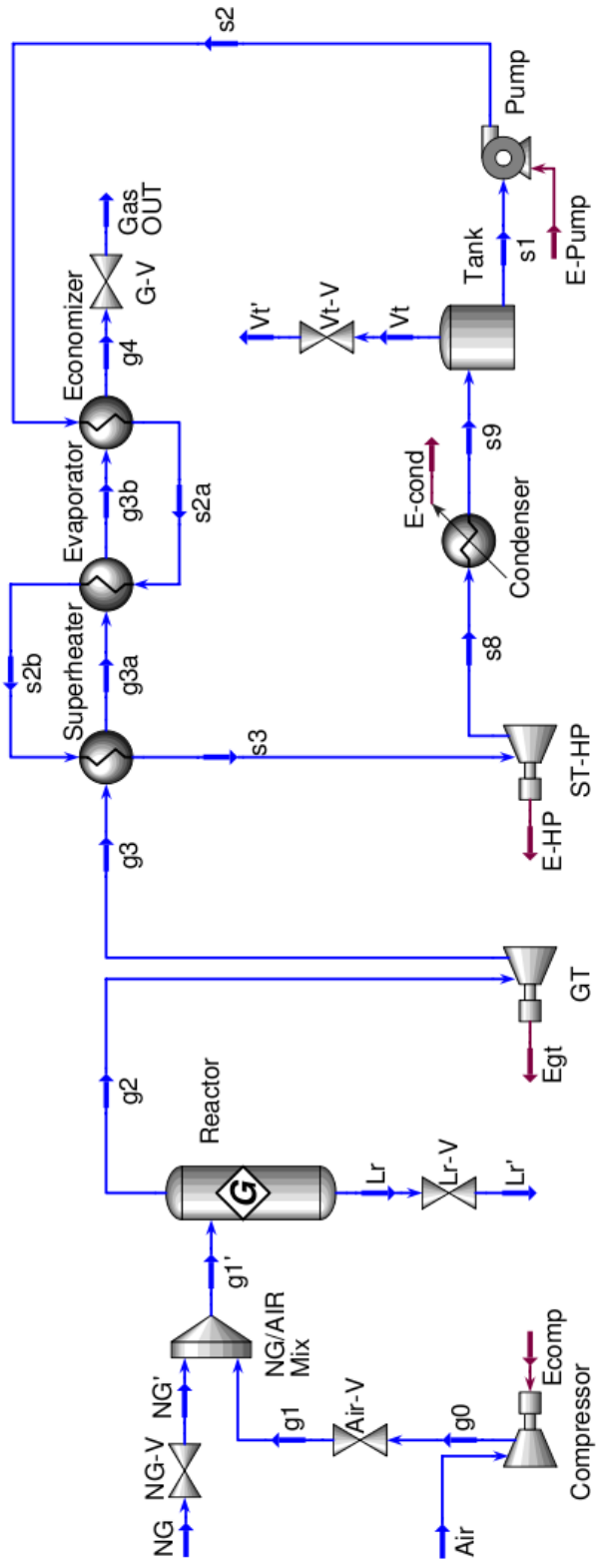

Figure 6.1: three exchangers CCGT model.

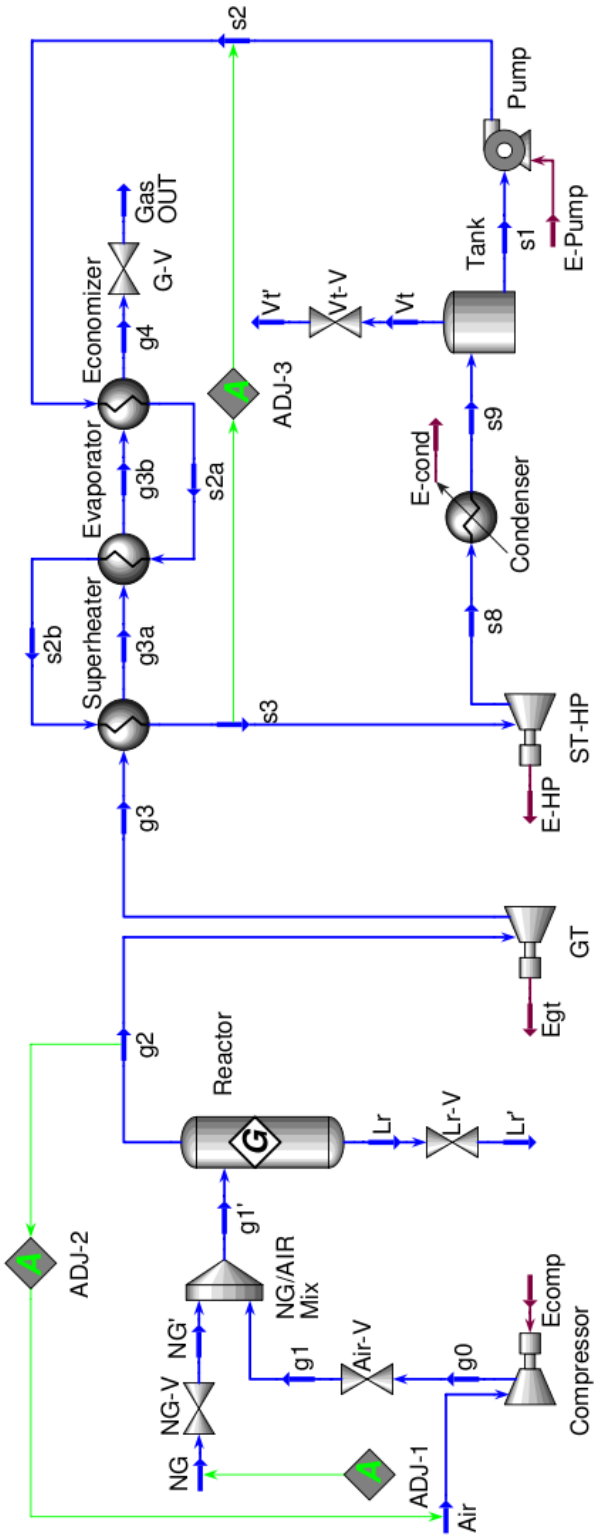

Figure 6.2: three exchangers CCGT model-adjusts.

6.2.1 Parametric Analysis

The variables used in the parametric analysis are the same as in section 5.5.1, the natural gas pressure and the water high pressure. The water low pressure has been set to 0.15 bar, if the low pressure is higher, the efficiency decreases.

We used three different adjust as in the simple combined cycle model,the first one (*ADJ-1* in figure 6.2) sets the net power output to 100 *MW* via the natural gas mass flow, the second one (*ADJ-2* in figure 6.2) sets the combustion chamber outlet gas temperature around 1250°C using the air mass flow and the third one (*ADJ-3* in figure 6.2) sets the steam temperature around 550°C before entering the steam turbine using the water mass flow.

Several problems appear during the parametric analysis due to the fact that there are a lot of different pressure combinations to achieve the same net power output. This can be solved with an accurate Adjust setting. *ADJ-1* has a tolerance of 100 kW to allow an easier and faster system convergence, the step size, set to 1500 kg/h, is crucial because a greater one may drastically modify the system configuration. *ADJ-2* has a tolerance of 5°C in order to avoid the temperature increase (1250°C is the limit due to mechanical problems). *ADJ-3* has soft restrictions with a tolerance of 15°C.

Figure 6.3 represents the efficiency analysis using the natural gas pressure and water high pressure variation. The higher efficiency trend is reached when the high water pressure is at its limits.

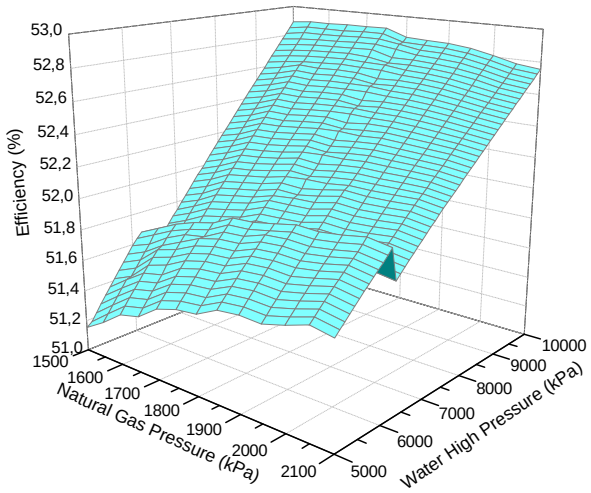

Figure 6.3: Efficiency vs Pressures.

6.2.2 Optimization

This configuration reaches a net efficiency of 53.06% (table 6.1). It is interesting to focus on the natural gas pressure of 16.39 bar, in this case the optimized value is not close to the limit.

Table 6.1: CCGT with three exchangers model data

Parameter	Symbol	Standard	Optimized	Unit
Natural Gas	Mass Flow ($\dot{m}_{NG}$)	$1.424 \cdot 10^4$	$1.394 \cdot 10^4$	kg/h
	Pressure (P_{NG})	18.00	16.39	bar
Air	Mass Flow ($\dot{m}_{Air}$)	$6.536 \cdot 10^5$	$6.230 \cdot 10^5$	kg/h
	Pressure (P_{air})	1	1	bar
Compressor	Adiabatic Eff. (η_{Ac})	88	88	%
	Polytropic Eff. (η_{Pc})	91.53	91.45	%
	Duty (E_{Comp})	$7.84 \cdot 10^4$	$7.12 \cdot 10^4$	kW
Reactor	Efficiency (η_R)	99.9	99.9	%
	g1′ Pressure ($P_{g1'}$)	17.80	16.04	bar
	g2 Temp. (T_{g2})	1251	1255	°C
Gas Turbine	Adiabatic Eff. (η_{Agt})	90	90	%
	Polytropic Eff. (η_{Pgt})	86.78	86.95	%
	Duty (E_{gt})	$1.39 \cdot 10^5$	$1.29 \cdot 10^5$	kW
	g3 Temp. (T_{g3})	646.0	667.3	°C
Economizer	UA (UA_{Ec})	$5.81 \cdot 10^6$	$1.73 \cdot 10^7$	kJ/h°C
	Delta P shell (ΔP_{sh})	0.10	0.10	bar
	Delta P tube (ΔP_{tb})	0.20	0.20	bar
	s2 Temp. (T_{s2})	33.8	34.07	°C
	s2a Temp. (T_{s2a})	284.8	309.80	°C
	GasOut Temp. (T_{gO})	97.26	68.43	°C
Evaporator	UA (UA_{Ev})	$2.46 \cdot 10^6$	$2.33 \cdot 10^6$	kJ/h°C
	Delta P shell (ΔP_{sh})	0.10	0.10	bar
	Delta P tube (ΔP_{tb})	0.20	0.20	bar
	s2b Temp. (T_{s2b})	284.6	309.7	°C
	g3b Temp. (T_{g3b})	294.8	319.8	°C
SuperHeater	UA (UA_{Sh})	$4.76 \cdot 10^5$	$4.29 \cdot 10^5$	kJ/h°C
	Delta P shell (ΔP_{sh})	0.10	0.10	bar
	Delta P tube (ΔP_{tb})	0.20	0.20	bar
	s3 Temp. (T_{s3})	548.8	538.1	°C
	g3a Temp. (T_{g3a})	544.4	560.2	°C
Water	Mass Flow ($\dot{m}_w$)	$1.222 \cdot 10^5$	$1.297 \cdot 10^5$	kg/h
	Pressure (P_{s2})	70.00	99.93	bar
Steam Turbine	Adiabatic Eff. (η_{Ast})	90	90	%
	Polytropic Eff. (η_{Pst})	87.76	87.65	%
	Duty (E_{st})	$3.88 \cdot 10^4$	$4.16 \cdot 10^4$	kW
	s4 Pressure P_{s4}	0.15	0.15	bar
Condenser	Delta P (ΔP_{cond})	0.10	0.10	bar
	Duty E_{cond}	$2.76 \cdot 10^8$	$2.84 \cdot 10^8$	kJ/h
Pump	Adiabatic Eff. (η_{Ap})	75	75	%
	Delta P (ΔP_p)	69.95	99.88	bar
	Duty (E_{pump})	316.27	479.33	kW
Efficiency	Net Eff. (η_{CCGT})	51.99	53.06	%
	RW	62.42	69.64	%

6.3 COMBINED/COGENERATIVE CYCLE

The distinctive feature of this combined cycle model is that it allows the user to simulate a combined or a cogenerative cycle. It is composed by a standard gas cycle and a steam cycle with a three heat exchangers HRSG and three steam turbines in series (figure 6.4):

- *ST-HP*: high pressure steam turbine;
- *ST-IP*: intermediate pressure steam turbine;
- *ST-LP*: low pressure steam turbine.

The HP and IP steam turbine outlets are splitted into two more streams, one is used for cogeneration (s_{out1} and s_{out2}) while the other (s5 and s7) is sent to the lower pressure turbine. Thus we can have two streams at different pressures and different temperatures used as cogeneration. It is possible to specify, for instance, the two external utilities thermal energy and HYSYS calculate the stream flows needed to satisfy the request. If the user leaves the two duties empty, the model works as a combined cycle. It is also possible to use only one cogeneration stream.

The remained steam (s8) is condensed in a condenser after the low pressure turbine and stored in a tank. The two fractions used in the cogeneration (s'_{out1} and s'_{out2}) are mixed together and sent to the same tank closing the steam cycle.

The external utilities are represented by two coolers (U_{sout1} and U_{sout2}) that cool the streams to 40°C and expand them to 1 atm. The temperature and pressure set after the two coolers leave HYSYS to evaluate the pressure drops in the exchangers. Thus, the user can modify the two middle pressures in the spreadsheet to reach the desired temperatures needed in the external utilities. The user can also specify the desired temperatures required in the utilities (leaving the two utility powers specified) instead of the intermediate and low pressures, or can specify the two temperatures and the two pressures leaving HYSYS to evaluate the power produced in the utilities.

In the cogenerative model the two utility powers (E_{sout1} and E_{sout2}) have been set to 25 *MW* each one.

Each steam turbine has an adiabatic efficiency of 90% leaving HYSYS to evaluate the polytropic one.

In the standard model the natural gas pressure has been set to 18 bar and an high pressure of 70 bar, a intermediate pressure of 21 bar and a low pressure of 6 bar in the steam cycle. The pressure before the condenser has been set to 0.15 bar like the other models.

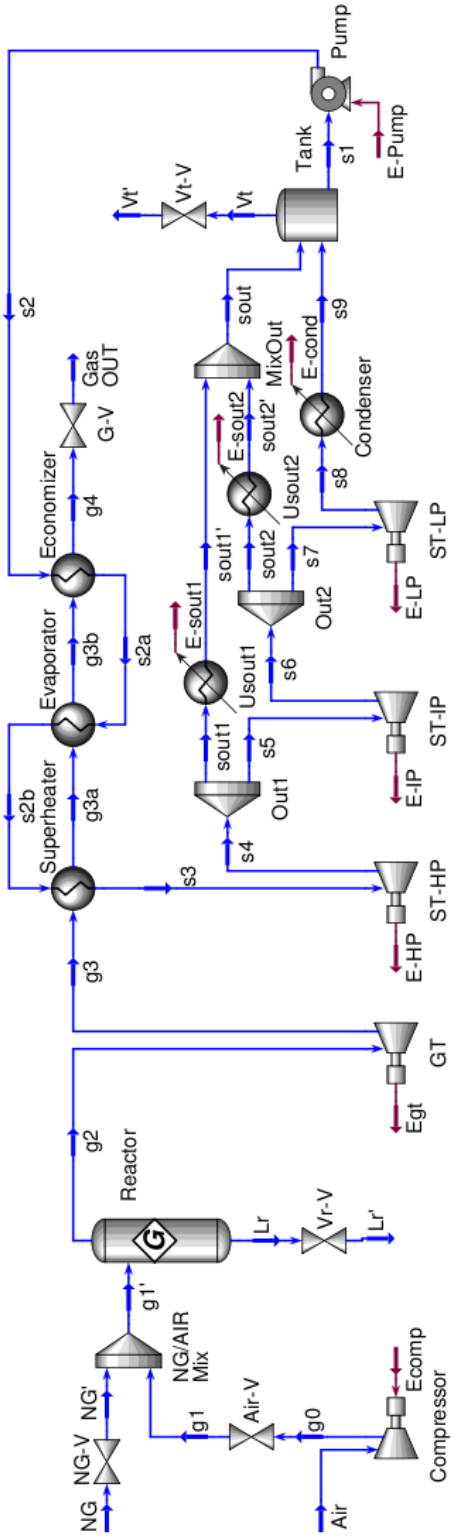

Figure 6.4: Combined/Cogenerative cycle model.

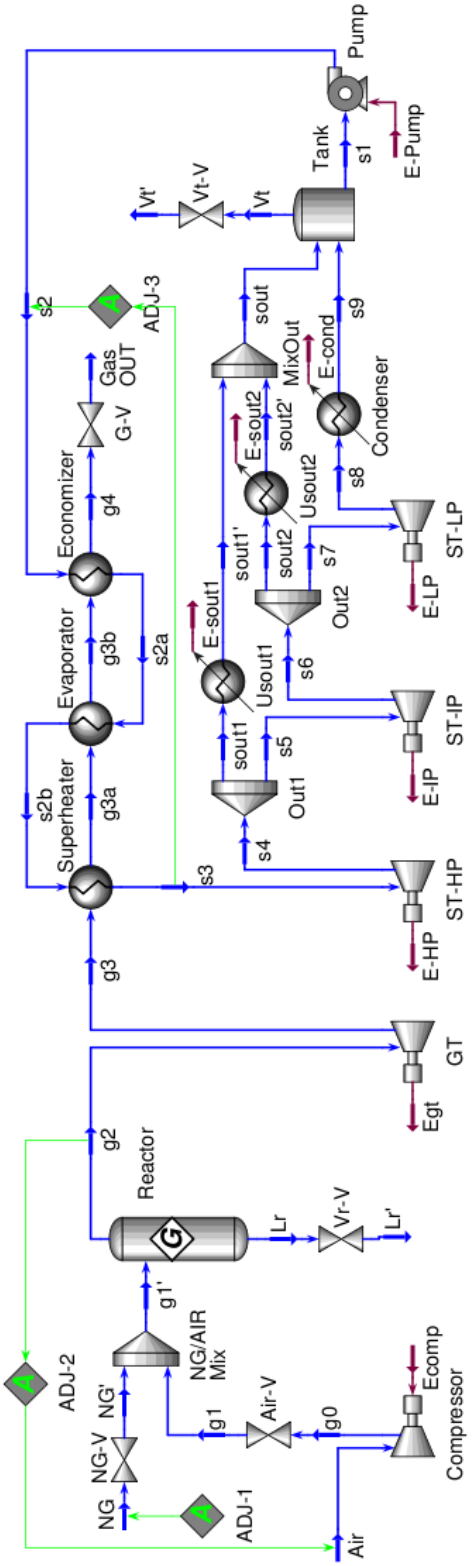

Figure 6.5: Combined/Cogenerative cycle model-adjusts.

6.3.1 Parametric Analysis

In order to make a parametric analysis, the model uses three adjusts (figure 6.5) as the previous one (section 6.2): *ADJ-1* sets the net power output to 100 *MW*, *ADJ-2* sets the exhaust gas temperature to 1250°C before entering the gas turbine and *ADJ-3* sets the steam temperature around 550°C before entering the steam turbine.

If the model works as a combined cycle, the efficiency is expressed by:

$$\begin{aligned}\eta_{CC} &= \frac{(E_{gt} - E_{comp}) + (E_{HP} + E_{IP} + E_{LP} - E_{pump}/0.6)}{\dot{m}_{NG}[LHV]_{NG}} \\ &= \frac{(E_{netGC} + E_{netSC})}{\dot{m}_{NG}[LHV]_{NG}} \\ &= \frac{E_{netCC}}{\dot{m}_{NG}[LHV]_{NG}}\end{aligned}$$

The parametric analysis of the combined cycle configuration model is similar to the previous models, the most important parameters are the pressure of natural gas and the water high pressure, their trends are similar to the previous models in which the efficiency is maximized working at the water high pressure limit (around 100 bar).

The two middle pressures variation does not provide relevant modification of the plant efficiency as shown in figure 6.6.

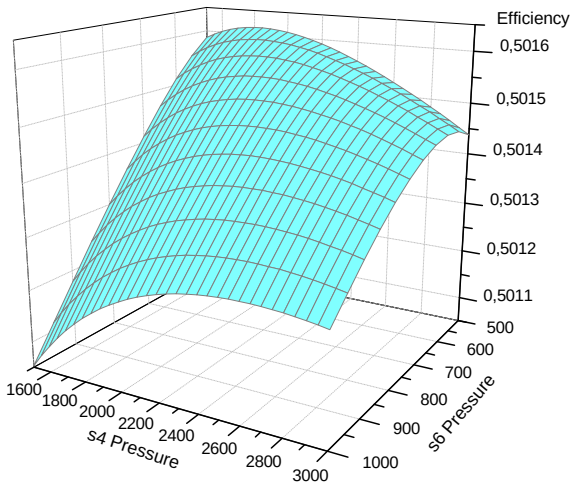

Figure 6.6: s4 and s6 pressures variations.

The criterion of performance used in the cogenerative model is the *fuel energy saving ratio* (section 3.4 on page 41) expressed for standard plants as

$$FESRa = 1 - \frac{\dot{m}_{NG}[LHV]_{NG}}{\frac{E_{netCC}}{0.38 \cdot p} + \frac{E_{sout1}}{0.9} + \frac{E_{sout2}}{0.9}}$$

and for advanced plants as

$$FESRb = 1 - \frac{\dot{m}_{NG}[LHV]_{NG}}{\frac{E_{netCC}}{0.5 \cdot p} + \frac{E_{sout1}}{0.9} + \frac{E_{sout2}}{0.9}}$$

and the *Ecabert efficiency*

$$R_E = \frac{E_{netCC}}{\dot{m}_{NG}[LHV]_{NG} - \frac{E_{sout1}}{0.9} - \frac{E_{sout2}}{0.9}}$$

The analysis has been made leaving the two utilities duties to 25 *MW* the steam intermediate pressure to 21 bar and the low pressure to 6 bar.

Figures 6.7 and 6.8 represent the fuel energy saving ratio and the Ecabert efficiency variations with the most important variables, natural gas pressure and water high pressure.

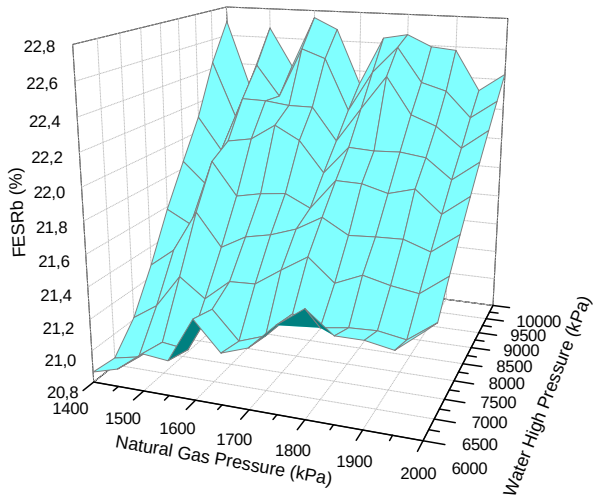

Figure 6.7: FESRb variation with pressures.

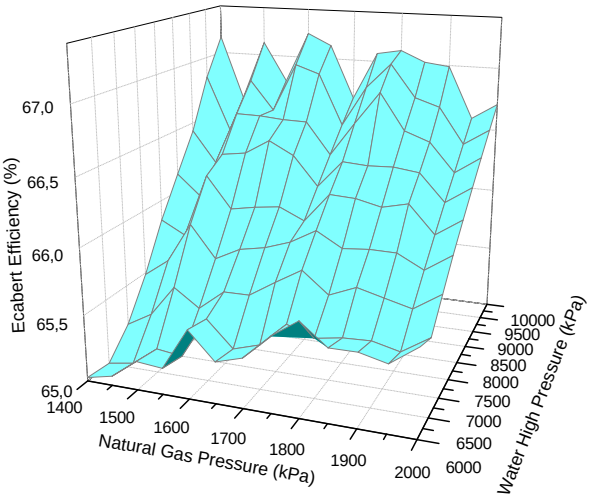

Figure 6.8: Ecabert efficiency variation with pressures.

6.3.2 Optimization

The optimization variables used in the combined cycle model are the natural gas mass flow and pressure, the air mass flow and the water mass flow and high pressure.

There are the same constraints used in the other models as the exhaust gas temperature below 1250°C and the steam temperature around 550°C. The objective function is the efficiency η_{CC}. The complete data are shown in table 6.2. As already discussed in the other models, the maximum efficiency is reached when the water high pressure is close to its limit (100 bar). On the contrary the natural gas pressure is optimal at 15.57 bar. After the optimization the natural gas and the air mass flow are slightly reduced, on the contrary the water mass flow is increase of 4000 kg/h. The efficiency increases from 53.75% to 54.77%. This is the model highest efficiency reached in this thesys and it can be explained because we have a satisfying heat exchange in the HRSG and an optimized allocation of the steam power produced using three steam turbine operating at three different pressures.

The cogenerative cycle is optimized using the same variables and constraints. The objective function is the FESRb index. After the optimization the index increases from 21.50% to 23.05% and the Ecabert efficiency increases from 65.74% to 67.60%. The optimization drastically reduces the air mass flow ($\simeq -50000$ kg/h) and, as expected, rises the water high pressure close to its limit.

Table 6.2: Combined cycle model data

Parameter	Symbol	Standard	Optimized	Unit
Natural Gas	Mass Flow ($\dot{m}_{NG}$)	$1.385 \cdot 10^4$	$1.355 \cdot 10^4$	kg/h
	Pressure (P_{NG})	18.00	15.57	bar
Air	Mass Flow ($\dot{m}_{Air}$)	$6.401 \cdot 10^5$	$5.994 \cdot 10^5$	kg/h
	Pressure (P_{air})	1	1	bar
Compressor	Adiabatic Eff. (η_{Ac})	88	88	%
	Polytropic Eff. (η_{Pc})	91.53	91.41	%
	Duty (E_{Comp})	$7.68 \cdot 10^4$	$6.68 \cdot 10^4$	kW
Reactor	Efficiency (η_R)	99.9	99.9	%
	g1′ Pressure ($P_{g1'}$)	17.80	15.37	bar
	g2 Temp. (T_{g2})	1246	1255	°C
Gas Turbine	Adiabatic Eff. (η_{Agt})	90	90	%
	Polytropic Eff. (η_{Pgt})	86.55	86.80	%
	Duty (E_{gt})	$1.42 \cdot 10^5$	$1.29 \cdot 10^5$	kW
	g3 Temp. (T_{g3})	616.5	650.2	°C
Economizer	UA (UA_{Ec})	$4.44 \cdot 10^6$	$8.89 \cdot 10^6$	kJ/h°C
	Delta P shell (ΔP_{sh})	0.10	0.10	bar
	Delta P tube (ΔP_{tb})	0.20	0.20	bar
	s2 Temp. (T_{s2})	33.8	34.07	°C
	s2a Temp. (T_{s2a})	284.8	309.80	°C
	GasOut Temp. (T_{gO})	113	90.01	°C
Evaporator	UA (UA_{Ev})	$2.35 \cdot 10^6$	$2.19 \cdot 10^6$	kJ/h°C
	Delta P shell (ΔP_{sh})	0.10	0.10	bar
	Delta P tube (ΔP_{tb})	0.20	0.20	bar
	s2b Temp. (T_{s2b})	284.6	309.7	°C
	g3b Temp. (T_{g3b})	294.8	319.8	°C
SuperHeater	UA (UA_{Sh})	$4.81 \cdot 10^5$	$5.29 \cdot 10^5$	kJ/h°C
	Delta P shell (ΔP_{sh})	0.10	0.10	bar
	Delta P tube (ΔP_{tb})	0.20	0.20	bar
	s3 Temp. (T_{s3})	540.4	567	°C
	g3a Temp. (T_{g3a})	525.3	540.5	°C
Water	Mass Flow ($\dot{m}_w$)	$1.103 \cdot 10^5$	$1.145 \cdot 10^5$	kg/h
	Pressure (P_{s2})	70.00	99.93	bar
HP Steam Turbine	Adiabatic Eff. (η_{Ahp})	90	90	%
	Polytropic Eff. (η_{Php})	88.65	88.17	%
	Duty (E_{st})	$1.03 \cdot 10^4$	$1.36 \cdot 10^4$	kW
	s4 Pressure P_{s4}	21	21	bar
IP Steam Turbine	Adiabatic Eff. (η_{Aip})	90	90	%
	Polytropic Eff. (η_{Pip})	88.53	88.51	%
	Duty (E_{st})	$8.46 \cdot 10^3$	$8.32 \cdot 10^3$	kW
	s4 Pressure P_{s4}	6.0	6.0	bar
LP Steam Turbine	Adiabatic Eff. (η_{Alp})	90	90	%
	Polytropic Eff. (η_{Plp})	88.82	88.82	%
	Duty (E_{st})	$1.68 \cdot 10^4$	$1.69 \cdot 10^4$	kW
	s4 Pressure P_{s4}	0.15	0.15	bar
Condenser	Delta P (ΔP_{cond})	0.10	0.10	bar
	Duty E_{cond}	$2.46 \cdot 10^8$	$2.51 \cdot 10^8$	kJ/h
Pump	Adiabatic Eff. (η_{Ap})	75	75	%
	Delta P (ΔP_p)	69.95	99.88	bar
	Duty (E_{pump})	285.40	422.93	kW
Efficiency	Net Eff. (η_{CCGT})	53.75	54.77	%
	RW	53.65	61.73	%

Table 6.3: Cogenerative cycle model data

Parameter	Symbol	Standard	Optimized	Unit
Natural Gas	Mass Flow ($\dot{m}_{NG}$)	$1.544 \cdot 10^4$	$1.507 \cdot 10^4$	kg/h
	Pressure (P_{NG})	18,00	15,37	bar
Air	Mass Flow ($\dot{m}_{Air}$)	$7.111 \cdot 10^5$	$6.647 \cdot 10^5$	kg/h
	Pressure (P_{air})	1	1	bar
Compressor	Adiabatic Eff. (η_{Ac})	88	88	%
	Polytropic Eff. (η_{Pc})	91.53	91.40	%
	Duty (E_{Comp})	$8.53 \cdot 10^4$	$7.35 \cdot 10^4$	kW
Reactor	Efficiency (η_R)	99.9	99.9	%
	g1′ Pressure ($P_{g1'}$)	17.80	15.17	bar
	g2 Temp. (T_{g2})	1248	1255	°C
Gas Turbine	Adiabatic Eff. (η_{Agt})	90	90	%
	Polytropic Eff. (η_{Pgt})	86.55	86.25	%
	Duty (E_{gt})	$1.58 \cdot 10^5$	$1.42 \cdot 10^5$	kW
	g3 Temp. (T_{g3})	618.3	652.9	°C
Economizer	UA (UA_{Ec})	$4.87 \cdot 10^6$	$1.26 \cdot 10^7$	kJ/h°C
	Delta P shell (ΔP_{sh})	0.10	0.10	bar
	Delta P tube (ΔP_{tb})	0.20	0.20	bar
	s2 Temp. (T_{s2})	33.8	34.07	°C
	s2a Temp. (T_{s2a})	284.8	309.8	°C
	GasOut Temp. (T_{gO})	113.8	80.2	°C
Evaporator	UA (UA_{Ev})	$2.60 \cdot 10^6$	$2.45 \cdot 10^6$	kJ/h°C
	Delta P shell (ΔP_{sh})	0.10	0.10	bar
	Delta P tube (ΔP_{tb})	0.20	0.20	bar
	s2b Temp. (T_{s2b})	284.8	309.7	°C
	g3b Temp. (T_{g3b})	294.8	319.8	°C
SuperHeater	UA (UA_{Sh})	$5.74 \cdot 10^5$	$4.80 \cdot 10^5$	kJ/h°C
	Delta P shell (ΔP_{sh})	0.10	0.10	bar
	Delta P tube (ΔP_{tb})	0.20	0.20	bar
	s3 Temp. (T_{s3})	549.5	540.4	°C
	g3a Temp. (T_{g3a})	524.4	549.5	°C
Water	Mass Flow ($\dot{m}_w$)	$1.221 \cdot 10^5$	$1.322 \cdot 10^5$	kg/h
	Pressure (P_{s2})	70.00	99.90	bar
HP Steam Turbine	Adiabatic Eff. (η_{Ahp})	90	90	%
	Polytropic Eff. (η_{Php})	88.65	88.15	%
	Duty (E_{st})	$1.15 \cdot 10^4$	$1.50 \cdot 10^4$	kW
	s4 Pressure P_{s4}	21	0.15	bar
IP Steam Turbine	Adiabatic Eff. (η_{Aip})	90	90	%
	Polytropic Eff. (η_{Pip})	88.53	88.63	%
	Duty (E_{st})	$7.19 \cdot 10^3$	$7.05 \cdot 10^3$	kW
	s4 Pressure P_{s4}	6.0	6.0	bar
LP Steam Turbine	Adiabatic Eff. (η_{Alp})	90	90	%
	Polytropic Eff. (η_{Plp})	88.82	88.82	%
	Duty (E_{st})	$9.09 \cdot 10^3$	$9.78 \cdot 10^3$	kW
	s4 Pressure P_{s4}	0.15	0.15	bar
sout1	Mass Flow ($\dot{m}_{sout1}$)	$2.966 \cdot 10^4$	$3.094 \cdot 10^4$	kg/h
	sout1 Temp. (T_{sout1})	369.3	310.9	°C
	Duty (E_{sout1})	$2.5 \cdot 10^4$	$2.5 \cdot 10^4$	kW
sout2	Mass Flow ($\dot{m}_{sout2}$)	$3.267 \cdot 10^4$	$3.386 \cdot 10^4$	kg/h
	sout2 Temp. (T_{sout2})	219.1	171.0	°C
	Duty (E_{sout2})	$2.5 \cdot 10^4$	$2.5 \cdot 10^4$	kW
Condenser	Delta P (ΔP_{cond})	0.10	0.10	bar
	Duty E_{cond}	$1.35 \cdot 10^8$	$1.48 \cdot 10^8$	kJ/h
Pump	Adiabatic Eff. (η_{Ap})	75	75	%
	Delta P (ΔP_p)	69.95	99.85	bar
	Duty (E_{pump})	315.85	488.45	kW
Efficiency	FESRa	37.17	38.40	%
	FESRb	21.50	23.05	%
	R_E	65.74	67.60	%
	RW	37.56	45.39	%

6.4 CCGT TRIPLE PRESSURE REHEAT CYCLE

The CCGT Triple pressure reheat steam cycle (R3PR) model (figure 6.10) is based on a gas turbine power plant working with a three pressure steps with reheating heat recovery steam generator [34] (figure 6.9). The feed water stream is splitted in three substreams and compressed at different pressures. After the vaporization and the superheating each stream is sent to a specific steam turbine working at high pressure, intermediate pressure and low pressure. After the HP steam turbine, the high pressure steam is reaheated and mixed with the IP steam before entering the IP steam turbine. This new IP stream, after the IP turbine, is mixed again with the LP steam before entering the LP steam turbine.

There are several new degrees of freedom in this model, so it has been followed the [34] model data. In the gas cycle it has been set the natural gas mass flow and pressure, and the air mass flow. In the steam cycle it has been set the water mass flow, the temperature and pressure of s_{tot} stream (110°C and 2 bar, i.e. [34]), the fractions in the TEE_{100}, the $saHP_1$ pressure, the $saIP_1$ pressure, the $saLP_1$ pressure, the phase fraction before and after each evaporator, s3 temperature, $s4_1$ temperature, sdIP temperature (290°C according with [34]), sdLP temperature (200°C according with [34]) and the s8 pressure.

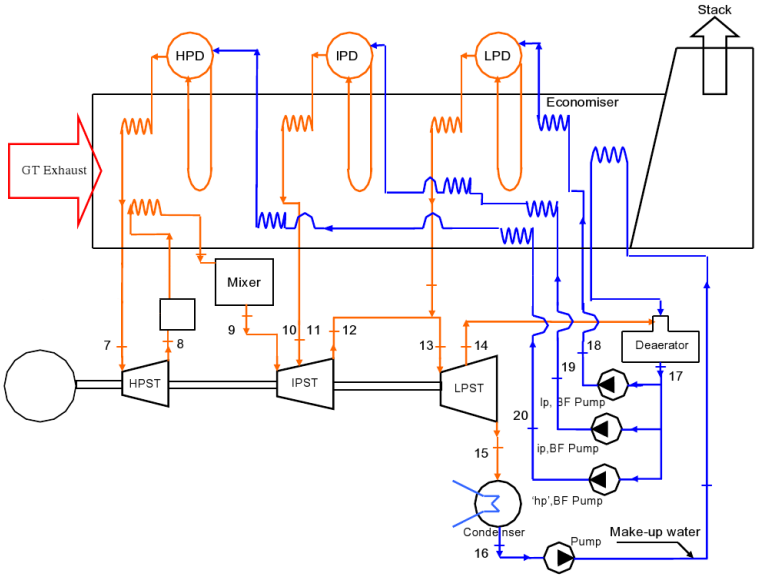

Figure 6.9: CCGT Triple pressure cycle scheme.

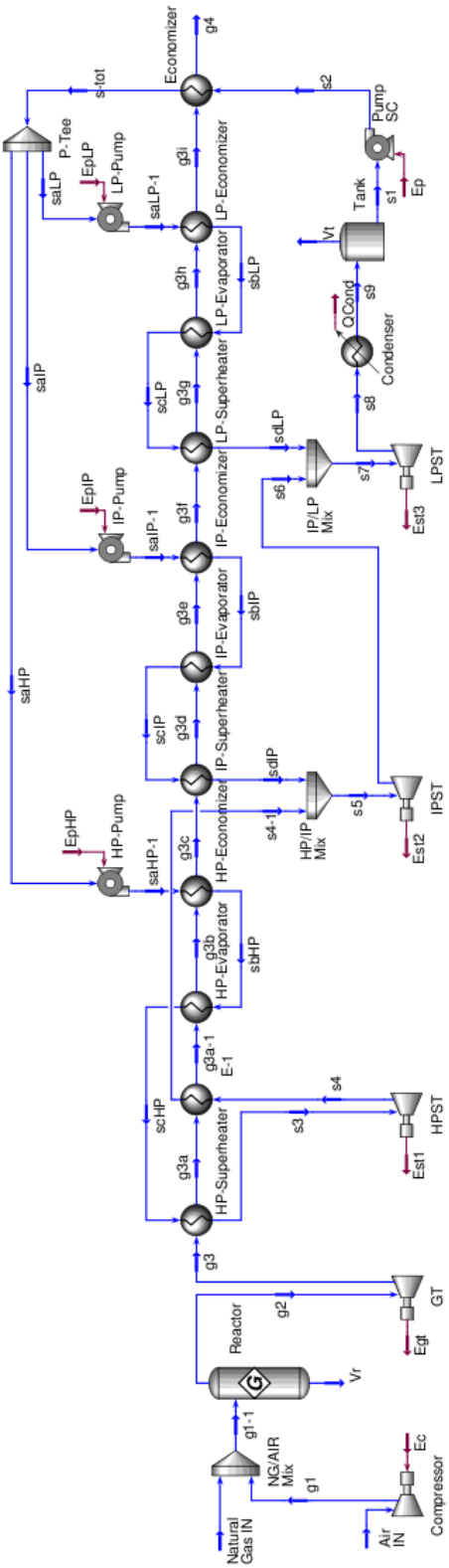

Figure 6.10: CCGT Triple pressure cycle model.

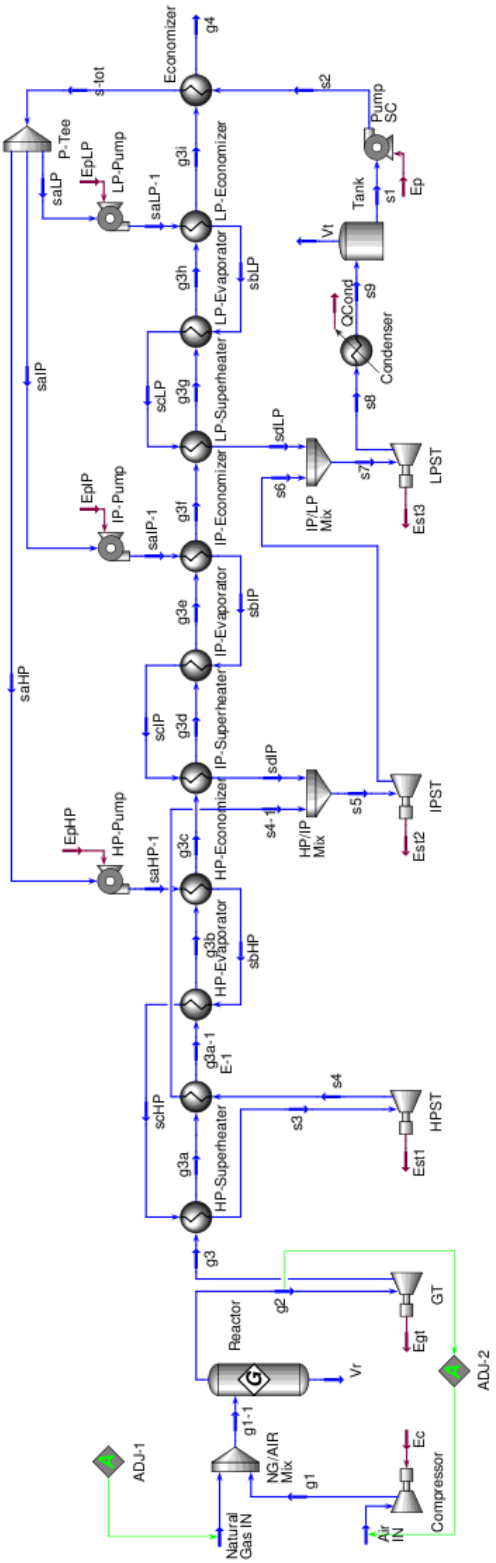

Figure 6.11: CCGT Triple pressure cycle model-adjusts.

6.4.1 Parametric Analysis

Two adjusts has been used (figure 6.11) operating only on the gas cycle: *ADJ-1* sets the net power output to 100 *MW* and *ADJ-2* sets the exhaust gas temperature to 1250°C before entering the gas turbine. Another adjust operating in the steam cycle has been used in the previous models in order to keep the s3 temperature around 550°C. On the contrary, in this case, a degree of freedom has been used to set s3 temperature, because using a minimum approach in the evaporators causes some problems of temperature cross in the superheaters.

The net efficiency is

$$\eta_{CC} = \frac{(E_{netGC} + E_{netSC})}{\dot{m}_{NG}[LHV]_{NG}} = \frac{E_{netCC}}{\dot{m}_{NG}[LHV]_{NG}}$$

where

$$E_{netGC} = E_{gt} - E_{comp}$$

$$E_{netSC} = E_{HP} + E_{IP} + E_{LP} - \sum_{i=1}^{4} E_{p,i}/0.6$$

The fractions in TEE_{100} are set as in [34]:

- $x_{saHP} = 0.64$,
- $x_{saIP} = 0.22$,
- $x_{saLP} = 0.14$.

This is the optimal setting, a variation on these fractions causes a reduction on the plant efficiency.

Furthermore, the variation of the sdIP and sdLP temperatures has been analysed. They are set to 290°C and 200°C, according to the model [34]. An increase on these temperature causes an increase of the efficiency around $0.02 \div 0.05\%$, but if $T_{sdIP} > 300°C$ or $T_{sdLP} > 210°C$ temperature crosses appear in intermediate pressure superheater or low pressure superheater respectively. Thus, it is better to leave a 10°C ΔT avoiding to work at limit conditions.

After a parametric analysis, the most important parameters that influence the efficiency are still the natural gas pressure and the water high pressure.

6.4.2 Optimization

The SQP optimization uses as optimization variables:

- the natural gas pressure (P_{NG}),
- the natural gas mass flow ($\dot{m}_{NG}$),
- the air mass flow ($\dot{m}_{Air}$),
- the water mass flow ($\dot{m}_{s2}$),
- the water high pressure (P_{saHP1}),
- the water intermediate pressure (P_{saIP1}),
- the water low pressure (P_{saLP1}),
- s3 temperature,
- s_{4-1} temperature,
- s_{tot} temperature.

The constraints are the net power produced ($99.9 \div 101 MW$), g2 temperature ($1225 \div 1255°C$) and other constraints to avoid temperature crosses:

- g3c temperature ($300 \div 400°C$),
- g3f temperature ($210 \div 300°C$),
- $\Delta T_{HP} = (T_{g3b} - T_{sbHP}) = (10 \div 150°C)$,
- $\Delta T_{IP} = (T_{g3e} - T_{sbIP}) = (10 \div 100°C)$,
- $\Delta T_{LP} = (T_{g3h} - T_{sbLP}) = (10 \div 100°C)$.

The objective function is the net efficiency η_{CC}. The highest efficiency (51.76%) is related to the water high pressure that is at its limit (100 bar), the complete data are shown on table 6.4. Other optimized models have also been realized with lower pressures, for a 70 bar water high pressure we have an efficiency of 50.91% with an $RW = 62.12\%$ and for a 90 bar high water pressure we have a 51.23% efficiency with an $RW = 63.54\%$.

Table 6.4: Triple pressure reheat cycle model data

Parameter	Symbol	Standard	Optimized	Unit
Natural Gas	Mass Flow ($\dot{m}_{NG}$)	$1.587 \cdot 10^4$	$1.433 \cdot 10^4$	kg/h
	Pressure (P_{NG})	18,00	21,00	bar
Air	Mass Flow ($\dot{m}_{Air}$)	$7.310 \cdot 10^5$	$6.826 \cdot 10^5$	kg/h
	Pressure (P_{air})	1	1	bar
Compressor	Adiabatic Effic. (η_{Ac})	88	88	%
	Polytropic Effic. (η_{Pc})	91.53	91.66	%
	Duty (E_{Comp})	$8.77 \cdot 10^4$	$8.84 \cdot 10^4$	kW
Reactor	Efficiency (η_R)	99.9	99.9	%
	g1′ Pressure ($P_{g1'}$)	17.80	21.00	bar
	g2 Temperature (T_{g2})	1248	1250	°C
Gas Turbine	Adiabatic Effic. (η_{Agt})	90	90	%
	Polytropic Effic. (η_{Pgt})	86.91	86.65	%
	Duty (E_{gt})	$1.52 \cdot 10^5$	$1.49 \cdot 10^5$	kW
	g3 Temperature (T_{g3})	658.5	630.3	°C
HP Economizer	UA (UA_{HP-Ec})	$3.43 \cdot 10^5$	$6.19 \cdot 10^5$	kJ/h°C
	Delta P shell (ΔP_{sh})	0.05	0.05	bar
	Delta P tube (ΔP_{tb})	0.20	0.20	bar
	saHP-1 Temp. (T_{saHP})	111.0	111.4	°C
	g3c Temp. (T_{g3c})	360.7	302.7	°C
HP Evaporator	UA (UA_{HP-Ev})	$5.67 \cdot 10^5$	$7.04 \cdot 10^5$	kJ/h°C
	Delta P shell (ΔP_{sh})	0.05	0.05	bar
	Delta P tube (ΔP_{tb})	0.20	0.20	bar
	sbHP Temp. (T_{sbHP})	284.8	309.9	°C
	g3b Temp. (T_{g3b})	439.8	405.7	°C
E-1	UA (UA_{E-1})	$7.96 \cdot 10^4$	$1.24 \cdot 10^5$	kJ/h°C
	Delta P shell (ΔP_{sh})	0.05	0.05	bar
	Delta P tube (ΔP_{tb})	0.20	0.20	bar
	s4 Temp. (T_{s4})	367.2	341.6	°C
	s4-1 Temp. (T_{s41})	450.0	450.0	°C
	g3a-1 Temp. (T_{g3a})	582.9	540.3	°C
HP SuperHeater	UA (UA_{HP-Sh})	$2.67 \cdot 10^5$	$3.80 \cdot 10^5$	kJ/h°C
	Delta P shell (ΔP_{sh})	0.05	0.05	bar
	Delta P tube (ΔP_{tb})	0.20	0.20	bar
	scHP Temp. (T_{scHP})	284.6	309.8	°C
	s3 Temp. (T_{s3})	550.0	564.4	°C
	g3a Temp. (T_{g3a})	599.2	563.4	°C
IP Economizer	UA (UA_{IP-Ec})	$1.15 \cdot 10^5$	$3.68 \cdot 10^5$	kJ/h°C
	Delta P shell (ΔP_{sh})	0.05	0.05	bar
	Delta P tube (ΔP_{tb})	0.20	0.20	bar

Table 6.4: Continued on next page

Table 6.4: continued from previous page

Parameter	Symbol	Standard	Optimized	Unit
	saIP-1 Temp. (T_{saIP})	110.3	110.3	°C
	g3f Temp. (T_{g3f})	276.8	211.8	°C
IP Evaporator	UA (UA_{IP-Ev})	$4.91 \cdot 10^5$	$1.56 \cdot 10^6$	kJ/h°C
	Delta P shell (ΔP_{sh})	0.05	0.05	bar
	Delta P tube (ΔP_{tb})	0.20	0.20	bar
	sbIP Temp. (T_{sbIP})	214.8	220.2	°C
	g3e Temp. (T_{g3e})	292.9	230.2	°C
IP SuperHeater	UA (UA_{IP-Sh})	$4.37 \cdot 10^4$	$1.16 \cdot 10^5$	kJ/h°C
	Delta P shell (ΔP_{sh})	0.05	0.05	bar
	Delta P tube (ΔP_{tb})	0.20	0.20	bar
	scIP Temp. (T_{scIP})	214.4	219.8	°C
	sdIP Temp. (T_{sdIP})	290.0	290.0	°C
	g3d Temp. (T_{g3d})	355.4	297.4	°C
LP Economizer	UA (UA_{LP-Ec})	$4.04 \cdot 10^4$	$1.34 \cdot 10^5$	kJ/h°C
	Delta P shell (ΔP_{sh})	0.05	0.05	bar
	Delta P tube (ΔP_{tb})	0.20	0.20	bar
	saLP-1 Temp. (T_{saLP})	110.1	110.0	°C
	g3i Temp. (T_{g3i})	225.8	156.1	°C
LP Evaporator	UA (UA_{LP-Ev})	$3.92 \cdot 10^5$	$1.32 \cdot 10^6$	kJ/h°C
	Delta P shell (ΔP_{sh})	0.05	0.05	bar
	Delta P tube (ΔP_{tb})	0.20	0.20	bar
	sbLP Temp. (T_{sbLP})	157.5	150.3	°C
	g3h Temp. (T_{g3h})	230.3	160.3	°C
LP SuperHeater	UA (UA_{LP-Sh})	$1.59 \cdot 10^4$	$5.96 \cdot 10^4$	kJ/h°C
	Delta P shell (ΔP_{sh})	0.05	0.05	bar
	Delta P tube (ΔP_{tb})	0.20	0.20	bar
	scLP Temp. (T_{scLP})	156.2	148.7	°C
	sdLP Temp. (T_{sdLP})	200.0	200.0	°C
	g3g Temp. (T_{g3g})	275.0	209.5	°C
Economizer	UA (UA_{Ec})	$2.76 \cdot 10^5$	$7.76 \cdot 10^5$	kJ/h°C
	Delta P shell (ΔP_{sh})	0.05	0.05	bar
	Delta P tube (ΔP_{tb})	0.20	0.20	bar
	s2 Temp. (T_{s2})	46.0	29.3	°C
	s-tot Temp. (T_{tot})	110.0	110.0	°C
	g4 Temp. (T_{g4})	183.2	97.7	°C
Water	Mass Flow ($\dot{m}_w$)	$1.247 \cdot 10^5$	$1.247 \cdot 10^5$	kg/h
	Pressure (P_{s2})	2.20	2.20	bar
HP-Pump	Adiabatic Effic. (η_{HP})	75	75	%
	Delta P (ΔP_{HP})	68.00	98.00	bar
	Duty (E_{HP})	213.94	308.323	kW

Table 6.4: Continued on next page

Table 6.4: concluded from previous page

Parameter	Symbol	Standard	Optimized	Unit
	saHP ($\dot{m}_{saHP}$)	$7.980 \cdot 10^4$	$7.980 \cdot 10^4$	kg/h
IP-Pump	Adiabatic Effic. (η_{IP})	75	75	%
	Delta P (ΔP_{IP})	19.00	21.26	bar
	Duty (E_{IP})	20.55	22.98	kW
	saIP ($\dot{m}_{saIP}$)	$2.743 \cdot 10^4$	$1.322 \cdot 10^5$	kg/h
LP-Pump	Adiabatic Effic. (η_{LP})	75	75	%
	Delta P (ΔP_{LP})	4.00	3.00	bar
	Duty (E_{LP})	2.75	2.06	kW
	saLP ($\dot{m}_{saLP}$)	$1.746 \cdot 10^4$	$1.322 \cdot 10^5$	kg/h
HP Steam Turbine	Adiabatic Effic. (η_{Ahp})	90	90	%
	Polytropic Effic. (η_{Php})	88.62	88.28	%
	Duty (E_{st})	$7.66 \cdot 10^3$	$9.01 \cdot 10^3$	kW
	s4 Pressure P_{s4}	20.6	22.86	bar
IP Steam Turbine	Adiabatic Effic. (η_{Aip})	90	90	%
	Polytropic Effic. (η_{Pip})	88.45	88.03	%
	Duty (E_{st})	$9.41 \cdot 10^3$	$1.12 \cdot 10^4$	kW
	s6 Pressure P_{s6}	5.4	4.4	bar
LP Steam Turbine	Adiabatic Effic. (η_{Alp})	90	90	%
	Polytropic Effic. (η_{Plp})	88.85	88.80	%
	Duty (E_{st})	$1.89 \cdot 10^4$	$1.95 \cdot 10^4$	kW
	s4 Pressure P_{s4}	0.15	0.09	bar
Condenser	Delta P (ΔP_{cond})	0.05	0.05	bar
	Duty E_{cond}	$2.77 \cdot 10^8$	$2.77 \cdot 10^8$	kJ/h
Pump	Adiabatic Effic. (η_{Ap})	75	75	%
	Delta P (ΔP_p)	2.1	2.2	bar
	Duty (E_{pump})	9.78	9.93	kW
Efficiency	Net Effic. (η_{CCGT})	47.01	51.76	%
	RW	54.98	64.51	%
	GC Effic. (η_{GC})	30.33	31.46	%
	SC Effic. (η_{SC})	16.68	20.30	%

7 CONCLUSIONS

The goal of this thesis was to explore the potential of using process simulators, namely Aspen HYSYS, to model and optimize different kinds of gas turbine cycles.

The second chapter dealt with a natural gas overview, typical compositions, formation and principal uses. The second part of this chapter was dedicated to an introduction on the principles of design and operation of simple gas turbine power plant configurations.

The third chapter was devoted to analyse the advanced gas turbine power plants starting from the combined cycle power plants, with different kinds of possible implementations, to the cogenerative cycle power plants.

In the fourth chapter several combined cycle and cogenerative cycle models found in the literature have been presented.

Chapters five and six explain the simple and advanced gas turbine power plant models realized using Aspen HYSYS. Each model has been developed starting from a model construction based on the literature. The gas cycle has been modelled using a compressor, a Gibbs reactor in which the reactions occur, and a gas turbine (expander) where the energy is produced. The steam cycle has been modelled in different ways starting from a simple steam cycle with one heat exchanger, as heat recovery steam generator, and one steam turbine. The heat recovery steam generator model has been improved using three heat exchangers, each one devoted to a peculiar application (economizing, evaporation and superheating). Furthermore, a combined/cogenerative model has been developed, in which there are a three heat exchangers steam generator and three steam turbines. The model considers a possible vapour draw, used for cogeneration, between one turbine and the subsequent one. This model represents in a fairly accurate way a typical modern combined cycle power plant in which we have a three pressure heat recovery steam generator and three steam turbine.

In each model the degrees of freedom definition has been very important to create a useful model for a parametric analysis. The main degrees have been used in the natural gas mass flow and pressure, the water pressure and the vapour phase fractions in the heat recovery steam generator. The use of Adjust blocks has

been necessary to satisfy the different constraints such as the combustion chamber outlet gas temperature or the superheated steam temperature.

Furthermore, a parametric analysis has been undertaken using the HYSYS Case Study utility, in which it is possible to specify several independent and dependent variables to analyse different configurations in a systematic way.

The analysis ends with a model's optimization via the Hyprotech SQP Optimizer, in which the user have to set the optimization variables, constraint functions and the objective function (to maximize or minimize).

The parametric analysis showed how the natural gas pressure is a crucial variable in the simple gas cycle, the efficiency raises with the pressure and lower mass flows are needed to achieve the same power production. The pressure is extremely important also in the steam cycle, the optimization shows that using the highest water pressure the efficiency is higher. In the combined cycles, the water high pressure is the main variable that maximizes the efficiency. Another important variable is the combustion chamber outlet gases temperature that can raise significantly the efficiency. Unfortunately, this temperature must be maintained below 1250°C, consistent with mechanical strength and corrosion resistance. Several studies have been made in order to raise this temperature, using gas turbines with air/steam blade cooling. An example is the *closed-loop-steam-cooling* (CLSC) [34] in which a part of exhaust steam from high pressure turbine is utilized for blade cooling, and while cooling the blades, it gets reheated, thereafter it is mixed with steam coming out from reheater of Heat Recovery Steam Generator (HRSG) for further expansion in steam turbine or the traditional *air-film-cooling* (AFC) technique [21].

In the combined cycles the optimal natural gas pressure is in the range $15.5 - 16.5$ bar differently from the simple gas cycle, and this is in accordance with the combined cycle literature.

Possible future works may include implementations of simulation models of different cycles, such as those with two or more gas turbines. Other extensions may consider the use of different types of reactors (kinetic, equilibrium, etc.) rather than the Gibbs one used in this work to model the combustion chamber. Furthermore, the use of Aspen HYSYS for dynamic simulation of simple and advanced cycles may be investigated.

BIBLIOGRAPHY

[1] P. Ailer, I. Santa, C. Szederkenyi, and K.M. Hangos. Nonlinear model-building of a lower power gas turbine. *Periodica Polytechnica Ser. Transp. Eng, vol. 29*, 2001. (Cited on page 46.)

[2] A. Bagnasco, B. Delfino, G.B. Denegri, and S. Massucco. Management and dynamic performance of combined cycle power plants during parallel and islanding operation. *IEEE Trans. Energy Convers., vol.13*, 1998. (Cited on pages 48, 70, and 71.)

[3] Cigre Task Force C4.02.25. *Modeling of Gas Turbines and Steam Turbines in Combined Cycle Power Plants*, 2003. (Cited on pages 46, 56, and 70.)

[4] Sadi Carnot. *Réflexions Sur la Puissance Motrice du Feu et Sur les Machines Propres á dÉvelopper Cette Puissance*. Sylvestre Bonnard, Paris, 1824. (Cited on page 19.)

[5] C. Casarosa, F. Donatini, and A. Franco. Thermoeconomic optimization of HRSG operative parameters for combined plants. In *Proceedings of the ECOS 2001 Conference vol. II*, Turkey, 2001. (Cited on page 36.)

[6] Y.A. Cengel and M.A. Boles. *Thermodynamics: An Engineering Approach*. McGraw-Hill, New York, 1994. (Cited on pages 46 and 52.)

[7] H. Cohen, G. Rogers, and H. Saravanamuttoo. *Gas Turbine Theory, 4th ed.*, 1996. (Cited on pages 46, 51, and 52.)

[8] G. Crosa, F. Pittaluga, A. Trucco, F. Beltrami, A. Torelli, and F. Traverso. Heavy-duty gas turbine plant aerothermodynamic simulation using simulink. *ASME J. Eng. Gas Turbines and Power, vol.120*, 1998. (Cited on page 46.)

[9] FP de Mello. Boiler models for system dynamic performance studies. *IEEE Trans, PWRS*, 1991. (Cited on page 63.)

[10] P.J. Deschamps. Advanced combined cycle alternatives with the latest gas turbines. *ASME Journal of Engineering for Gas Turbines and Power 120*, 1998. (Cited on page 36.)

[11] Alessandro Franco and Claudio Casarosa. On some perspectives for increasing the efficiency of combined cycle power plants. *Applied Thermal Engineering* 22, 2002. (Cited on page 35.)

[12] Tony Giampaolo. *Gas Turbine Handbook: Principles and Practices, Third Edition*. Fairmont Press, London SW15 2NU, UK, 2006.

[13] L. N. Hannett, G. Jee, and B. Fardanesh. A governor/turbine model for a twin-shaft combustion turbine. *IEEE Trans. Power syst., vol.10*, 1995. (Cited on page 53.)

[14] J.H. Horlock. *Advanced Gas Turbine Cycles*. Elsevier Science Ltd, Kidlington, Oxford OX5 lGB, UK, 2003.

[15] R. Kehlhofer. *Combined Cycle Gas and Steam Turbine Power Plants*. Fairmont Press, Lilburn, GA, 1991. (Cited on page 33.)

[16] J.H. Kim, T.W. Song, T.S. Kim, and S.T. Ro. Model development and simulation of transient behavior of heavy duty gas turbines. *ASME J. Eng. Gas Turbines and Power, vol.123*, 2001. (Cited on page 46.)

[17] T.J. Kotas. *The Exergy Method of Thermal Plant Analysis*. Butterworths, London, 1985. (Cited on page 36.)

[18] K. Kunitomi, A. Kurita, H. Okamoto, Y. Tada, S. Ihara, P. Pourbeik, and W.W. Price. Modeling frequency dependency of gas turbine output. In *IEEE Power Eng. Soc. Winter Meeting*, 2001. (Cited on pages 57, 65, and 66.)

[19] K. Kunitomi, A. Kurita, Y. Tada, S. Ihara, W.W. Price, L.M. Richardson, and G. Smith. Modeling combined-cycle power plant for simulation of frequency excursions. *IEEE Trans. Power syst., vol.18*, 2003. (Cited on pages 57 and 65.)

[20] Gillian Lalor, Julia Ritchie, Damian Flynn, and Mark J. O'Malley. The impact of combined-cycle gas turbine short-term dynamics on frequency control. *IEEE Trans. Power syst., vol.20*, 2005. (Cited on page 70.)

[21] J.F. Louis, K. Hiraoka, and M.A. El-Masri. A comparative study of influence of different means of turbine cooling on gas turbine performance. *ASME Paper no. 83-GT-180*, 1983. (Cited on page 114.)

[22] C.H Marston and M. Hyre. Gas turbine bottoming cycles: Triple-pressure steam versus kalina. *ASME Journal of Engineering for Gas Turbines and Power 117*, 1995. (Cited on page 35.)

[23] Lapo Filippo Mori. Scrivere la tesi di laurea con LaTeX 2ε. *ArsTeXnica*, 2007.

[24] M. Nagpal, A. Moshref, G.K. Morison, and P. Kundur. Experience with testing and modeling of gas turbines. In *IEEE Power Eng. Soc. General Meeting*, 2001. (Cited on page 54.)

[25] Tobias Oetiker. *The Not So Short Introduction to LaTeX 2ε*, September 27, 2005.

[26] Tobias Oetiker, Hubert Partl, Irene Hyna, and Elisabeth Schlegl. *The Not So Short Introduction to LaTeX 2ε*, 2005.

[27] Working Group on Prime Mover and Energy Supply Models for System Dynamic Performance Studies. Dynamic models for combined cycle plants in power system studies. *IEEE Transactions on Power System, Vol. 9, No. 3*, 1994. (Cited on pages 50, 59, and 70.)

[28] Lorenzo Pantieri. *L'arte di Scrivere con LaTeX*, 2008. http://www.lorenzopantieri.net/.

[29] L. Pereira, J. Undrill, D. Kosterev, D. Davies, and S. Patterson. A new thermal governor modeling approach in the WECC. *IEEE Trans. Power syst., vol.18*, 2003. (Cited on pages 54 and 55.)

[30] P. Pourbeik. *The Dependance of Gas Turbine Power Output on System Frequency and Ambient Conditions*. Cigre, 2002. (Cited on page 57.)

[31] W.I. Rowen. Simplified mathematical representations of heavy-duty gas turbines. *ASME J. Eng. Power, vol. 105*, 1983. (Cited on pages 47, 49, 50, 70, and 71.)

[32] W.I. Rowen. Simplified mathematical representations of single shaft gas turbines in mechanical drive service. In *Int. Gas Turbine and Aeroengine Congr. and Expo.*, Cologne, Germany, 1992. (Cited on pages 48, 49, and 70.)

[33] P.A. Rufli. A systematic analysis of the combined gas-steam cycle. In *Proc. ASME COGEN-Turbo I*, 1987. (Cited on page 31.)

[34] Y. Sanjay, Onkar Singh, and B.N. Prasad. Energy and exergy analysis of steam cooled reheat gas-steam combined cycle. *Applied Thermal Engineering*, 2007. (Cited on pages 105, 108, and 114.)

[35] S. Suzaki, K. Kawata, M. Sekoguchi, and M. Goto. Mathematical model for a combined cycle plant and its implementation in an analogue power system simulator. In *IEEE Power Eng. Soc. Winter Meeting*, 2000. (Cited on page 52.)

[36] Wenguo Xiang and Yingying Chen. Performance improvement of combined cycle power plant based on the optimization of the bottom cycle and heat recuperation. *Journal of Thermal Science Vol.16, No.1*, 2007. (Cited on page 40.)

[37] Soon Kiat Yee, Jovica V. Milanovic, and F. Michael Hughes. Overview and comparative analysis of gas turbine models for system stability studies. *IEEE Transactions on Power Systems, vol 23*, 2008.

[38] Q. Zhang and P.L. So. Dynamic modelling of a combined cycle plant for power system stability studies. In *presented at the IEEE Power Eng. Soc. Winter Meeting*, 1998. (Cited on page 48.)